Utilizing Asphaltenes and Polyethylene Terephthalate Fibres in Developing High-Performance Asphalt Concrete

by

Nirob Ahmed

A thesis submitted in partial fulfillment of the requirements for the degree of

Master of Science

in

Civil (Cross-Disciplinary)

Department of Civil and Environmental Engineering
University of Alberta

Abstract

Asphalt pavement performance is significant in order to ensure safety, longevity, cost-effectiveness, environmental sustainability, and the overall socio-economic well-being. A substantial amount of financial allocation is dedicated every year to enhance the performance of asphalt pavement in a more sustainable manner, due to the increasing global concern for sustainable infrastructure development. This has stimulated investigations into waste materials and different methodologies that reduce environmental footprints while simultaneously enhancing the lifespan of asphalt pavement with improved capacity. In this context, this research explored the incorporation of waste additives, specifically asphaltenes and polyethylene terephthalate (PET) fibres, in the development of high-performance asphalt concrete (HPAC). HPAC is an innovative paving material for high-traffic roads, known for its superior strength, rutting resistance, and fatigue resistance.

In the initial stage of this study, asphaltenes, a sustainable and cost-effective waste material, was used as an additive in the asphalt binder modification process. Two different asphalt binders were used in this study—one derived from crude oil and the other from Alberta oilsands bitumen. The binders were modified with an optimum concentration of 12% (by weight of binder) asphaltenes to assess their rheological and aging properties utilizing multiple stress creep recovery (MSCR) and frequency sweep (FS) tests. These tests were conducted on a dynamic shear rheometer (DSR) device with different plate geometry. MSCR test results demonstrated that binders modified with asphaltenes exhibited a reduction in non-recoverable creep compliance (J_{nr}), satisfying the criteria for extremely heavy traffic conditions, as evidenced by J_{nr} values consistently below 0.5 kPa^{-1}. All the binders met the stress sensitivity requirement, with $J_{nr\ diff}$ values being lower than 75%. $J_{nr\ slope}$ results, on the other hand, indicated lower stress sensitivity in the asphaltenes-modified

ii

binders. Results from the FS tests revealed improved rutting resistance in the asphalt binders post asphaltenes modification with increased complex shear modulus and rutting parameter values. Lower phase angle values strongly indicated a shift toward increased elasticity and reduced viscous behaviour in binders subsequent to the asphaltenes incorporation. Additionally, complex shear modulus aging index (CAI) results demonstrated that the asphaltenes-modified binders were better resistant to short-term aging.

Finally, asphalt mixes were prepared with the inclusion of asphaltenes, and three different lengths of PET fibres. An indirect tensile cracking test (IDEAL-CT) was performed to evaluate the cracking resistance properties of these mixes using a universal testing machine (UTM). The tests were performed at a typical intermediate temperature of 25 °C. Another target test temperature of 37 °C was determined based on the PG of the asphalt binder. The test results showed a clear impact of PET fibre incorporation at 37 °C, with significant improvement in the cracking tolerance (CT_{Index} values for control asphaltenes-modified, 6-mm, 12-mm, and 18-mm PET fabricated samples were found to be 61, 87, 105, and 99, respectively) and failure energy (5,475 J/m^2, 6,752 J/m^2, 7,005 J/m^2, and 6,902 J/m^2 for control asphaltenes-modified, 6-mm, 12-mm, and 18-mm PET fabricated samples, respectively), with this effect becoming more pronounced with increasing fibre length.

Preface

This thesis is an original work carried out by Nirob Ahmed at the University of Alberta, under the supervision of Dr. Leila Hashemian.

Chapters 1 and 2, are composed of introduction and literature review on asphaltenes-modified asphalt binders and polyethylene terephthalate (PET) fibres reinforced asphalt mixes.

Chapter 3 of this work, "Exploring the Influence of Asphaltenes on Rheology and Aging Characteristics of Asphalt Binders", has been submitted to C&B.

Chapter 4, "Investigating the Influence of Polyethylene Terephthalate Fibres with Different Lengths on the Cracking Resistance of High-Performance Asphalt Concrete", has been submitted to Canadian Journal of Civil Engineering (CJCE), and at this moment is under review.

Chapter 5 presents a summary and conclusions of this work.

Dedicated to my beloved parents, my eldest brother, and my loving wife.

Acknowledgment

I would like to express my sincerest appreciation to Dr. Leila Hashemian, my supervisor at the University of Alberta, for her unwavering support, patience, guidance, and encouragement during my years of research. Additionally, I would like to express gratitude to my committee members, Dr. Alireza Bayat, Dr. Bo Zhang, and Dr. Maricor Arlos.

I extend my cordial thanks to Dr. Taher Baghaee Moghaddam, and Mohamed Saleh, for their assistance, invaluable suggestions, and motivating inputs at each phase of my research work.

I am grateful to the faculty and staff of the department for providing me with the necessary resources and facilities needed for the progression of my research. My gratitude also extends to Alberta Innovates for providing financial assistance throughout this research.

Lastly, I want to thank my family for their unconditional love and support, a consistent source of motivation and inspiration throughout this journey.

Table of Contents

List of Tables

List of Figures

Chapter 1. Introduction

1.1 Introduction

Road infrastructure is the most valuable asset for a nation's economic growth and prosperity. Road infrastructure includes components such as pavement, bridges, tunnels, drainage, bus stops, terminals and others. Pavement is one of the most essential component of road infrastructure, which provides smooth all-weather travelling surface for a range of vehicles and the commuters. Pavement can be categorised in two main types; one is rigid pavement and the other one is flexible pavement. Rigid pavement is basically a one-layer structure which is constructed by laying a reinforced or unreinforced in-situ concrete slab over a granular subbase. Flexural strength of the pavement is responsible for supporting the loads, and the loads are transferred to a wider subgrade area. Most US Interstate network and European highway network use rigid pavements, while, Canada, on the other side, have an estimated 95% flexible pavements of the entire paved road network [1].

Flexible pavement, also known as asphalt road, is constructed with multiple layers, and protects the subgrade under the pavement. Most commonly adopted road construction type is the flexible pavement, and the average design life for flexible pavement is about 20-30 years [2]. Design of a flexible pavement is mainly dependent on load distribution characteristics of different layers. It has the advantage of having the ability to freely contract and expand, that eliminates thermal stresses [3]. However, several pavement failures such as cracking, rutting, and thermal cracking can occur which can damage the overall design life of the pavement. Such failures in the flexible pavement can occur due to adverse weather conditions, use of chemicals and salts in colder region, repetitive loads from vehicles, and aging. Thus, the maintenance of flexible pavements is very critical, which requires substantial amount of financial allocation every year. Adoption of High-

performance asphalt concrete (HPAC) can be an innovative solution to mitigate such issues and increase the lifespan of asphalt paved roads.

HPAC is an inventive paving material designed to achieve an asphalt mix with high mechanical properties. These properties include high elastic stiffness, high resistance to deformation and good fatigue resistance, all while maintaining adequate workability and durability [4], [5]. HPAC can also be defined as a material that maintains flexibility and stress relaxation properties in cold temperatures, and shows least deformation in high temperatures [6]. The main application of HPAC is in base course, although, it has already been utilized in the surface [7]. The fundamental elements for HPAC are hard grade binders and continuous dense-graded mineral skeletons [8]. Different studies have been carried out, over the years, in the development of HPAC such as optimization of the aggregate packing characteristics for design, fibre reinforcement in warm mix asphalt, Marshall design based HPAC [9], [10], [11]. Use of asphaltenes and polyethylene terephthalate (PET) fibres altogether in the development of HPAC is relatively unexplored and can be a good addition for the betterment in the pavement industry.

Asphalt binder is a hydrocarbon substance primarily derived from crude oil or oilsands refineries using fractional distillation as its main production process [12]. It is an integral element of an asphalt mix and can greatly affect the properties and performance of asphalt mixtures. Some distresses such as fatigue cracking, rutting, and thermal cracking are linked to the complex rheological properties of asphalt binders [13]. Attempts have been made to modify the properties of binders through the use of various modifiers, including fillers, fibres, extenders, plastics, anti-stripping agents, oxidizing agents, antioxidants, reclaimed rubber, polymers to mitigate above mentioned pavement distresses [14]. Asphaltenes is a waste material which is produced at a higher rate in the oil industry, can also be used to modify neat asphalt binders. Previous studies indicated

an improved aging resistance and stiffness of asphalt binders with asphaltenes-modification [15], [16]. However, there is more to be investigated in terms rutting resistance, viscoelastic behaviour, stress sensitivity, elastic recovery of the asphaltenes-modified asphalt binders.

PET stands out as the most widely used thermoplastic polyester, a type of long-chain polymer categorised under polyesters [17]. Known for its easy handling, durability, strength, low gas permeability, thermal and chemical stability [18], PET is commonly found in municipal solid waste in the form of waste plastic bottles [19]. Introduction of PET fibres into the asphalt pavement industry emerges as a sustainable solution to the ever-increasing plastic waste globally. Over the years, numerous studies have explored the utilization of PET fibres in the asphalt mixes, revealing improved fatigue life and rutting performance [20], [21]. Consequently, the investigation of the combined effect of asphaltenes and PET fibres in improving the cracking performance of the asphalt mixes would be a quality addition to the existing literature.

1.2 Objectives

This study has two main goals: to investigate the impact of asphaltenes on the rheological properties of two asphalt binders from different sources, and to explore the performance properties of asphaltenes-modified and PET-fabricated HPAC.

1.3 Methodology

In the initial stage of this research, two distinct binder types, designated as A and B, were selected for modification with asphaltenes. To identify the optimum asphaltenes content, PG and SARA analyses were conducted on both the unmodified binders and those modified with varying asphaltenes concentration, specifically focusing on binder A. Following this, MSCR and FS tests were conducted using a DSR device on both unmodified binders and those modified with optimum asphaltenes content for binders A and B. MSCR tests were exclusively performed on the RTFO-

4

aged samples, while FS tests were carried out on both unaged and RTFO-aged samples. Results from MSCR test, including average non-recoverable creep compliance (J_{nr}), average percent recovery (R), and stress sensitivity indices ($J_{nr\ diff}$, and $J_{nr\ slope}$), were determined. FS tests, on the other hand, were employed to develop complex shear modulus (G*) and phase angle (δ) master curves. Furthermore, the rutting parameter (G*/sin[δ]) and aging indices (CAI, and PAI) were evaluated through FS tests. An in-depth analysis of all these parameters was carried out to assess the impact of asphaltenes-modification on asphalt binders.

Subsequently, the study was extended to asphalt mixes containing unmodified and asphaltenes-modified (with optimum content) binder A and different lengths of PET fibres (6-, 12-, and 18-mm), wherein an IDEAL-CT test was conducted at two test temperatures (25 °C and 37 °C) utilizing a Universal Testing Machine (UTM). The IDEAL-CT test aimed to acquire cracking parameters such as cracking tolerance index (CT_{Index}), failure energy (FE), and indirect tensile strength (ITS). These parameters were analyzed to determine the impact of fibre addition on the asphalt mixes. The methodology flowchart, as depicted in Figure 1-1, provides a visual representation of the steps involved in both the binder and asphalt mix testing phases of this research.

```mermaid
flowchart TD
    A[Materials selection (**asphaltenes**, binders **A** and **B**, **aggregates**, and **PET fibres**)]
    B[Asphalt **binder modification** with asphaltenes]
    C[Determining **optimum asphaltenes content**]
    D[Performing **short-term aging** on the asphalt binders (**A and B**) with **RTFO** oven]
    E[**Aggregates**, **binder (A)**, and **PET fibres** preparation for the designed mixes]
    F[**MSCR** test on the **RTFO aged** asphalt binders]
    G[**FS** test on both **unaged** and **RTFO aged** asphalt binders]
    H[Mixing the aggregates, binder and PET fibres]
    I[Analyzing Jnr, Jnr diff, Jnr slope, and R results obtained from MSCR test]
    J[Analyzing G*, δ, G*/sin[δ], CAI, and PAI results obtained from FS test]
    K[Sample compaction using a Superpave gyratory compactor]
    L[Performing ideal cracking test (**IDEAL-CT**)]
    M[Analyzing **ITS**, **FE**, and CT Index results from **IDEAL-CT**]
    N[Conclusion and Recommendation]
```

Figure 1-1. Methodological Flowchart

1.4 Thesis Structure

This thesis is organized into five chapters and has the following structure:

Chapter 1 – Introduction: A background of the research topic, motivations for the study, objectives, methodology, and thesis structure are briefly described.

Chapter 2 – Literature Review: Common distresses in asphalt pavement, asphalt binder modification with asphaltenes, and incorporation of polyethylene terephthalate (PET) fibres in asphalt mixes are discussed in this chapter. Also, relevant studies on the investigation of the rheological properties of the asphalt binder, and cracking performance of high-performance asphalt concrete (HPAC) are cited.

Chapter 3 – Exploring the Influence of Asphaltenes on Rheology and Aging Characteristics of Asphalt Binders: In this chapter, the optimal concentration of asphaltenes is evaluated using the results from PG and SARA analyses. The rutting resistance, viscoelastic properties, and aging resistance of the neat and asphaltenes-modified binders are determined using MSCR and FS test results.

Chapter 4 – Investigating the Influence of Polyethylene Terephthalate Fibres with Different Lengths on the Cracking Resistance of High-Performance Asphalt Concrete: The cracking performance of HPAC, with the incorporation of three different lengths (6-, 12-, and 18-mm) of PET fibres, is investigated utilizing IDEAL-CT test at 25 °C and 37 °C test temperatures. The cracking tolerance index (CT_{Index}), failure energy (FE), indirect tensile strength (ITS) results are analyzed to assess the impact of PET fibres addition in the asphalt mixes.

Chapter 5 – Summary and Conclusions: The impact of asphaltenes on the rheological and aging properties of asphalt binder and the combined effect of asphaltenes and different lengths of PET fibres on the HPAC are summarized in this chapter.

Chapter 2. Literature Review

2.1 Flexible Pavement

Flexible pavements are widely used for roads with low to medium traffic volumes, and they are also prevalent in high traffic areas, including interstate highways and airfield runways, taxiways and aprons that are subjected to substantial loads from aircraft gear and wheels [3]. Approximately 95% of the world's roads utilize flexible pavements [22]. In flexible pavement, the wheel load is distributed to a larger area, resulting in decreased stress with increase in depth. The design of flexible pavement is based on this stress distribution characteristic, typically incorporating many layers, as shown in Figure 2-1 [23]. This layered system helps the roads to flex and bend without the development of cracks in the pavement. Among these layers, the base course layer holds the most structural significance, and serves as the load-bearing component [24].
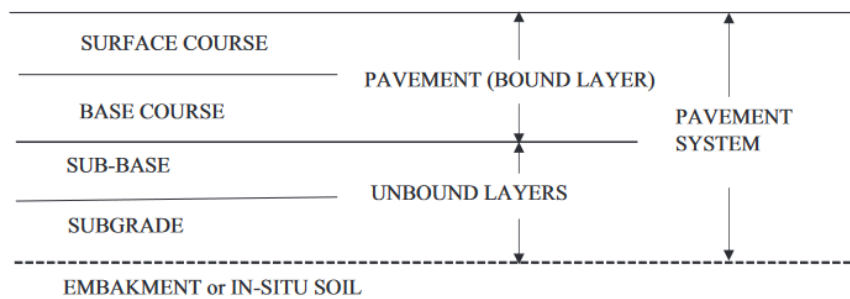
Figure 2-1. Basic layers in flexible pavement [25]

2.2 Distresses in Flexible Pavement

Pavement distress is defined as the potential flaws in the design, performance, and serviceability of a pavement surface over its lifetime [26]. Multiple factors influence the longevity and performance of a pavement, including subgrade characteristics, pavement materials, traffic loads, and moisture and temperature conditions. The distresses in asphalt pavement (Figure 2-2) can be categorized as surface cracking, surface deformation, deterioration, and mat problems [27].

Figure 2-2. Distresses in flexible pavement [28]

Surface cracking refers to the formation of cracks on the pavement surface; longitudinal cracks are parallel to the road, whereas transverse cracks cut across it. These cracks initially appear with significant gaps and gradually evolve into closely spaced. Fatigue cracking is a form of surface cracking that arises from the repeated and fluctuating stress levels, causing fractures to develop when the maximum stress falls below the tensile strength of the material. The fatigue cracking is primarily caused by the repetitive stress exerted by traffic [29], [30]. Surface deformation involves the deterioration of structural layers due to the impact of heavy traffic loads. The problem can be attributed to the degradation of the subsurface layers, and subgrade. Rutting is a distinct type of surface deformation identified by longitudinal depressions running parallel to the wheel path, perhaps accompanied by transverse displacement. It can occur due to a permanent loss in volume and permanent movement of the materials while maintaining a constant volume, or a combination of both factors [31].

Pavement deterioration refers to the breakage of segments of the pavement, and it is highly influenced by the development of cracking and rutting in the pavement. Potholes, which are bowl-shaped depressions formed gradually from small cracks and holes, are a visible sign of pavement deterioration. Mat problems are limited to the surface layer of the pavement and include issues such as bleeding, segregation, and delamination [32]. The quality of aggregates, and asphalt binder properties significantly influence the overall performances of asphalt pavement in terms of resisting various distresses.

2.3 Asphalt Binder

The asphalt binder, also known as asphalt cement binder, serves as the adhesive in asphalt concrete that holds the aggregates together. It is a by-product of the petroleum-refining process that generally produces gasoline, diesel fuel, lubricating oil, and other petroleum products [33]. It is obtained from the dense residue left after petroleum distillation. Asphalt binder is a viscoelastic material, which can behave viscous, elastic, or a combination of the two depending on temperature and time. It is to be noted, the binder's behaviour at high temperatures for short durations is equivalent to that observed at low temperatures for extended periods. This concept, referred as time-temperature superposition (TTS), is usually applied at various temperatures, frequencies, and conditions to examine the behaviour of asphalt [34].

The asphalt binder significantly influences the overall resilience of asphalt mixtures in resisting pavement damage. Hence, it is imperative to conduct a comprehensive assessment of the rheological properties of the asphalt binder before its application in the field. Typically, the suitable asphalt binder is selected through the performance evaluation, utilizing a grading system [35]. The Superpave performance grade (PG) system is a dual-digit categorization that offers details regarding the binder. The first value represents the average seven-day maximum design

temperature in degrees Celsius, whereas the second number indicates the minimum design temperature in degrees Celsius that the pavement will encounter.

2.4 Aging in Asphalt Binder

Asphalt binders utilized in the construction of asphalt concrete pavements undergo aging both at their initial installation and throughout their operational lifespan. Aging occurs due to the evaporation of volatile substances and the chemical reactions of asphalt binder compounds with oxygen. The process of aging has a considerable impact on the rheological characteristics of asphalt binders [36], [37]. The Superpave testing and specification system employs two laboratory tests, the Rolling Thin Film Oven (RTFO) and the Pressure Aging Vessel (PAV), to assess the aging of binders before examining their rheological properties.

Figure 2-3. (a) Rolling thin film oven (RTFO), (b) RTFO carriage inside the oven

The RTFO test is a method used to simulate the aging of asphalt binders in pavement construction by exposing them to heat and air on a continuously moving film. This brief period of aging is carried out in accordance with AASHTO T240-17 [38]. Each glass bottle receives quantities of the binder weighing 35 ± 0.5 g and is left on a rack for 60-min at room temperature. Subsequently, the

glass bottles are inserted into the carriage within the oven. The process of aging lasts for 85-min in the RTFO oven (Figure 2-3), set at a temperature of 163 °C. During this time, the bottles are rotated at a constant rate of 15 ± 0.2 rev/min, while the airflow is maintained at a rate of 4000 ± 300 mL/min.

Figure 2-4. (a) Pressure aging vessel (PAV), (b) Binder samples in a PAV rack

The PAV test process is specifically developed to replicate the oxidative aging that occurs during the lifespan of an asphalt pavement while it is in use. A portion of the residue, aged using the RTFO, is utilized to replicate the prolonged aging of asphalt. This is done to evaluate the performance grade of the asphalt binder at intermediate and low temperatures using a PAV (Figure 2-4), following the guidelines of AASHTO R28-16 [39]. Each PAV pan is filled with approximately 50 g of the residue that has been aged using the RTFO. These pans are then placed in a sample rack specifically designed for the PAV test. The samples are thereafter exposed to a pressure of 2.1 MPa and a constant temperature of 100 °C for a period of 20 h. Subsequently, the remaining substance in each pan is carefully collected and transferred into a single container. This container is then introduced into a vacuum oven set at a temperature of 170 °C for a duration of 30-min, with the purpose of eliminating any surplus gas present in the sample.

2.5 Performance Grading of Asphalt Binder

The assessment of a binder's PG adheres to the procedures outlined in AASHTO R29-18 [40]. This process designates the initial investigation for the binder's high-temperature verification as the primary grading step. A DSR device is used to perform this test on an asphalt binder sample in accordance with AASHTO T315-16 [41], as shown in Figure 2-5.
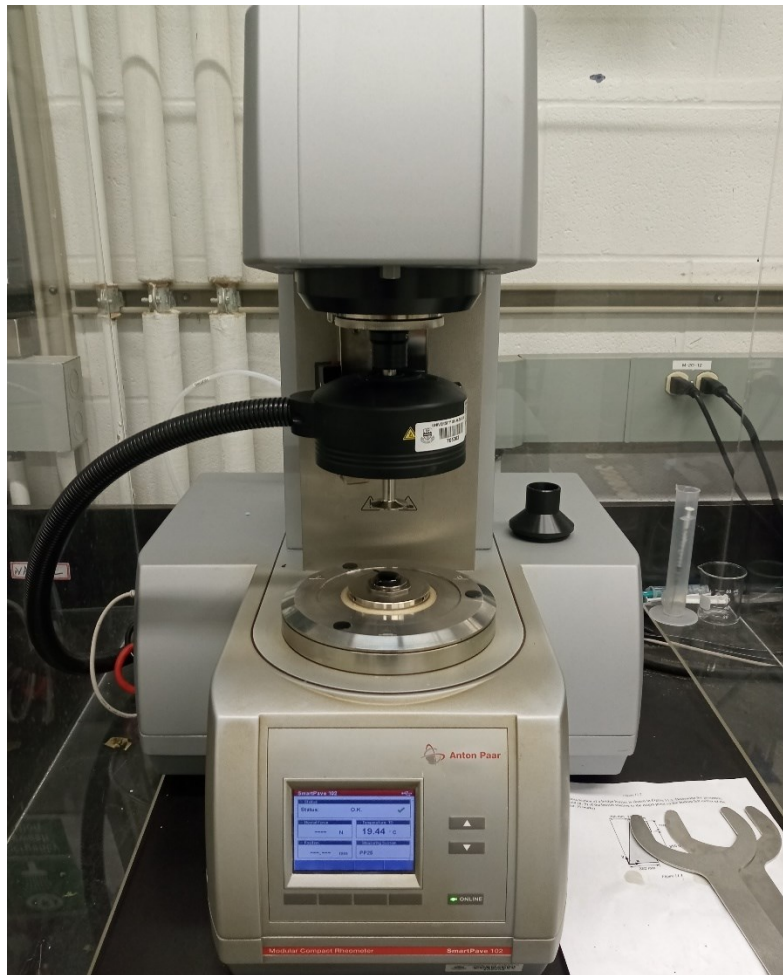
Figure 2-5. A dynamic shear rheometer (DSR) device

In order to evaluate stress and the resulting strain response in binder samples, the DSR applies sinusoidal shear loading. The device uses this information to calculate the phase angle (δ) and complex shear modulus (G^*) for viscoelastic materials. The ratio of the maximum applied shear

stress to the peak strain value is denoted by G^*, and the time lag between the shear stress and the shear strain response is represented by δ. The binder's G^* and δ are initially evaluated at 58 °C. The test temperature is then decreased or increased by 6 °C at a time until $G^*/\sin[\delta]$ is less than or equal to 1.0 kPa. According to AASHTO M320-17 [42], $G^*/\sin[\delta] \geq 1.0$ kPa indicates the highest binder grade. RTFO-aged asphalt that has undergone post-initial grading is subjected to the same testing technique, but with a change in $G^*/\sin[\delta]$ magnitude to 2.2 kPa, as outlined in AASHTO T315-16 [41]. The difference in value between the original and RTFO-aged binders is used to calculate the high-temperature grade, and the continuous high PG is the minimum of these two values.

PAV-aged asphalt binders are tested under sinusoidal shear loading using a DSR as per AASHTO T315-16 [41] to assess the performance of binders at intermediate temperatures. AASHTO M320-17 [42] specifies the testing temperatures for the binder, and failure occurs when $G^*.\sin[\delta]$ surpasses 5,000 kPa at a loading frequency of 10 rad/s.

For characterizing the rheological properties of asphalt binders at low temperatures, a bending beam rheometer (BBR) is utilized as depicted in Figure 2-6, in accordance with AASHTO T313-16 [43]. The test is carried out at a temperature specified by AASHTO M320-17 [42] on PAV-aged samples. Creep stiffness and the m-value are the two parameters—determined through BBR at a loading time of 60 seconds—that are crucial to the sample failing. Creep stiffness assesses how the asphalt binder withstands constant loading, while the m-value measures how the binder's stiffness changes under applied loads. The stiffness of a small asphalt beam (127 mm×12.7 mm×6.35 mm) is calculated by tracking its deflection during the application of a creep load using BBR [44]. According to AASHTO M320-17 [42], the criteria for determining the low PG involve

identifying the lowest temperature where the creep stiffness (S) is less than or equal to 300 MPa and the slope value (m) is greater than or equal to 0.300.
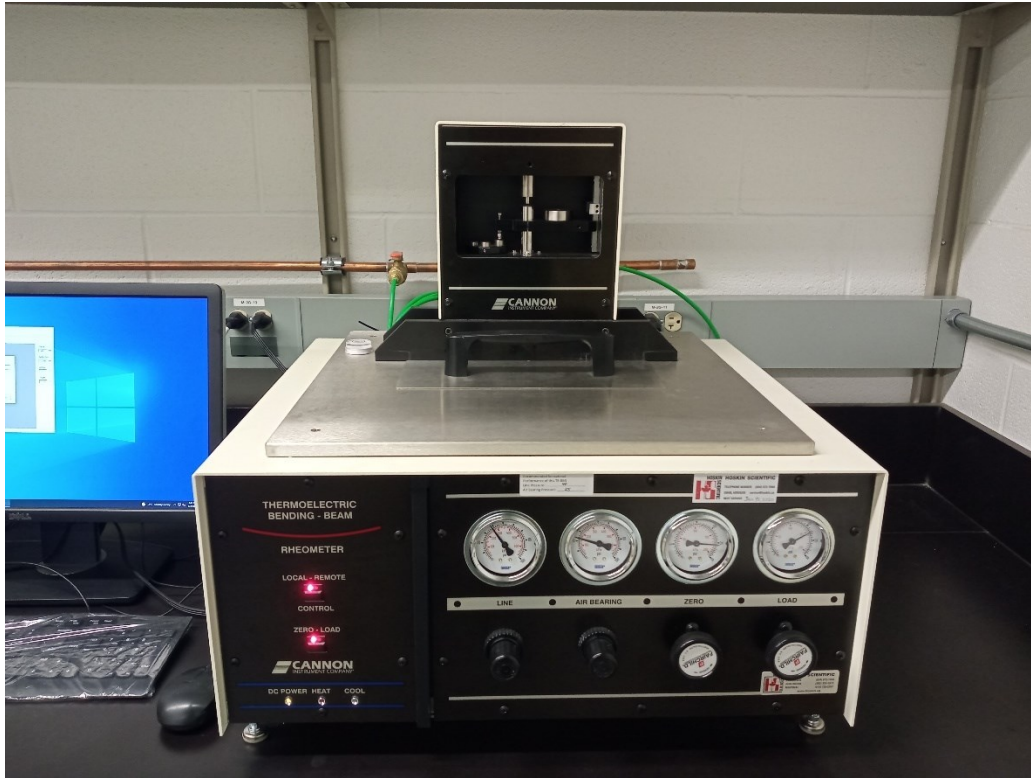
Figure 2-6. A bending beam rheometer (BBR) device

2.6 Asphalt Binder Viscosity

The temperature during construction phase has a significant impact on the quality of asphalt pavements. Exceedingly high mixing temperature in the manufacturing of asphalt concrete leads to a reduction in the viscosity of the asphalt binder. Consequently, this prevents the production of a thick layer of binder for proper adhesion between the aggregates, thus the asphalt binder gets easily separated from the aggregates [45], [46]. On the other hand, in cases where the construction temperature is very low, the asphalt binder becomes highly viscous, obstructing the homogeneous blending with the aggregates. Additionally, the process of compacting the asphalt mix during paving becomes challenging, and the quality and performance are compromised [47]. The

determination of the mixing and compaction temperatures rely on identifying the temperature intervals that correspond to the specified viscosity [48].

The Superpave method necessitates the determination of mixing and compaction temperatures utilizing a rotational viscometer (RV) [49]. The RV measures the torque needed to rotate a spindle within the asphalt binder sample at a particular speed and temperature. The torque is subsequently transformed into the viscosity of the sample [44]. The viscosity of the asphalt binder at different temperatures is measured using an RV (Figure 2-7), following the guidelines in AASHTO T316-17 [50]. Viscosity measurements are obtained from the apparatus at 1-minute intervals over a period of 3 minutes for each temperature. The viscosities for the mixing and compaction temperature ranges are plotted as 0.17 ± 0.02 Pa-s and 0.28 ± 0.03 Pa-s, respectively [51].

Figure 2-7. A rotational viscometer (RV)

2.7 SARA Analysis

The SARA components test serves to evaluate the proportion of saturates, aromatics, resins, and asphaltenes in asphalt binder [52], [53]. Researchers have extensively explored the correlation between these SARA fractions in asphalt binders and their physical and engineering characteristics over the past few decades. It was discovered that while saturates and aromatics contribute to the soft and plasticizing properties of the asphalt binder, asphaltenes and resins help to improve the stiffness of the material [54]. The viscosity of the oil sand binder is reduced as the maltenes percentage rises, whereas the addition of asphaltenes increases asphalt binder viscosity [55].

Asphaltenes and maltenes separation can be achieved through the solvent extraction technique outlined in ASTM D6560-17 [56]–[58]. In this process, a sample of the binder is initially blended with heptane and then subjected to reflux heating. The resulting precipitated asphaltenes and maltenes are collected on a filter paper, with the maltenes subsequently separated through a procedure involving hot heptane washing in an extractor and dissolution in hot toluene. Further subdivision of maltenes into saturates, aromatics, and resins is accomplished using clay-gel adsorption chromatography as per the guidelines provided in ASTM D2007-19 [59]–[61]. Initially, the specimen is diluted before being passed through a percolation column containing clay and silica gel. N-pentane is utilized to collect the resulting liquid. The upper clay segment undergoes a n-pentane wash and subsequent desorption with a toluene-acetone blend. The lower gel column is desorbed through toluene recirculation. Extracted solvents are eliminated from the n-pentane and toluene-acetone fractions, and the remaining residues are quantified for saturates and polar compound levels. Aromatics and resins can be identified using the difference method or by measuring what remains after the toluene has evaporated [61]. Saturates appear as a transparent or

lightly tinted liquid, aromatics as a yellow to deep-red liquid, resins as a dark-brown to black solid, and asphaltenes as a black powder at ambient temperature. [16], [62].

The colloidal index (CI) of asphalt binders is calculated to assess the stability of the asphaltenes phase within the maltenes matrix. It can be defined as the ratio of the combined quantities of saturates and asphaltenes to the combined quantities of resins and aromatics, as shown in Equation 2-1 [63], [64]. The asphaltenes component in the maltenes matrix tends to be unstable when the CI value is greater than 1.2 [65].

$$CI = \frac{Saturates\ (\%) + Asphaltenes\ (\%)}{Resins\ (\%) + Aromatics\ (\%)} \tag{2-1}$$

2.8 Asphaltenes as Binder Modifier

Asphaltenes plays a crucial role in determining the elastic properties of asphalt binder. It is defined as the component of the binder that does not dissolve in low carbon number n-alkanes (such as n-hexane, n-heptane, or n-pentane) but may dissolve in light aromatic hydrocarbons (such as toluene and benzene) [16], [66], [67]. Asphaltenes, the most dense and intricate component of crude oil, composed of concentrated polynuclear aromatics and contains minor quantities of heteroatoms (S, N, and O) as well as traces of nickel and vanadium [68], [69]. Asphaltenes is the primary source of issues in the catalytic processing of petroleum residua. It has a negative impact on the overall hydride-sulfurization rate, contributing to the deactivation of catalysts [70]. Consequently, it is regarded as a waste and insignificant material with limited uses, derived using the solvent deasphalting method in oil refineries.

This method of extracting asphaltenes utilizes the solubility-based characteristics of asphaltenes. N-alkanes, specifically n-heptane or n-pentane, are used as anti-solvents to induce the precipitation of asphaltenes particles [60], [71]. In order to ensure complete precipitation of asphaltenes

20

particles, it is recommended to use an anti-solvent volume that is at least 40 times the volume of the oils and to allow a contact duration of at least 8 h [56], [72]. Figure 2-8 displays the solid asphaltenes produced by the refinery. To obtain powdered asphaltenes, the solid asphaltenes are initially subjected to crushing to break them into smaller particles, which are subsequently ground into finer particles. The resulting finer particles are further sieved using a No. 100 sieve with a 150 μm mesh size to transform them into a powdered state.
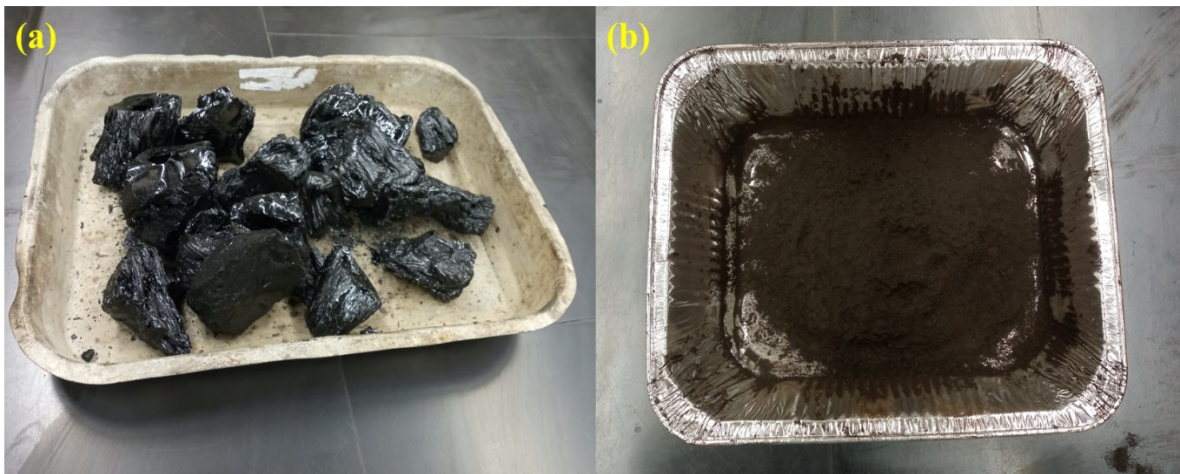
Figure 2-8. Asphaltenes in (a) Solid form, (b) Powder form

Multiple researches have been undertaken to assess the impact of asphaltenes modification on the asphalt binder performance. The researchers have identified two general approaches for altering the asphaltene content in asphalt binders [57], [73]. The first approach involves utilizing a mechanical stirrer to blend asphalt binder with a substance that contains a high concentration of asphaltenes (such as propane deasphalting tar (PDA) and natural bitumen, recovered binder, and polyphosphoric acid (PPA)) at elevated temperatures [15], [74]. The second approach is where the solvent dissolution process is applied to obtain asphaltenes from an asphalt binder. These recovered asphaltenes are subsequently reintroduced into the asphalt binder in specific proportions [16], [73], [75].

Improving the rheological properties of asphalt binder can be effectively achieved by incorporating polymers into it [76]. However, polymers tend to be expensive and this increases the cost of polymer modification process. Therefore, utilizing asphaltenes as a waste material has the potential to alter the rheological properties of asphalt binder at a minimal expense. Prior studies indicate that the binder stiffness and elasticity are improved with asphaltenes incorporation. Although, a higher concentration of asphaltenes reduces the stability of the asphalt binder, the high PG required for high stiffness asphalt mix is achieved with 12% (by the weight of binder) asphaltenes concentration with a well-maintained asphalt binder stability [77]. An increase in the concentration of asphaltenes in asphalt binder leads to a reduction in penetration and an elevation in softening point [78]. Furthermore, the inclusion of asphaltenes has been found to improve the viscosity of the asphalt binder [79]. Even the inclusion of small amounts of asphaltenes was discovered to significantly decrease creep compliance and enhance stiffness. Thus, the asphaltenes modification of the asphalt binder has a positive impact on the mechanical properties of asphalt mixes [16], [73].

2.9 Polyethylene Terephthalate (PET) Fibres in Asphalt Mixes

One of the most dispersed thermoplastic polymers on the market is polyethylene terephthalate, or PET for short [80]. It is a polymer that belongs to the polyester family and is semi-crystalline. It is practically insoluble in water with a melting point of greater than 250 °C [81], [82]. PET is the preferred material, particularly when making containers for the mass beverage industry. Consequently, PET is a material that is frequently found in municipal solid waste [83]. One drawback of the continually growing volume of plastic waste is that it is not biodegradable and the use of PET in the pavement industry could be a potential revolutionizer.

Figure 2-9 illustrates the process of developing PET fibres, starting with the sorting and shredding of waste plastic bottles into flakes. The flakes are then vacuum-dried and cleaned before going through the last extrusion step. The first step in the extrusion process is to feed the plastic flakes through a hopper into a barrel. A 110-rpm revolving screw inside the barrel drives the plastic forward, melting it bit by bit as it passes through three zones: the metering, melt, and feed zones. A circular band heater raises the barrel's temperature to 260° C, and a thermocouple maintains temperature control to stop plastic from degrading. Melted plastic exits the screw at the front of the barrel, where it is blown with compressed air to form a continuous synthetic fibre [82].
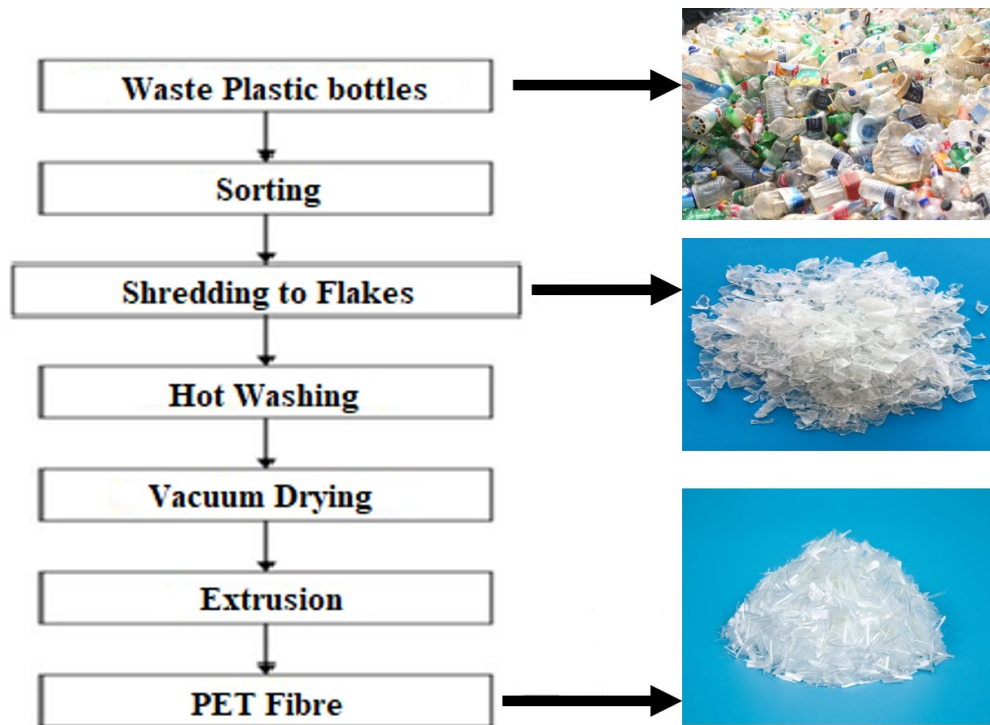
Figure 2-9. PET fibre generation flowchart [82]

Recycled PET fibre has been found to enhance asphalt concrete mixtures' resilience to rutting and fatigue. Furthermore, at lower temperatures, the resilience modulus of PET-reinforced asphalt concrete improves more significantly in comparison with higher temperature [20]. According to

Ma and Hesp's observation in 2022, the dimensions of PET fibre—including both length and diameter—have an impact on the fibre's ability to reinforce hot mix asphalt (HMA) against cracking. The few trials that have been done seem to indicate that the asphalt mixture cracking resistance is increased more successfully with longer PET fibres with bigger diameters. Similarly, PET fibre with a rough surface is favoured because it could strengthen the fibre's reinforcing function through improved interaction with aggregates and/or asphalt [84]. Saleh et al. in 2023 evaluated asphalt mix performance with different dosage of PET fibres, and they concluded that a 0.15% content of PET fibres considerably improves the stiffness, fracture energy, and tensile strength of the asphalt mixtures [85]. Ahmadinia et al. conducted experimental research on stone mix asphalt modified with PET fibre to assess its resistance to rutting, moisture susceptibility, resilient modulus, and drain-down tolerance. The authors came to the conclusion that the PET modified mixes improved and controlled the detailed performance tests at a certain fibre content [86]. Dehghan et al. assessed the fatigue life of fibre-reinforced HMA while taking various PET fibre lengths and amounts into account. Following the four-point bending test evaluation of the fatigue response at the strain range of 300, 500, and 700 microstrains, the fatigue lifetimes at each of the three microstrains were enhanced by more than 100% [87].

2.10 High-Performance Asphalt Concrete (HPAC)

Numerous studies have endeavoured to introduce and enhance HPAC by focusing on its resistance properties, each presenting distinct limitations, approaches, and concentrated scopes. The primary focus of HPAC's development was on optimizing the aggregate packing properties for the asphalt pavement's design. For the purpose of choosing the HPAC aggregate structure, some particular guidelines were created. The application of aggregate packing techniques to asphalt concrete has proven beneficial [9]. Subsequent studies explored the impact of introducing fibres into HPAC,

utilizing warm mix asphalt. Findings revealed that the simultaneous use of polyolefin-aramid FORTA polymer fibres and fischer-tropsch paraffin wax (Sasobit) not only significantly enhances the resistance of the asphalt mixture but also improves workability throughout the entire process, including mixing, transportation, paving, and compacting [10]. Latvia has previously developed HPAC, utilizing local mineral materials and recycled modifiers such as fibreglass and crumb rubber [88]. Moreover, Silva et al. conducted a comprehensive investigation of HPAC in 2011, emphasizing rutting and stiffness criteria. Their objective was to assess the potential benefits of incorporating polyethylene-based waste materials into asphalt mixtures, specifically high-density polyethylene (HDPE) as a binder modifier and cross-linked polyethylene (PEX) as a partial substitute for aggregates [89].

A well-structured aggregate gradation from different fractions is required for the development of HPAC; the gradation used in this research was derived from studies on high-modulus asphalt concrete (HMAC). This particular asphalt mixture demands higher voids in the mineral aggregate (VMA) values to accommodate the increased asphalt binder content [90]. Consequently, the use of fully crushed aggregates contributes to an increase in VMA owing to their surface area and texture [91]. In order to standardize the mixture design process with regard to aggregate gradation in HMAC, a number of nations and regions, such as Australia, France, South Africa, and the United Kingdom, have designed unique gradation envelopes [5], [92]–[94]. While some studies are using strategies to optimize aggregate gradations for improved performance, others are creating their own gradations that may or may not match standard envelopes [8], [95].

Unlike traditional methods, volumetric properties are not used to determine the amount of asphalt binder in HPAC mix design procedures. Instead, it is established through the calculation of a richness factor denoted as K [91]. This K factor, integral to the French asphalt mix design

25

approach, is a proportional variable linked to the binder film thickness enveloping the aggregate [90]. The required asphalt binder content can be calculated using Equation 2-2 given below.

$$TL_{est} = K\alpha\sqrt[5]{\Sigma}$$ (2-2)

where,

TL_{est} = percent binder by mass of mixture,

K = richness factor,

α = correction coefficient for relative density of aggregates, and

Σ = specific surface area of aggregates.

2.11 Testing Programs

2.11.1 Multiple Stress Creep Recovery (MSCR) Test

The MSCR test has recently gained acceptance in assessing rutting in the Superpave PG system efficiently. Many consider it to be the best available test method for evaluating the high-temperature performance of asphalt binders [96], [97]. The MSCR test can act as a substitute for the existing DSR test in characterizing high-temperature properties related to rutting in HMA [98]. Following AASHTO T350-19 [99] guidelines, the MSCR test is conducted on RTFO-aged residue using a DSR at a specific temperature. While the test temperature can vary, it is recommended to choose one representative of the temperature range where rutting occurs in the field [100], [101]. Employing a 25-mm parallel plate geometry with a 1-mm gap setting, the sample undergoes creep at stress levels of 0.1 kPa and 3.2 kPa, followed by recovery at each stress level. The creep stage lasts for 1 s, succeeded by a 9 s recovery. The test involves 20 cycles at the 0.1-kPa stress level and 10 cycles at the 3.2-kPa stress level. The initial 10 cycles at 0.1 kPa are meant for specimen conditioning only and are not used in the calculation. There are no intervals between creep and recovery cycles or changes in stress levels [99].

Average non-recoverable creep compliance (J_{nr}), stress sensitivity evaluation indices ($J_{nr\ diff}$, and $J_{nr\ slope}$), and average percent recovery (R) are the results determined through MSCR test. The average non-recoverable creep compliance values are determined following Equation 2-3 and 2-4 at two different stress levels of 0.1 kPa and 3.2 kPa, respectively.

At 0.1 kPa:

$$J_{nr_{0.1}} = \frac{SUM[J_{nr}(0.1,N)]}{10} \text{ for N} = 11 \text{ to } 20 \qquad (2\text{-}3)$$

where,

$\qquad$ N = cycles.

At 3.2 kPa:

$$J_{nr_{3.2}} = \frac{SUM[J_{nr}(3.2,N)]}{10} \text{ for N} = 1 \text{ to } 10 \qquad (2\text{-}4)$$

The percent difference in non-recoverable creep compliance between 0.1 kPa and 3.2 kPa ($J_{nr\ diff}$) is used to assess the stress sensitivity in asphalt binder, which is calculated using Equation 2-5.

$$J_{nr\ diff} = \left(\frac{J_{nr}3.2 - J_{nr}0.1}{J_{nr}0.1} \right) . 100\% \qquad (2\text{-}5)$$

The relationship between the non-recoverable creep compliance variable and the rut variable can be better described by a new modified stress sensitivity evaluation index ($J_{nr\ slope}$), according to numerous researchers who have discovered that there is no significant correlation between $J_{nr\ diff}$ and rutting test findings. The $J_{nr\ slope}$ values are evaluated following Equation 2-6.

$$J_{nr\ slope} = \left(\frac{J_{nr}3.2 - J_{nr}0.1}{3.1} \right) . 100\% \qquad (2\text{-}6)$$

Average percent recovery can be calculated at 0.1 kPa and 3.2 kPa stress levels using Equation 2-7 and 2-8, respectively.

At 0.1 kPa:

$$R_{0.1} = \frac{SUM[\epsilon_r(0.1,N)]}{10} \text{ for N} = 11 \text{ to } 20 \qquad (2\text{-}7)$$

where,

ϵ_r = The strain value at the end of the recovery portion.

At 3.2 kPa:

$$R_{3.2} = \frac{SUM[\epsilon_r(3.2,N)]}{10} \text{ for N} = 1 \text{ to } 10 \qquad (2\text{-}8)$$

2.11.2 Frequency Sweep (FS) Test

One common method for evaluating the rheological properties of asphalt binders is the FS test. Carried out within the linear viscoelastic (LVE) range, this test utilizes a DSR to measure viscoelastic parameters across various temperatures and frequencies [102]. Asphalt, behaving as a viscoelastic material, demonstrates rheological properties in line with the time–temperature superposition (TTSP) principle. This principle establishes a correlation between frequency and temperature, allowing consistent rheological behavior to be obtained under different experimental conditions [103]. The complex modulus and phase angle's dependency on temperature, frequency, or loading time can be presented through isochronal and isothermal plots, respectively [104]. The rheological properties of the material, displayed in these charts, offer important insights into how the material behaves at various temperatures and frequencies.

The strain amplitude applied during the test can be calculated performing a linear amplitude sweep test before the frequency sweep test, ensuring it stays within the LVE range of the asphalt binder. The typical test setting for lower temperature (≤ 30 °C) involves the use of an 8-mm diameter plate with 2-mm gap, while for higher temperatures (≥ 30 °C) it is recommended to use 25-mm plate geometry with 1-mm gap setting (Figure 2-10). This specific choice minimizes torque measurement inaccuracies and prevents misleading phase angles [105].
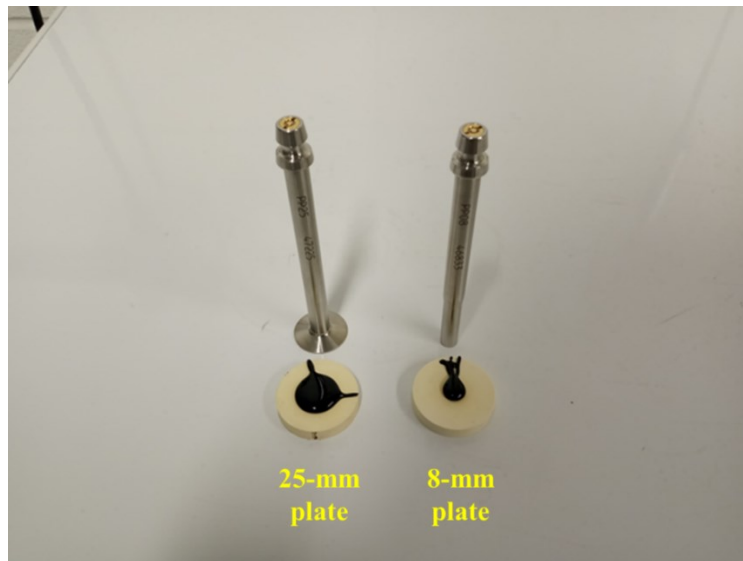
Figure 2-10. Different plate geometry in DSR
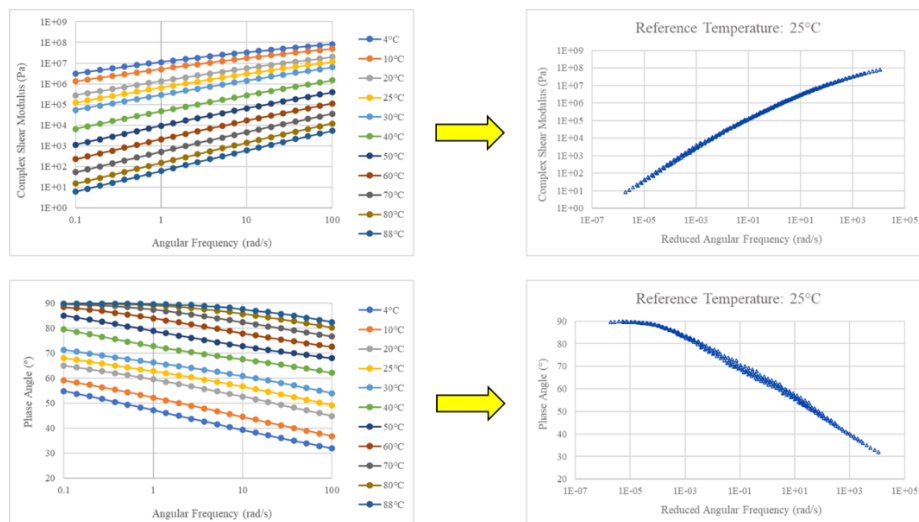
Figure 2-11. Master curves development from isotherms using TTSP method

29

Using the TTSP technique, the complex shear modulus (G^*) and phase angle (δ) master curves can be developed post-test. This involves horizontally shifting the results from each isothermal frequency sweep with respect to a reference temperature, aligning them into an overall continuous curve at a reduced frequency [16], [106]. In this approach, the curves are converged into a unified, smooth function with the application of shift factors to frequency values, assuming different values for each temperature data series, as shown in Figure 2-11 [107].

Rheological aging indices, including the complex modulus aging index (CAI) and phase angle aging index (PAI), are determined using Equation 2-9 and 2-10, respectively. A lower CAI value signifies a stronger resistance to aging in the asphalt binder, whereas a higher PAI value indicates superior aging resistance performance [108]–[110].

$$CAI = \frac{G^*_{aged\ binder}}{G^*_{unaged\ binder}} \tag{2-9}$$

$$PAI = \frac{\delta_{aged\ binder}}{\delta_{unaged\ binder}} \tag{2-10}$$

2.11.3 Indirect Tensile Cracking Test (IDEAL-CT)

The IDEAL-CT stands out as an innovative test method designed to accurately assess asphalt mixture fatigue cracking [111]. It offers a straightforward, convenient, and efficient testing approach that eliminates the need for complex specimen preparation involving cutting, gluing, drilling, notching, or instrumentation. Notably, the IDEAL-CT demonstrates a significantly lower coefficient of variation when compared to conventional repeated load cracking tests [112]. The testing procedure, outlined in ASTM D8225-19 [113], involves the use of a UTM. A Superpave gyratory compacted cylindrical specimen, with a diameter of 150 ± 2 mm and a thickness of 62 ± 1 mm (for mixtures with a nominal maximum aggregate size (NMAS) of 19 mm or less), is

centrally positioned in the fixture, as depicted in Figure 2-12(a). The test fixture incorporates a load cell, loading strips measuring 19.05 ± 0.3 mm in width, a data collection system, and specimen deformation measurement tools. To make sure all contact surfaces are clear of debris and clean, the fixture needs to be inspected.

The standard intermediate test temperature is set at 25 °C, and the preconditioning of the test specimen involves placing it in an environmental chamber for 2 h ± 10 min. Alternative intermediate test temperatures can be calculated based on the PG of the asphalt binder as per Equation 2-11:

$$\text{PG IT} = \frac{\text{PG HT} + \text{PG LT}}{2} + 4 \qquad (2\text{-}11)$$

where:

    PG IT = intermediate PG temperature (°C),

    PG HT = climatic high PG temperature (°C), and

    PG LT = climatic low PG temperature (°C).
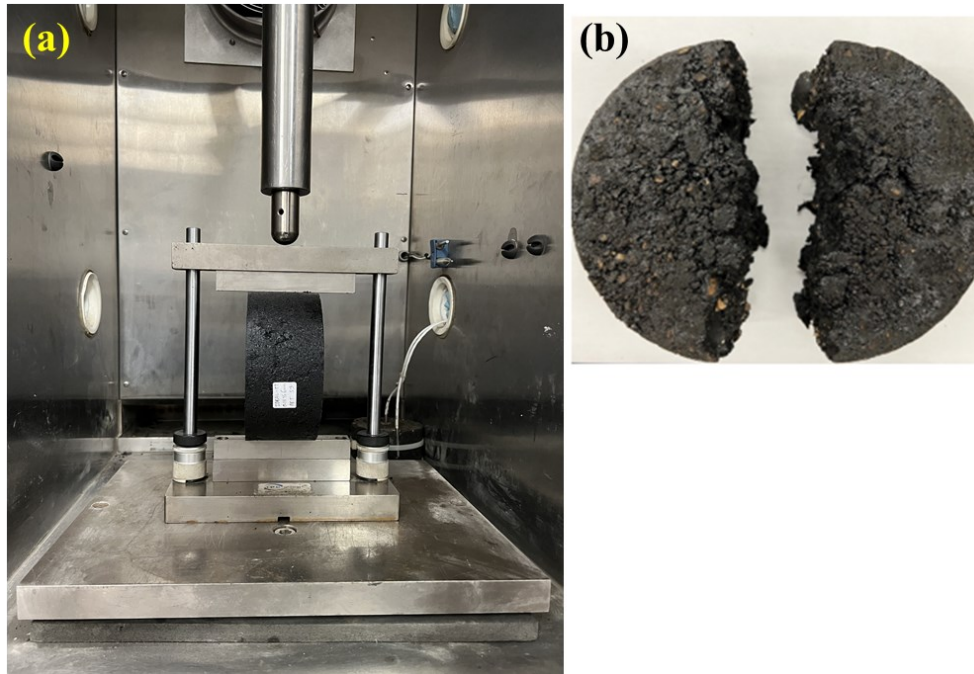
Figure 2-12. Test specimen (a) Inside the UTM chamber, (b) After the test

The application of load maintains a consistent load-line displacement (LLD) rate of 50 ± 2 mm/min throughout the test, with the test being stopped once the load drops below 100 N. A cracked sample after the test is done is presented in Figure 2-12(b). The time, load and LLD are measured at a minimum rate of 40 sampling data points per second throughout the entire test duration for a smooth load-LLD curve (Figure 2-13). This test procedure takes into account both the initiation and propagation of cracks in asphalt mixtures.
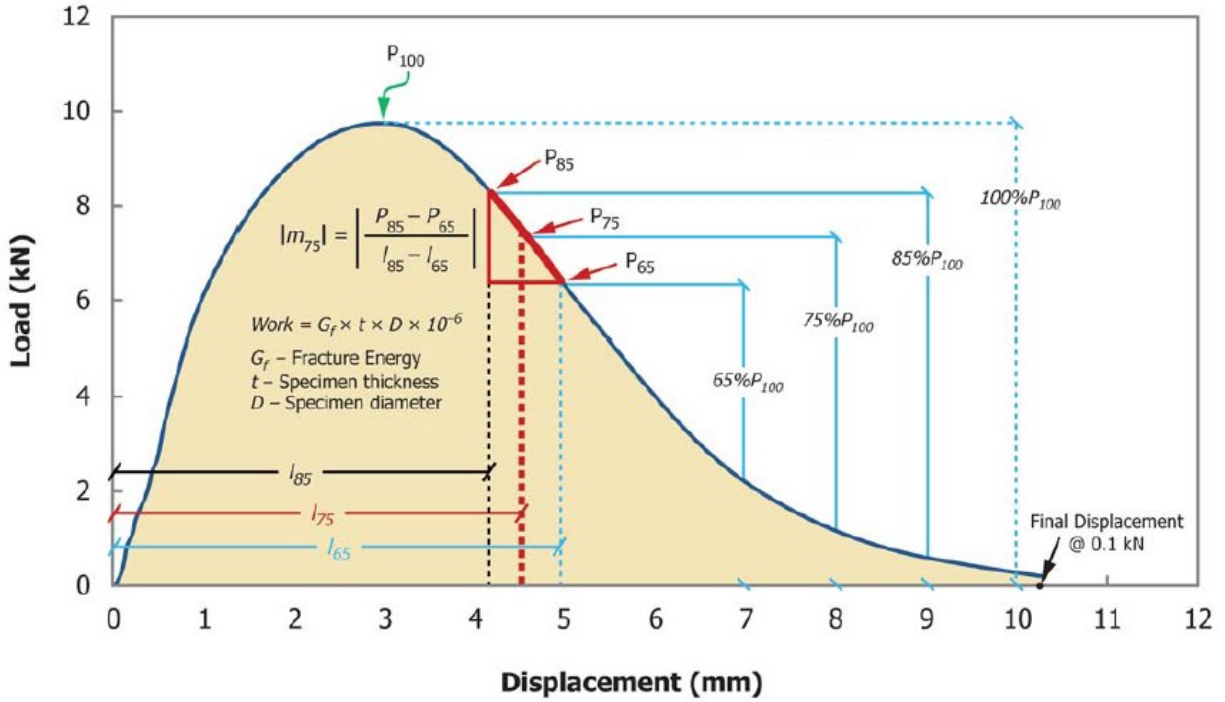
Figure 2-13. A load vs displacement graph [113]

FE can be obtained by calculating the area under the load-displacement graph using Equation 2-12. The CT_{Index}, a cracking resistance performance indicator of asphalt mixtures with good correlations with the fatigue life of the asphalt binders, can be calculated using Equation 2-13 [113], [114].

$$G_f = \frac{W_f}{D \times t} \times 10^6 \tag{2-12}$$

where:

   G_f = FE (J/m^2),

   W_f = work of failure (J),

   D = diameter (mm) of the specimen, and

   t = thickness of the specimen (mm).

$$CT_{Index} = \frac{t}{62} \times \frac{l_{75}}{D} \times \frac{G_f}{|m_{75}|} \times 10^6 \tag{2-13}$$

where:

CT_{Index} = cracking tolerance index,

$|m_{75}|$ = absolute value of the post-peak slope m75 (N/m),

l_{75} = displacement at 75% the peak load after the peak (mm), and

$\dfrac{t}{62}$ = unitless correction factor for specimen thickness.

ASTM D6931-17 [115] outlines the Equation 2-14 for the evaluation of ITS for the asphalt mixes.

$$ITS = \frac{2000.P}{\pi.t.D} \qquad\qquad (2\text{-}14)$$

where:

ITS = indirect tensile strength (kPa), and

P = maximum load (N).

Chapter 3. Exploring the Influence of Asphaltenes on Rheology and Aging Characteristics of Asphalt Binders

3.1 Abstract

Asphalt pavement, crucial for road infrastructure in Northern America, faces challenges like rutting, reduced elasticity, and aging in binders, necessitating sustainable solutions. This study explored asphaltenes, an oil refinery by-product, as an additive for asphalt binder modification, utilizing two distinct binder types. The goal was to evaluate the rutting resistance, elasticity improvement and aging resistance performance of asphalt binders modified with an optimal concentration of asphaltenes. Binders, both neat and modified with an optimum asphaltenes concentration of 12% (by weight of binder), underwent multiple stress creep recovery (MSCR) and frequency sweep (FS) tests. MSCR test results revealed that asphaltenes-modified binders had reduced non-recoverable creep compliance (J_{nr}), meeting requirements for extremely heavy traffic conditions with J_{nr} values being lower than 0.5 kPa^{-1}. Stress sensitivity was notably reduced, emphasizing the stabilizing effect of asphaltenes. FS test results indicated improved stiffness, rutting resistance, and aging resistance, underscoring the promising use of asphaltenes in sustainable asphalt binder modification.

3.2 Introduction

Asphalt concrete easily surpasses the quality of the most used pavement surfaces, and around 90% of the paved roads in the Northern America are constructed of asphalt concrete [116]. Asphalt concrete consists of mineral aggregates glued together with asphalt binder. The asphalt binder is a by-product derived from the petroleum-refining system, which also produces gasoline, diesel fuel, lubricating oil, and various other petroleum-based products. Asphalt binder as an integral part of asphalt concrete, plays an important role in the performance and longevity of asphalt paved roads. In order to ensure good performance, the properties of the asphalt binders must be controlled carefully. However, different challenges including rutting, reduced elasticity, and susceptibility to

aging of asphalt binder continue to pose threats in the field of asphalt pavement engineering [117]–[119].

Asphalt pavement rutting is a significant form of distress influenced by factors such as high pavement temperatures, high traffic volumes, heavy axle loads, slow-moving traffic, and insufficient resistance to rutting in asphalt binders or mixes [120]. The development of rutting in asphalt pavement is a result of a combination of densification and shear deformation, manifesting as depressions along the wheel paths and minor upheavals at the edges [121]. The elastic property of asphalt binder poses a considerable impact on the overall structural integrity of the asphalt pavement, where the binders with lower elasticity are more prone to cracking and can also contribute to severe rutting [119].

Another noteworthy challenge in the asphalt pavement is the aging of the asphalt binder, which can negatively impact the rheological properties of the binder, ultimately causing decline in mixture performance. The aging process of asphalt binders is influenced by several factors, including oxidation, volatilization, polymerization, thixotropy, syneresis and separation. It is to be noted, the rate of aging is more severe during the production and construction phase of the mixture (short-term aging) due to exposure to high temperature [122], [123].

In search of effective solutions to address these drawbacks, previous studies looked into different binder additives (e.g. polymer modifier, nanoclay, wax additive, and asphaltenes) that can be used for asphalt binder modification, to enhance crucial binder properties [77], [124]–[128]. However, in light of growing public concerns regarding sustainability, and considering the substantial cost associated with some modifiers, researchers are currently more focused on the utilization of waste materials to enhance asphalt binder properties [129], [130]. Asphaltenes is considered a by-product

generated at a significant rate in crude oil refineries through the process of deasphaltation, with an estimated production rate of 17.5% of asphalts in northern Alberta facilities of Canada [131].

There are two approaches available for incorporating asphaltenes into the asphalt binder. The initial method involves the use of a mechanical stirrer to blend the asphalt binder with materials rich in asphaltenes [74], [78]. The other method is to reintroduce the asphaltenes, which have been extracted from the asphalt binder using n-heptane, back into the binder [57]. Asphaltenes certainly plays a vital role in the traditional viscoelastic behaviour, contributing to the elasticity and stiffness of a binder [16]. However, the dosage at which asphaltenes are added into the asphalt binder is crucial because an increase in asphaltenes content leads to higher stiffness and elasticity in the binder. An excessive rise in stiffness adversely impacts the cracking resistance property at lower temperature. Furthermore, a higher asphaltenes content can also create stability issues in the asphalt binder [77]. Other waste additives, including waste polyethylene, rubber, packaging tape, cooking oil, and lignin have been used to alter the rheological properties of the asphalt binders in the recent past years [130], [132]–[134].

Literature study revealed that more research should be conducted to bridge the gap in rutting resistance, elasticity performance, and aging behavior of asphalt binders modified with asphaltenes. Consequently, our study aimed to contribute valuable insights to the existing literature by providing a comprehensive understanding of how the introduction of asphaltenes can strengthen the asphalt binder network, ultimately improving its resistance to rutting and aging, while enhancing overall elasticity.

3.3 Objectives

The primary goal of this research was to explore the potential use of asphaltenes, a waste material, as an additive for asphalt binder modification, utilizing two distinct types of binders. By adopting

different binder testing programs, this study focused on to reveal the impact of asphaltenes content in enhancing key asphalt binder properties, such as elasticity, rutting resistance, and aging resistance. By investigating the effectiveness of asphaltenes, this study makes a meaningful contribution toward sustainable practices in asphalt pavement construction. This has the potential to reduce the need for more conventional additives and promote environmentally friendly alternatives.

3.4 Methodology

In the initial phase of this experimental study, two distinct types of binders, labeled A and B, were chosen for modification with asphaltenes. In order to select the optimum asphaltenes content, PG, SARA analyses were conducted on the neat and those modified with varying percentages of asphaltenes for binder A. The asphalt binders were then subjected to short-term aging using a rolling thin film oven (RTFO). Subsequently, MSCR and FS tests were performed using a DSR device on both unmodified binders and those modified with optimum asphaltenes content for binders A and B. It is worth noting that MSCR tests were performed on the RTFO-aged samples only, while FS tests were conducted on both unaged and RTFO-aged samples. Average non-recoverable creep compliance (J_{nr}), average percent recovery (R), and stress sensitivity indices ($J_{nr\ diff}$, and $J_{nr\ slope}$) are the results calculated from MSCR tests, while FS tests were used to generate master curves for complex shear modulus (G^*) and phase angle (δ). Additionally, the rutting parameter ($G^*/\sin[\delta]$) and aging indices were determined through FS tests. Figure 3-1 shows the methodological steps adopted in this study.
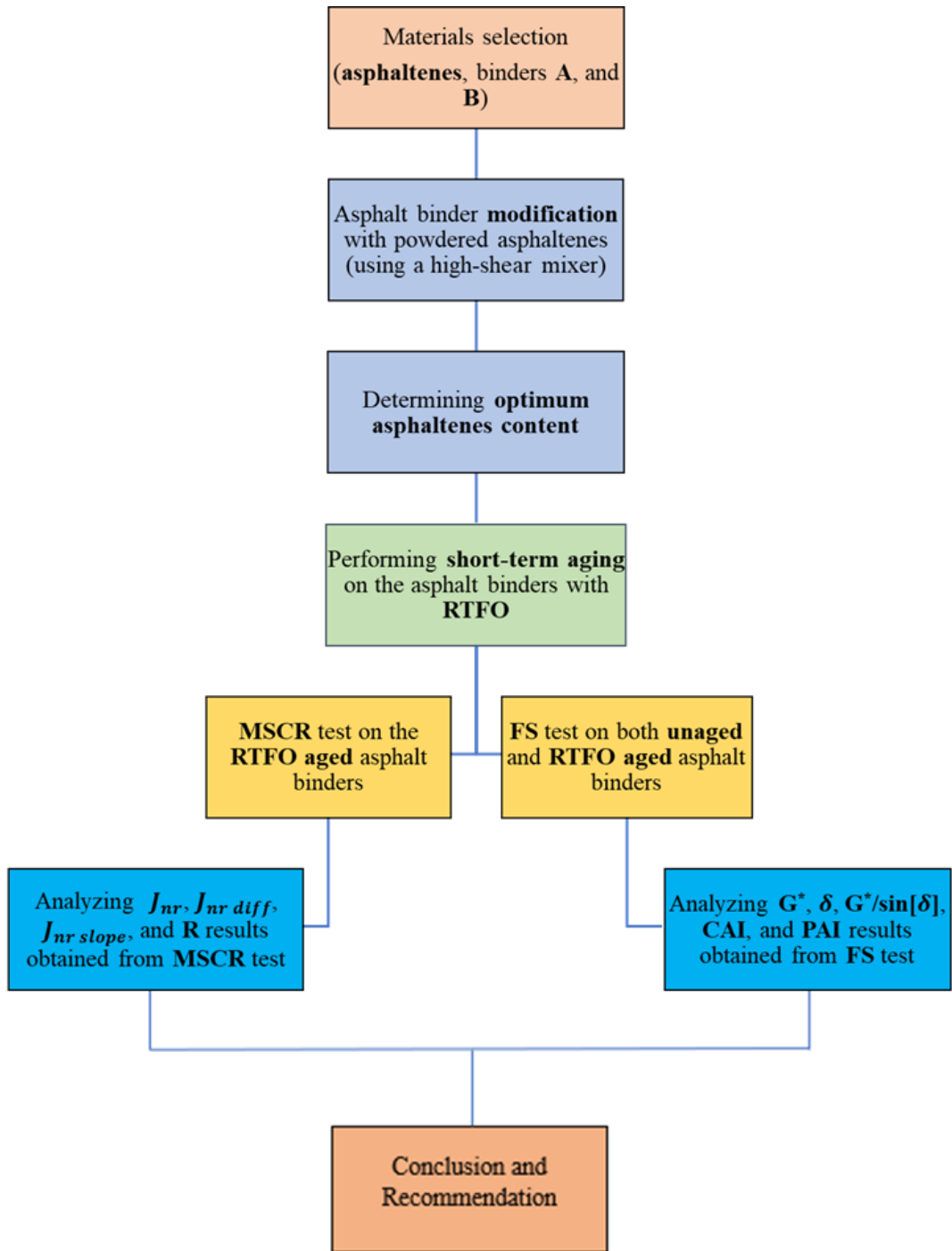
Figure 3-1. Methodological flowchart

3.5 Materials and Experiments

3.5.1 Materials

In this research, the used asphalt binders were designated as A and B. Binder A is derived from crude oil and is commercially provided by Husky Energy. On the contrary, Binder B is obtained from Alberta oilsands bitumen, and it is currently under study. The standard PG of neat binder A was 70-22, while the true PG was 70.2-25.9. For neat binder B, on the other hand, the standard and true PG were 64-22, and 69-26.6, respectively. The asphaltenes additive, was sourced as a waste by-product from Alberta oil-sand bitumen. Initially in solid form (Figure 3-2(a)), the material was turned into powder form by grinding and sieving through a No. 100 sieve with a mesh size of 150 μm. The four fractions, namely saturates, aromatics, resins, and asphaltenes (SARA) of the asphaltenes were determined, revealing that the majority was constituted by asphaltenes at 79.62%, while saturates comprised 6.85%, aromatics made up 9.68%, resins formed 3.85%. Powdered asphaltenes were blended with asphalt binders using a high shear mixer (Figure 3-2(b)), operated at a speed of 2,000 rpm for 60 min at a temperature of 140 °C.
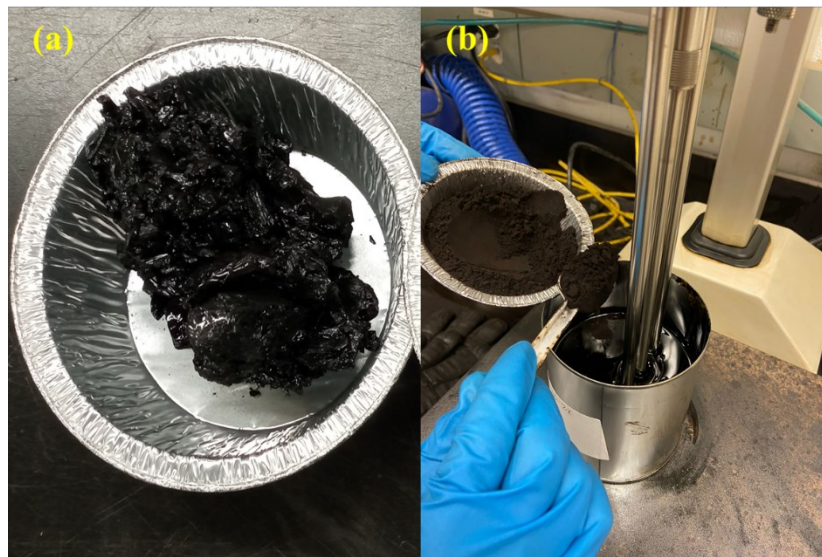
Figure 3-2. (a) Solid asphaltenes, and (b) Asphalt binder modification with a high shear mixer

3.5.2 Optimum Asphaltenes Content

The investigation for the optimal asphaltenes content in asphalt binder modification was adopted from a study conducted by Ghasemirad, Bala, and Hashemian in 2020 [77], driven by the findings obtained through both PG and SARA analyses. The intention was to refine the asphalt binder properties and select the ideal asphaltenes content in achieving improved performance characteristics.

3.5.2.1 PG Analysis

In order to get the high PG of 82 °C, required for the preparation of high-performance asphalt concrete (HPAC) in the other phase of this research, binder A was modified with different concentrations (0 to 20% with 3% interval) of asphaltenes (by weight of asphalt binder). DSR tests were carried out on the binders to assess their high PG characteristics as per AASHTO T315-16 [41], and the results are detailed in Table 3-1. It can be observed that there was a consistent increase in high PG with the progressive addition of asphaltenes, indicating an improvement in the stiffness of the asphaltenes-modified binders. Interestingly, each 6% increment in asphaltenes content corresponded to a one-interval rise in the high PG of the asphalt binders. The required high PG of 82°C was achieved with 12%, 15%, 18%, and 20% concentrations of asphaltenes. According to Ghassemirad et al. [94], a selected gradation combined with a binder of 82 °C high PG meets one of the principal specifications of high-modulus asphalt concrete, and this criterion is adopted in HPAC preparation as well.

Table 3-1. High PG results for binder A with different asphaltenes concentration

Binder A + % Asphaltenes (by weight of binder)	True High PG (°C)	Standard High PG (°C)
0% Asph.	70.2	70
3% Asph.	73.9	70
6% Asph.	76.5	76
9% Asph.	81.1	76
12% Asph.	82.9	82
15% Asph.	85.9	82
18% Asph.	88.0	88
20% Asph.	89.9	88

3.5.2.2 SARA Analysis

SARA analysis was performed on the neat binder A and some selected asphaltenes-modified binders with which the required high PG was achieved. The process involved initial separation of asphaltenes from the sample using n-heptane as the solvent, following ASTM D6560-17 [58]. Afterwards, the maltenes (saturates, aromatics, and resins) fractions were determined through clay-gel adsorption chromatography, as outlined in ASTM D2007-19 [61]. In addition, the colloidal index (CI) values for the asphalt binders were calculated using Equation 3-1.

$$CI = \frac{Saturates\ (\%) + Asphaltenes\ (\%)}{Resins\ (\%) + Aromatics\ (\%)} \qquad (3\text{-}1)$$

Table 3-2. SARA and CI results for chosen asphalt binders A

Binder A + % Asphaltenes (by weight of binder)	Saturates (%)	Aromatics (%)	Resins (%)	Asphaltenes (%)	Polar Fraction	Non-polar Fraction	CI
0% Asph.	25.41	20.36	31.58	22.59	54.17	45.77	0.92
12% Asph.	21.63	20.94	24.75	32.17	56.92	42.57	1.18
18% Asph.	18.83	20.25	25.23	35.16	60.39	39.08	1.19
20% Asph.	17.93	19.74	21.57	39.76	61.33	37.67	1.40

As presented in Table 3-2, there was a rise in polar fraction values of the asphalt binders with the addition of asphaltenes, which is responsible for increased stiffness, viscosity, and elasticity of the asphalt binders [77]. In terms of stability, the asphaltenes fraction within the maltenes matrix tends to be unstable when the CI value exceeds 1.2, as indicated by Lesueur [65]. It was observed that

the addition of asphaltenes increased the instability, and the asphalt binder modified with 20% asphaltenes demonstrated least stability with a CI value of 1.4.

Therefore, taking into account the analyses of both PG and SARA results, it can be concluded that a concentration of 12% asphaltenes is ideal for asphalt binder modification. This concentration achieves the necessary high PG while simultaneously maintaining the stability of the asphalt binder.

The asphalt binder labeled B was then modified with a concentration of 12% asphaltenes, resulting in a true PG of 82-21.9. Asphalt binder A when combined with 12% asphaltenes had a true PG of 82.9-21.8, while both binder A and B modified with optimal asphaltenes content exhibited an identical standard PG of 82-16. This indicates that the rate at which the high temperature PG improved (increase in high PG by 12 °C for binder A, and 18 °C for binder B) with the addition of asphaltenes at the optimal concentration was greater than the adverse effect observed in the low temperature PG (increase in low PG by 6 °C).

3.5.3 Rolling Thin Film Oven (RTFO) Aging

The RTFO aging is carried out for the laboratory simulation of the short-term aging of asphalt, reflecting the conditions during the production and compaction of HMA mixtures, utilizing a rolling thin film oven (RTFO) as per AASHTO T240-17 [38]. During this process, glass containers designed for RTFO were filled with asphalt binder samples, each weighing approximately 35 ± 0.5 g. The glass containers were rotated and allowed to cool in a rack for 60-min before being placed in the RTFO carriage inside the oven. To facilitate the aging process, each container was placed in such a way that the top opening faced a directed air supply within the oven. The oven was then sealed and a temperature of 163 °C was maintained, while the carriage was rotating at a constant speed of 15 rev/min throughout the 85-min aging duration.

3.5.4 Multiple Stress Creep Recovery (MSCR) Test

The MSCR test is widely recognized as the most reliable method to assess the high-temperature performance of asphalt binders [135], [136]. In this study, both neat and asphaltenes-modified (with optimum asphaltenes content) binders for types A and B were subjected to MSCR test to determine the average non-recoverable creep compliance and percent recovery using a DSR device, following the guidelines outlined in AASHTO T350-19 [99]. It was intended for use with the RTFO aged residue at a specified temperature, applying two stress levels of 0.1 kPa and 3.2 kPa over ten cycles of creep stress and recovery. The chosen testing temperature for this study was 64 °C, which corresponds to the lowest high PG of the studied asphalt binders and is closer to the temperature range at which rutting occurs in the field [97], [100]. The test was operated using a 25-mm plate geometry with 1-mm gap setting. The average non-recoverable creep compliance (J_{nr}) values can be calculated using Equation 3-2 and 3-3, at stress levels of 0.1 and 3.2 kPa, respectively.

At 0.1 kPa:

$$J_{nr_{0.1}} = \frac{SUM[J_{nr}(0.1,N)]}{10} \text{ for N = 11 to 20} \tag{3-2}$$

where,

      N = cycles.

At 3.2 kPa:

$$J_{nr_{3.2}} = \frac{SUM[J_{nr}(3.2,N)]}{10} \text{ for N = 1 to 10} \tag{3-3}$$

Additionally, the average percent recovery (R) results at 0.1 and 3.2 kPa stress levels were evaluated through Equation 3-4 and 3-5, respectively.

At 0.1 kPa:

$$R_{0.1} = \frac{SUM[\epsilon_r(0.1,N)]}{10} \text{ for N = 11 to 20} \tag{3-4}$$

where,

ϵ_r = The strain value at the end of the recovery portion.

At 3.2 kPa:

$$R_{3.2} = \frac{SUM[\epsilon_r(3.2,N)]}{10} \text{ for N = 1 to 10} \tag{3-5}$$

The stress sensitivity of the asphalt binders can be evaluated using Equation 3-6 following AASHTO T350-19 [99], where $J_{nr\ diff}$ is the difference between the J_{nr} values at stress levels of 3.2 kPa and 0.1 kPa. Moreover, a modified stress sensitivity evaluation index ($J_{nr\ slope}$) proposed by Stempihar, Gundla, and Underwood [137] was calculated using Equation 3-7.

$$J_{nr\ diff} = \left(\frac{J_{nr}3.2 - J_{nr}0.1}{J_{nr}0.1}\right).100\% \tag{3-6}$$

$$J_{nr\ slope} = \left(\frac{J_{nr}3.2 - J_{nr}0.1}{3.1}\right).100\% \tag{3-7}$$

3.5.5 Frequency Sweep (FS) Test

The FS test is conducted using a DSR device within the linear viscoelastic (LVE) range of the asphalt binders to assess their viscoelastic properties at various temperatures and frequencies. Complex shear modulus (G^*) and phase angle (δ) master curves can be developed through the application of time-temperature superposition (TTSP) principle by horizontally shifting the test results from each isothermal frequency sweep with respect to one reference temperature [16], [106]. In this particular study, the FS test was carried out over a frequency range of 0.1 rad/s to

100 rad/s at different temperatures on both the unaged and RTFO aged asphalt binders. A DSR test setting of 8-mm plate geometry with 2-mm gap was selected for the lower temperatures ranging from 4 to 30 °C, while a 25-mm plate with 1-mm gap test setting was used for higher temperatures (30 to 88 °C) depending on the high PG of the binder. This specific choice of test setting was made to remove the torque measurement inaccuracies and avoid erroneous phase angles [105].

The strain applied for the test was set at 0.5% within the LVE range, and this value was determined through a linear amplitude sweep test prior to the FS test. The G^*, δ master curves were developed at a reference temperature of 25 °C using TTSP principle, as this temperature was successfully applied in the investigation of asphalt binder fatigue behavior [138]. Furthermore, the complex shear modulus aging index (CAI) and phase angle aging index (PAI) were calculated using Equation 3-8 and 3-9, respectively.

$$CAI = \frac{G^*_{aged\ binder}}{G^*_{unaged\ binder}} \tag{3-8}$$

$$PAI = \frac{\delta_{aged\ binder}}{\delta_{unaged\ binder}} \tag{3-9}$$

3.6 Results and Discussion

3.6.1 Multiple Stress Creep Recovery (MSCR) Test Results

3.6.1.1 Average Non-recoverable Creep Compliance

The MSCR test can be used to evaluate the rutting properties of both unmodified and modified binders, and it has the capacity to establish a considerably better correlation to mixture rutting compared to the Superpave binder criteria [139]. As shown in Figure 3-3, at a stress level of 0.1 kPa, the J_{nr} value for binder A decreased by 87.8% following asphaltenes-modification, and at the 3.2 kPa stress level, the J_{nr} value dropped by 88.5%. A comparable pattern can be observed for

binder B, where the J_{nr} values minimized by 83.2%, and 83.6% at stress levels of 0.1 kPa, and 3.2 kPa, respectively, after asphaltenes-modification. A reduced J_{nr} value indicates a slower rate of deformation, implying enhanced elasticity and increased resistance to rutting [140]. This suggests that the stability of the asphalt binders against rutting was strengthened after the introduction of asphaltenes.
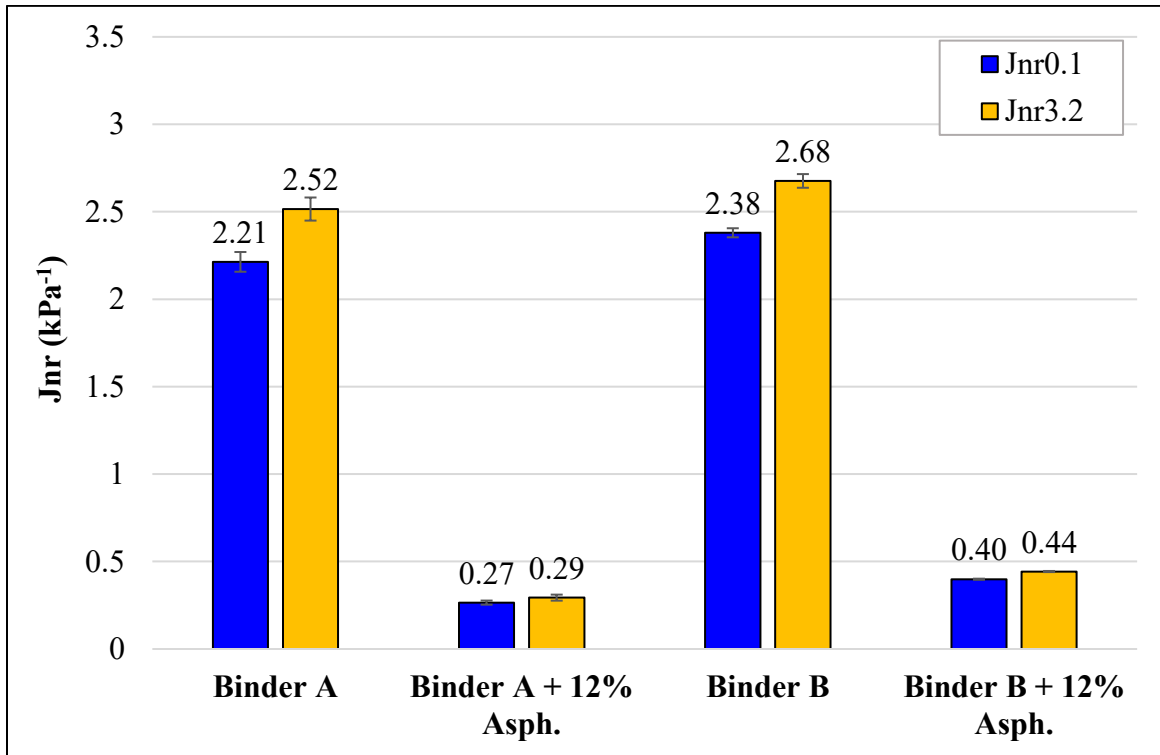
Figure 3-3. Comparison of J_{nr} results at two stress levels of 0.1 kPa and 3.2 kPa

The neat binders A and B met the criteria for the standard traffic 'S' grade (as, 2 kPa^{-1} < J_{nr}3.2 ≤ 4.5 kPa^{-1}), while both the asphaltenes-modified binders satisfied the requirements for the extremely heavy traffic 'E' grade (as, J_{nr}3.2 ≤ 0.5 kPa^{-1}), as outlined in AASHTO M332-20 [141]. The 'S' grade designation is typically applicable for traffic levels less than 10 million equivalent single axle loads (ESALs) and traffic speeds surpassing 70 km/h. On the other hand, the 'E' grade designation is generally for traffic levels more than 30 million ESALs and standing traffic with speeds less than 20 km/h.

3.6.1.2 Stress Sensitivity
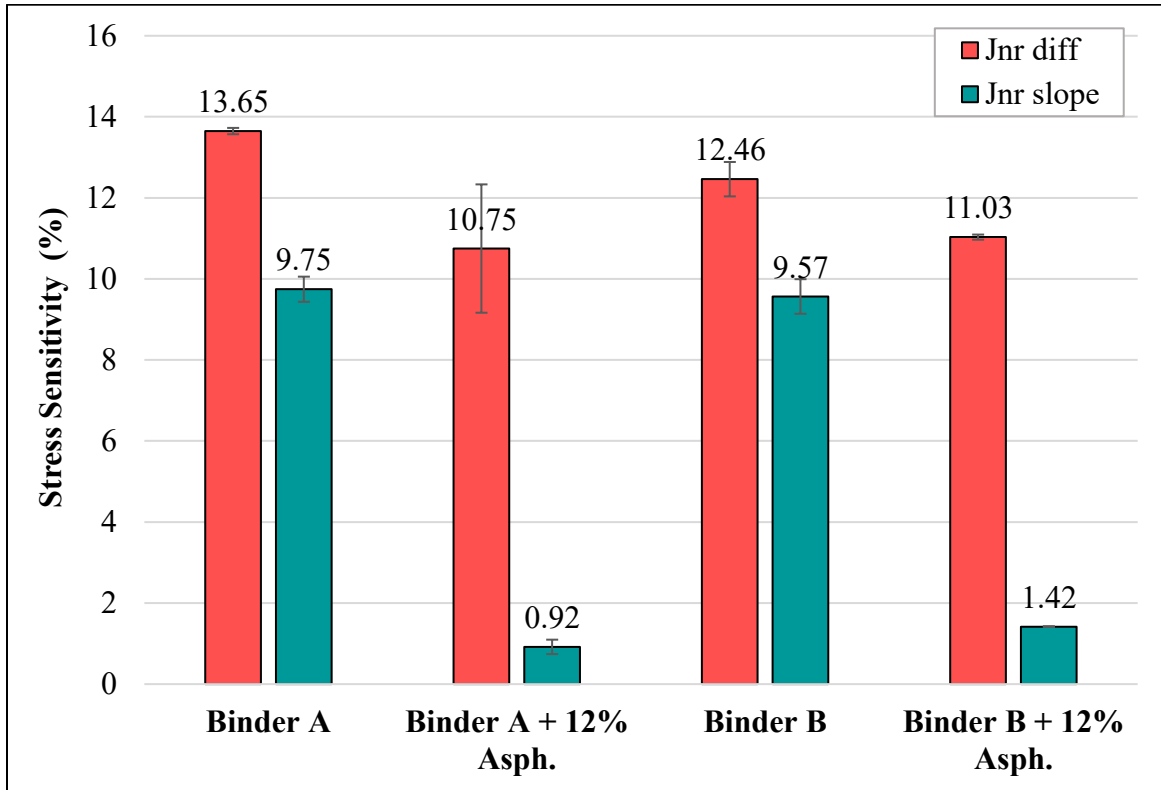
Figure 3-4. Comparison of stress sensitivity of neat and asphaltenes-modified binders

From Figure 3-4, it can be observed that the $J_{nr\,diff}$ values were less than 75% for all the binders, thereby meeting the AASHTO M332-20 [141] requirement for stress sensitivity. Furthermore, it is apparent that the asphalt binders, when modified with asphaltenes, showed less stress sensitivity irrespective of their type. However, some studies have found that there is no significant correlation between $J_{nr\,diff}$ and rutting test results, and a new modified stress sensitivity evaluation index ($J_{nr\,slope}$) can better describe the relationship between the non-recoverable creep compliance variable and the rut variable [137], [142], [143]. The difference in $J_{nr\,slope}$ values between neat and asphaltenes-modified binders observed in this study aligns with this prior theory. Specifically, it is observed that after asphaltenes-modification, binder A demonstrated a 90.6% decrease in $J_{nr\,slope}$, and for binder B, $J_{nr\,slope}$ minimized by 85%. It is to be noted, lower $J_{nr\,slope}$ values

correspond to less stress sensitivity. This suggests that the asphaltenes-modified binders could maintain their stiffness and viscosity under high stress conditions, contributing to stable pavement performance.

3.6.1.3 Average Percent Recovery

Table 3-3. Average percent recovery results at 0.1 and 3.2 kPa stress levels

Binder types	R0.1 (%)	R3.2 (%)
Binder A	4.18	0.1
Binder A + 12% Asph.	22.46	16.28
Binder B	3.76	0
Binder B + 12% Asph.	18.23	11.58

Considering the results of average percent recovery, as presented in Table 3-3, it is evident that for asphaltenes-modified binder A the average percent recovery at 0.1 and 3.2 kPa stress levels was 22.46% and 16.28%, respectively. This is considerably higher compared to the unmodified binder A, which exhibited 4.18% at 0.1 kPa and 0.1% at 3.2 kPa. Similarly, for binder B, after asphaltenes modification, the average percent recovery was 18.23% and 11.58% at 0.1 and 3.2 kPa stress levels, respectively, whereas the neat binder showed 3.76% average percent recovery at 0.1 kPa stress with no recovery at the higher stress level of 3.2 kPa. This suggests an increase in the elastic recovery of asphalt binders with asphaltenes modification. Additionally, R0.1 of all binders was greater than R3.2, indicating that recovering the deformation of asphalt binder under high-stress horizontal shear is more challenging than that under low-stress horizontal shear.

3.6.2 Frequency Sweep (FS) Test Results

3.6.2.1 Complex Shear Modulus

The complex shear modulus master curves were developed for asphalt binders A (Figure 3-5(a)), and B (Figure 3-5(b)) under both unaged and RTFO aged conditions, at a reference temperature of 25 °C. Under unaged condition at a reduced angular frequency of 1 rad/s, asphaltenes-modified

binder A showed a 546% higher complex shear modulus compared to unmodified binder A, while

binder B, post-asphaltenes introduction, demonstrated an increase of 497% compared to the neat

binder B. Additionally, at the highest testing frequency of 100 rad/s, a 220% rise can be seen in the

complex shear modulus value for asphaltenes-modified binder A in comparison with unmodified

binder A, and asphaltenes-modified binder B showed a 202% increase compared to the unmodified

binder B. This considerable increase in complex shear modulus values throughout the entire

reduced angular frequency range for both asphalt binders A, and B could improve the rutting

resistance in the asphalt binders after asphaltenes-modification.
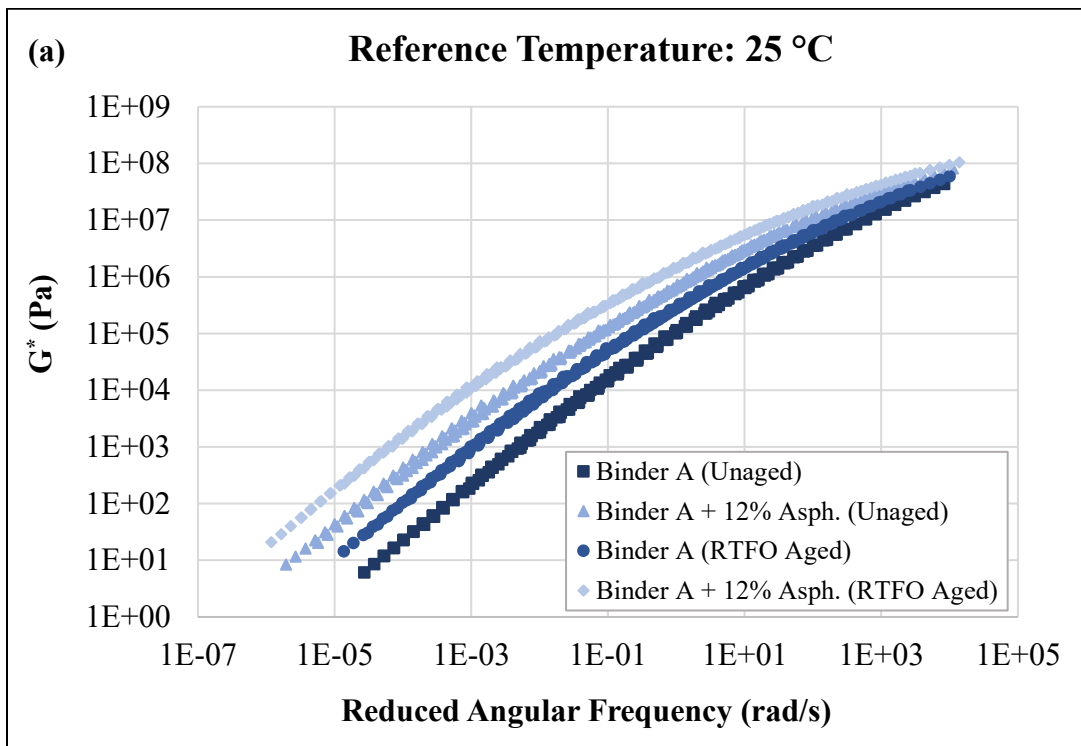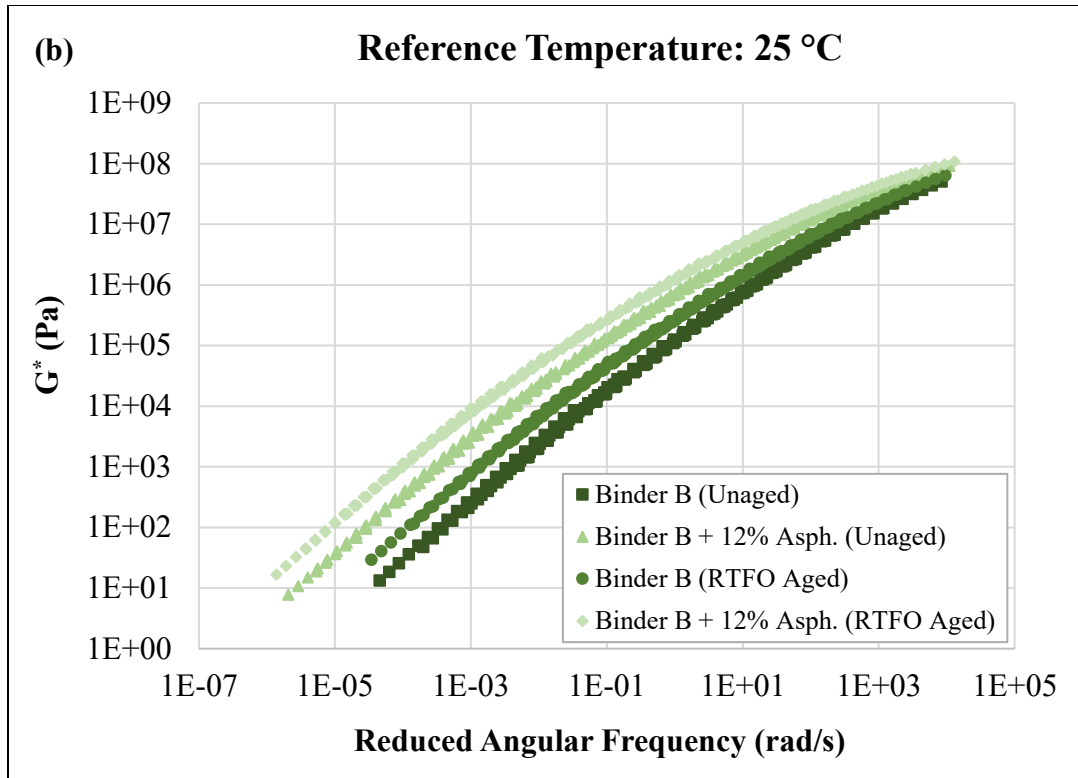
Figure 3-5. G^* master curves for (a) Binder A, and (b) Binder B

The complex shear modulus values were increased after the asphalt binders subjected to RTFO aging, reaching the highest level for the asphaltenes-modified RTFO-aged binders. Specifically, at a low frequency of 1 rad/s, RTFO-aged binder A, when modified with asphaltenes, demonstrated 118% higher complex shear modulus compared to the unaged asphaltenes-modified binder A. Similarly, for asphaltenes-modified binder B, the RTFO-aged sample exhibited a 78% jump when compared with unaged asphaltenes-modified binder B. This is evident that the asphalt binders became stiffer following RTFO aging. The increase in complex shear modulus values could be due to the greater stiffness of the asphalt binder resulting from the enhanced molecular structure brought about by the introduction of asphaltenes.

3.6.2.2 Phase Angle

Phase angle is an indicative of the viscoelastic behaviour of the asphalt binders. Analysis of the phase angle master curves, as shown in Figure 3-6(a) and Figure 3-6(b), reveals lower values for both asphaltenes-modified binders A and B compared to their respective unmodified counterparts. At a reduced angular frequency of 1 rad/s and unaged condition, asphaltenes-modified binder A had 16.5% lower phase angle value, compared to the unmodified binder A, while asphaltenes-modified binder B displayed a 15% drop compared to the neat binder B. Furthermore, both asphaltenes-modified binder A, and B exhibited a 22% lower phase angle in comparison with their respective unmodified binders at 100 rad/s reduced angular frequency. This strongly suggests a shift toward increased elasticity and reduced viscous behaviour in the binders following the inclusion of asphaltenes in response to the applied frequencies.
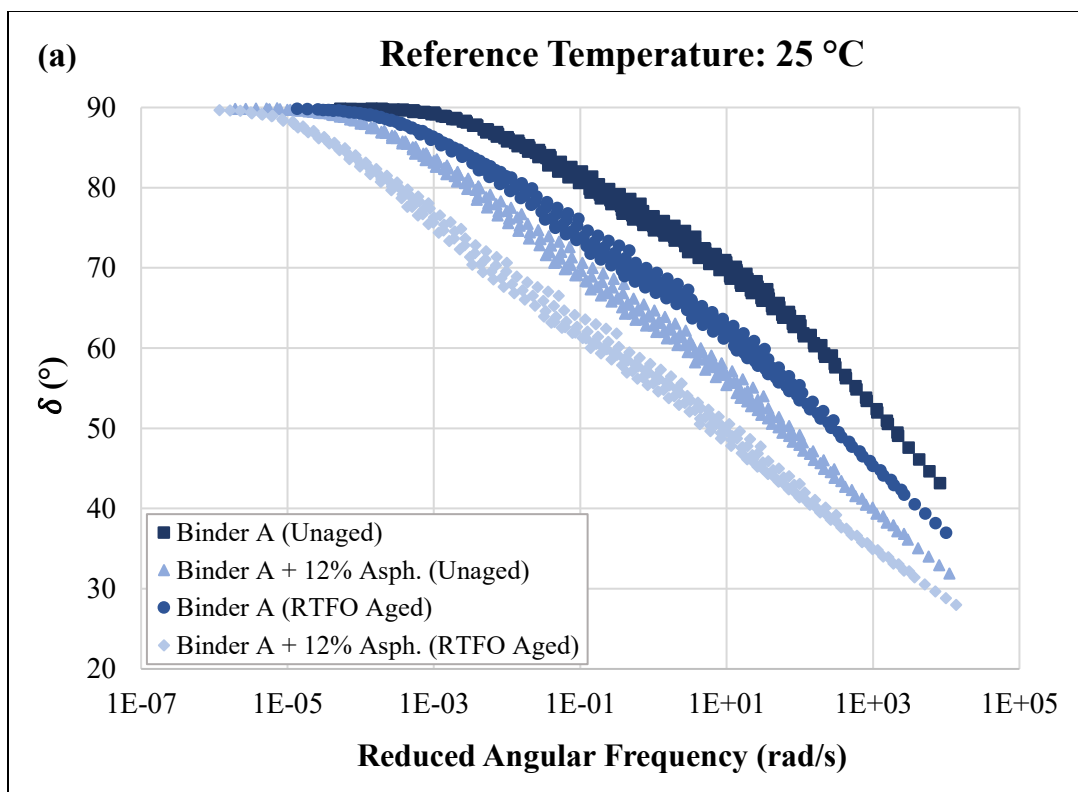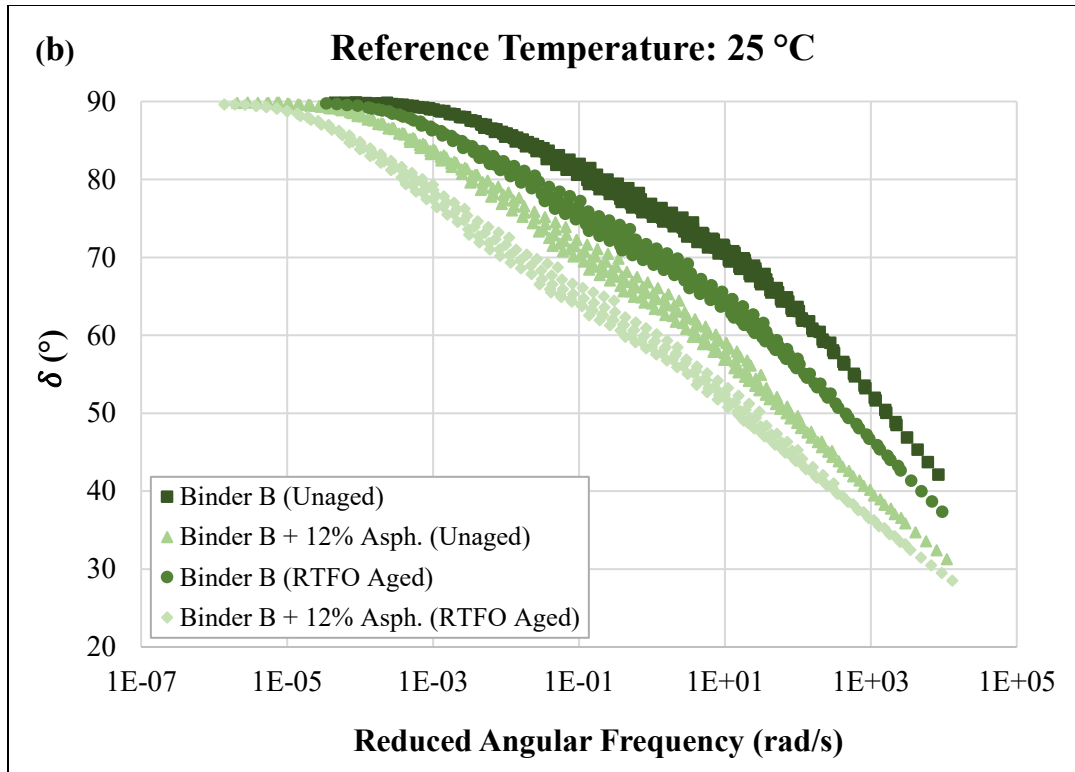
Figure 3-6. δ master curves for (a) Binder A, and (b) Binder B

At a low frequency, specifically 1 rad/s, it is noteworthy that the least phase angle values were evident in the case of asphaltenes-modified samples following RTFO aging. The asphaltenes-modified RTFO-aged binder A had a phase angle value of 55.57°, marking 12% reduction compared to the unaged sample of asphaltenes-modified binder A. Correspondingly, for RTFO-aged asphaltenes-modified binder B, the phase angle was lowered by 9% in comparison to the asphaltenes-modified binder B in unaged condition. The decreased phase angle values observed in the RTFO-aged samples indicate that the elasticity of the asphalt binders had increased after short-term aging.

3.6.2.3 Rutting Parameter

Lastly, to evaluate the performance of the asphalt binders in terms of rutting resistance post-asphaltenes modifications, a rutting parameter $G^*/\sin[\delta]$ was calculated and the findings are

presented in Figure 3-7(a) and Figure 3-7(b). It is to be noted, a higher $G^*/\sin[\delta]$ indicates greater rutting resistance. In an unaged state, the asphaltenes-modified binder A exhibited $G^*/\sin[\delta]$ values of 732 kPa at 1 rad/s and 15,355 kPa at 100 rad/s. These values were significantly higher when compared with neat binder A, which recorded 104 kPa at 1 rad/s and 4,065 kPa at 100 rad/s.

Comparably, when asphaltenes was introduced to binder B, there was a notable increase in $G^*/\sin[\delta]$, reaching 751 kPa and 16,667 kPa at 1 rad/s and 100 rad/s, respectively. In contrast, the unmodified binder B demonstrated lower $G^*/\sin[\delta]$ values of 117 kPa at 1 rad/s and 4,687 kPa at 100 rad/s. Post RTFO aging, the $G^*/\sin[\delta]$ values were considerably escalated for both binder types, with the highest values observed for asphaltenes-modified binders (1718 kPa for binder A and 1413 kPa for binder B at 1 rad/s). This underscores that asphaltenes-modified binders were more resistant to rutting when compared with neat binders. Moreover, the rutting resistance property of the asphaltenes-modified binders further increased following short-term aging.
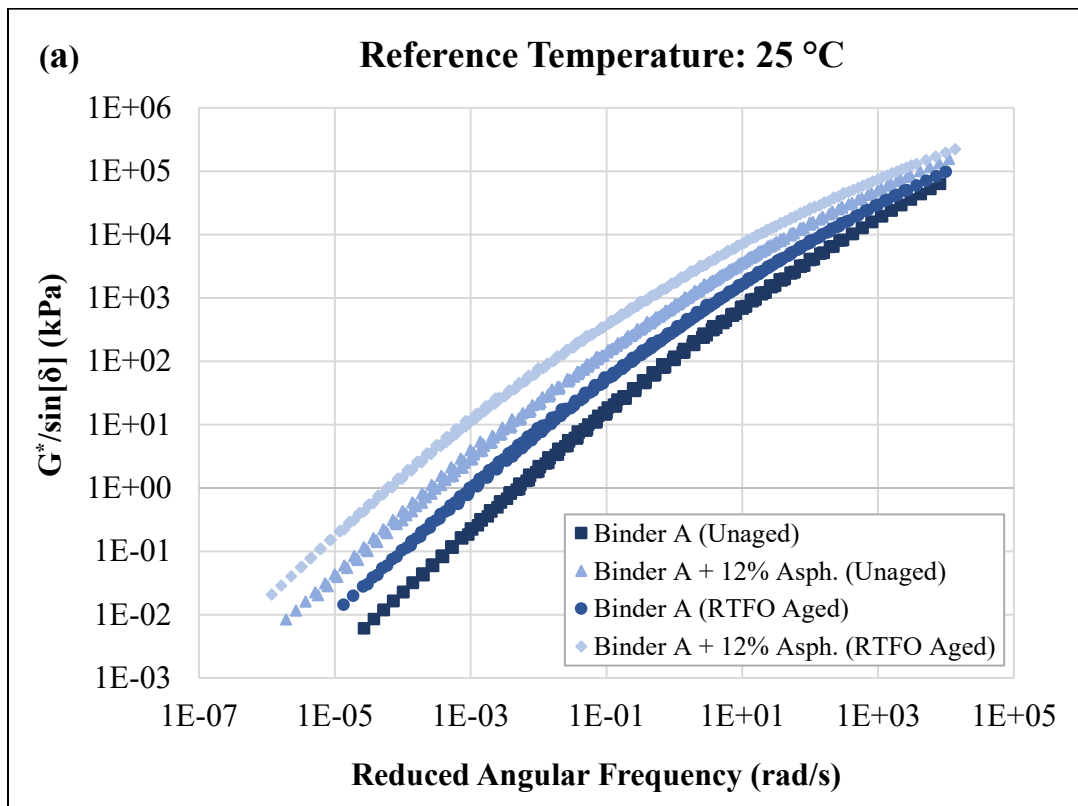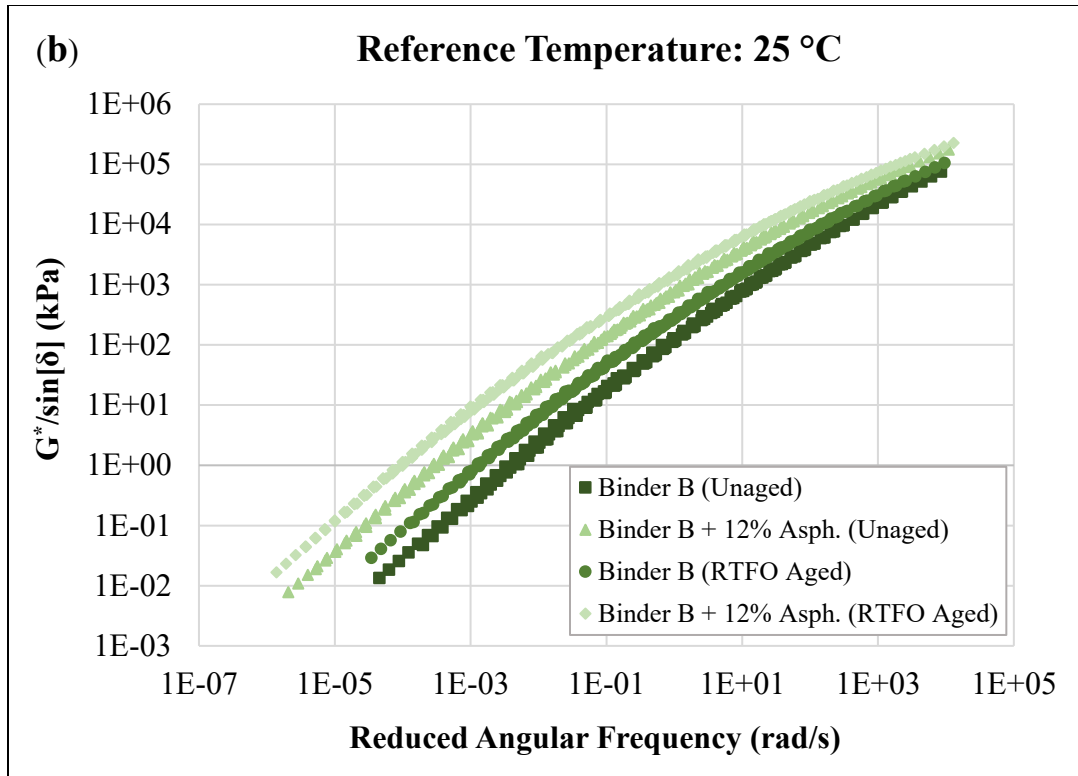
Figure 3-7. Rutting parameter results for (a) Binder A, and (b) Binder B

3.6.2.4 Aging Indices

To assess the impact of short-term aging on both neat and asphaltenes-modified binders, aging indices such as CAI and PAI were calculated at the reference temperature of 25 °C. It is to be noted, smaller CAI values indicate improved aging resistance, while a higher degree of aging is caused by smaller PAI values [144], [145]. As depicted in Figure 3-8, at 0.1 rad/s, asphaltenes-modified binder A had a CAI value of 2.63, which was lower than the unmodified binder A with a value of 3.27. This trend continued with increasing frequencies, reaching a 15% lower CAI value for the binder A with added asphaltenes compared to the unmodified binder A at the highest testing frequency of 100 rad/s. Asphaltenes-modified binder B, on the other hand, displayed 23% and 16% lower CAI values at 0.1 and 100 rad/s, respectively, compared to the unmodified binder B. Therefore, it is evident that the asphaltenes-modified binders, regardless of the binder source,

showed better short-term aging resistance for the entire angular frequency range when contrasted with neat binders as per the CAI results.
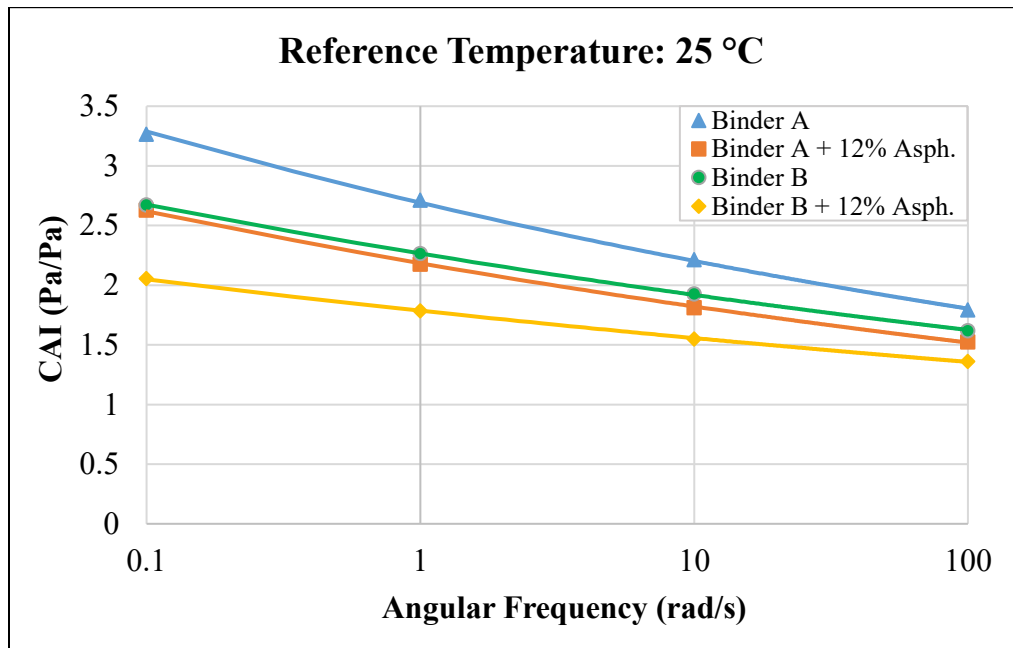
Figure 3-8. CAI graphs for the asphalt binders

Analyzing the PAI results presented in Figure 3-9, it is evident that at lower frequencies, the asphaltenes-modified binders had smaller PAI values compared to their unmodified counterparts, for both asphalt binders A and B. However, at the highest testing frequency of 100 rad/s, unmodified binders A and B had the PAI values of 0.87 and 0.89, respectively. After asphaltenes modification the PAI values for binders A and B increased to 0.88 and 0.91, respectively. Notably, the rate at which the PAI values decreased was considerably higher for both unmodified binders in comparison with modified binders. Considering the CAI and PAI results for the entire frequency range, the asphaltenes-modified binders were showing better resistance to short-term aging.
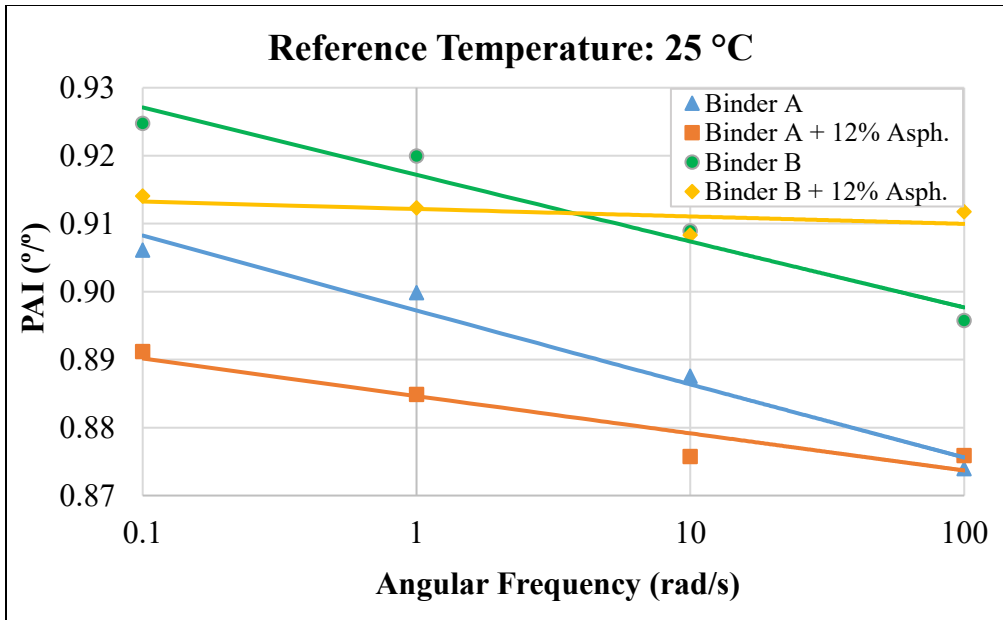
Figure 3-9. PAI graphs for the asphalt binders

An Analysis of Variance (ANOVA) on the aging indices was performed with a 0.05 significance level (α) to assess the statistical significance of differences. In ANOVA, the comparison of variability within group, specifically within asphaltenes content and frequency, against variability between groups was conducted to calculate F-values. For asphaltenes content, the F-critical value obtained was 9.277, and for frequency, it was 10.128. Analyzing the F-values for CAI, as shown in Table 3-4, it is evident that both asphaltenes content and frequency had values exceeding their respective F-critical values for binders A and B. This suggests a statistically significant impact of both asphaltenes content and frequency on CAI values. However, for PAI, the F-values were lower than their corresponding F-critical values for both asphaltenes content and frequency in binders A and B. This indicates that the differences in PAI values between neat and asphaltenes-modified binders were insignificant, and the impact observed for frequency was minor.

Table 3-4. ANOVA results for the aging indices

Aging index	Binder types	Asphaltenes content		Frequency	
		P-value	F-value[a]	P-value	F-value[b]
CAI	Binder A	0.011	32.888	0.005	48.014
	Binder B	0.011	32.328	0.013	24.256
PAI	Binder A	0.091	6.043	0.073	6.939
	Binder B	0.912	0.014	0.389	1.426

[a] F-crit (asphaltenes content) = 9.277. [b] F-crit (frequency) = 10.128.

3.7 Conclusion

This study investigated the impact of asphaltenes modification on the rheological and aging properties of asphalt binders, utilizing two distinct types of binders A and B. The results demonstrated a substantial improvement in elasticity, rutting resistance and short-term aging resistance of the asphalt binders post asphaltenes introduction. In context of the results obtained from PG and SARA analysis, MSCR, and FS tests the following conclusions can be inferred:

- The required high PG of 82 °C was successfully attained by incorporating 12% asphaltenes concentration without compromising the low-temperature performance of the asphalt binders. Additionally, the stability of the asphalt binders was maintained at this asphaltenes concentration based on the CI results.

- The average non-recoverable creep compliance (J_{nr}) values indicated a substantial decrease following asphaltenes modification for both types of binders, suggesting improved elasticity and enhanced rutting resistance. Notably, at the maximum stress level of 3.2 kPa, the lowest J_{nr} value of 0.29 kPa^{-1} was observed for asphaltenes-modified binder A. The modified binders met the requirement for the extremely heavy traffic 'E' grade, highlighting their potential to withstand high-stress conditions.

- All asphalt binders fulfilled the stress sensitivity criteria, exhibiting $J_{nr\ diff}$ values less than 75%. However, a modified stress sensitivity index $J_{nr\ slope}$ results made the comparison between neat and asphaltenes-modified binders more evident. Specifically, binders A and B showed 90.6% and 85% lower $J_{nr\ slope}$ values, respectively, after asphaltenes modification, signifying less stress sensitivity in the asphaltenes-modified binders.

- The outcomes of the complex shear modulus (G^*) master curves revealed a significant increase in stiffness for the binders modified with asphaltenes, particularly under RTFO aging. Higher G^* could enhance the binder ability to resist rutting. Furthermore, the reduced phase angle (δ) values of the asphaltenes-modified binders indicated a shift towards improved elasticity and reduced viscous property, providing further evidence of the positive effects of asphaltenes modification.

- Rutting parameter ($G^*/\sin[\delta]$) values displayed a remarkable surge for the modified binders, with the highest values being observed for RTFO-aged asphaltenes-modified binders, highlighting their superior ability to resist deformation.

- The asphalt binders showed enhanced resistance to aging following the introduction of asphaltenes. This could be attributed to the complex molecular structure and chemical composition of the asphaltenes, serving as both a reinforcing agent and antioxidant within the binder matrix. These properties contribute to the maintenance of the asphalt binder's structural integrity and the mitigation of detrimental effects from oxidation over time. However, statistical analysis confirmed that the differences observed in PAI values between unmodified and asphaltenes-modified binders were minimal.

For future research, it is recommended to prepare asphalt mixtures using asphaltenes-modified binders and assess their rutting performance using a Hamburg wheel-track machine. In addition, performance evaluation of the asphaltenes-modified binders at cold temperature conditions would contribute valuable insights to the field of asphalt materials engineering.

Chapter 4. Investigating the Influence of Polyethylene Terephthalate Fibres with Different Lengths on the Cracking Resistance of High-Performance Asphalt Concrete

4.1 Abstract

High-performance asphalt concrete is an innovative paving material that typically relies on the properties of polymer-modified asphalt binders. However, the application is limited due to their high cost and phase separation issues. A solution is explored in the present study by blending 12% asphaltenes and a straight-run asphalt binder with a true performance grade of 70.2-25.9, resulting in a true performance grade of 82.9-21.8, which elevates the binder's stiffness. Three lengths of polyethylene terephthalate fibres are used to improve the cracking resistance of these asphaltenes-modified mixes. An indirect tensile cracking test is conducted at 25 °C and 37 °C, revealing a significant improvement in cracking tolerance and failure energy, particularly at 37 °C. The CT_{Index} value peaked at 105 for 12-mm polyethylene terephthalate fabricated sample, while control asphaltenes-modified, 6-mm, and 18-mm polyethylene terephthalate fabricated samples achieved 61, 87, and 99, respectively, with failure energy increasing with longer fibres.

4.2 Introduction

A safe and efficient road network is essential to a country's economic prosperity, with flexible pavement being the most widely employed road surface in road networks around the world today. Increasing the lifespan of asphalt concrete roads and enhancing its mechanical properties are among the top priorities for transportation authorities. In Canada, the world's second-largest country by land area, connecting urban cities with rural areas requires a substantial pavement infrastructure. The combination of excessive traffic and various weather conditions creates premature distresses in the pavement, potentially reducing the service life if the pavement is not maintained properly. One common issue is cracking, often triggered by abrupt temperature changes and repetitive stress from vehicle traffic. Given the stresses to which pavements are

63

subjected, substantial financial resources are allocated annually for the purpose of rehabilitation and construction of new asphalt pavements [146].

Numerous studies have been conducted to enhance the overall performance of asphalt pavements by seeking alternative and innovative materials for modification, whether it be modification of the asphalt binder or of the asphalt mixture. Polymer-modified asphalt, for instance, represents a notable technological enhancement in road pavement in which polymers are blended into asphalt, resulting in a superior road construction material [147]. In recent years, the use of waste materials such as asphaltenes in asphalt binder modification has become increasingly popular due to its sustainability and cost reduction benefits. Asphaltenes have a relatively high rate of production in refineries and it offers potential applications in asphalt binder modification. Ghasemirad et al. in 2020, observed a significant improvement in the high-temperature Performance Grade (PG) of asphaltenes-modified binders compared to a base binder, high-temperature PG being indicative of resistance to permanent deformation [77]. Asphaltenes also enhance the elasticity and stiffness in the conventional viscoelastic properties of a binder. Moreover, it has been noted that the inclusion of asphaltenes as a separate modifier has the potential to improve characteristics such as viscosity, resistance to rutting, and stiffness of asphalt mastic [79]. However, polymer modification of asphalt binders can also result in stability issues, as the blend may experience phase separation when stored at high temperatures. This can be a challenge during transportation and application of the binder [148]. Moreover, the modification process is often costly, making polymer-modified binders considerably more expensive than unmodified binders.

The addition of fibres as a reinforcement in asphalt pavement has been in practice for many years, as per the National Cooperative Highway Research Program (NCHRP) Report 475 [149]. Traditionally, fibres have been used primarily to control the drain-down effect in asphalt cement,

but more recently the inclusion of fibres in asphalt mixes has emerged as a promising solution due to the excellent mechanical properties of fibres [150]. Fibres, when used in asphalt pavement, function as a bridge to distribute stress amid cracking effects [151]. The reinforcing effect of fibres in asphalt mixtures, it should be noted, depends on factors such as the mechanical properties (tensile strength) of the fibres, their physical dimensions (length and diameter), as well as their dispersion within the asphalt mixes. To ensure adequate bonds between fibres, binder, and aggregates, sufficient dispersion is crucial [152]. The concentration of fibre content is also of great significance, given that exceeding the optimal fibre content can lead to fibre clustering and result in undesirable outcomes [153]. The length of fibres can also affect the performance of asphalt mixes. Although it may be easier for shorter fibres to be incorporated into the mix than for longer fibres [154], the effect of the former on the asphalt mixes may not be substantial [155]. Longer fibres contribute to better interlocking among the components of asphalt concrete compared to shorter fibres [150]. On the other hand, the blending process and the interlocking of aggregates may be hampered by "balling" issues when the fibres are excessively long [156].

Polyethylene terephthalate (PET) is semi-crystalline, thermoplastic, and non-biodegradable polymer, originating from a group of polyesters and commonly present in municipal solid waste such as waste plastic bottles [157]. To produce PET fibres, plastic bottles are sorted, shredded, washed, and extruded. The extrusion process involves melting the plastic in a heated barrel and creating continuous synthetic fibres [82]. PET fibres are beneficial as an additive to asphalt pavement due to their strength and resistance to degradation, making them valuable as a reinforcement material in asphalt concrete. This is particularly important given the global increase in plastic waste and the urgent need for proper end-of-life management.

PET fibres generated from plastic waste have been used in various research studies either as a binder additive or as an asphalt mixture reinforcement to improve the mechanical performance of Hot Mix Asphalt (HMA) [158]. Underscoring another benefit of the use of fibres in asphalt, a recent study investigated the potential of recycled polyethylene terephthalate (PET) fibre to enhance the fatigue life of asphalt mixes [20]. Their findings indicated that the fatigue performance of asphalt mixtures reinforced with recycled PET fibre was considerably improved, particularly at elevated strain levels. Remarkably, PET fibres retained their properties even when exposed to extreme heat and heavy loads, rendering them a recyclable product. A higher stiffness modulus and increased fatigue life can also be achieved by using crushed PET particles in asphalt concrete mixes [159]. Meanwhile, Jegatheesan et al. observed improvement in the binder properties, as well as in the mix properties, with the addition of PET fibres as a binder additive by comparing modified mixtures containing varying concentrations of PET fibres [160].

High-performance asphalt concrete (HPAC), often referred to as high-performance HMA or Superpave, is designed to withstand heavy traffic loads, resist rutting and cracking, and provide superior durability compared to conventional asphalt mixes. HPAC can be defined as a paving material that exhibits minimal deformation at high temperatures and that maintains flexibility and stress relaxation characteristics at low temperatures [6]. Unlike the design of traditional asphalt mixes, the design of HPAC considers not only empirical properties but also performance-based criteria, including tests for rutting, stiffness modulus, and fatigue cracking [161]. Despite these superior properties, though, in colder regions HPAC may be vulnerable to cracking, potentially reducing its lifespan and hampering its performance.

Cracking is one of the most prevalent defects in the asphalt layer, and the initiation and propagation of cracks across asphalt overlays are influenced by factors such as traffic loads, thermal stresses,

and temperature variations [162]. The Indirect Tensile Asphalt Cracking Test (IDEAL-CT) is an indirect tension test method used for determining the cracking potential of an asphalt mixture. Callomamani et al. in 2022, conducted a study in which they fabricated asphalt mixtures with different fibre types, such as Polyethylene terephthalate, Polyacrylonitrile, and Aramid. The cracking resistance of the mixes was determined using the IDEAL-CT test, which revealed that fibre-incorporated mixes had better cracking resistance compared to the mixes with no fibres [163]. Johnson et al., meanwhile, performed an IDEAL-CT test on asphalt mixtures with nanomaterial-modified binder in order to evaluate the cracking resistance, observing the impact of nanomaterial modification of the binder in improving the cracking performance at intermediate pavement service temperatures [164]. In this context, our study evaluated the impact of PET fibres on the cracking properties of asphalt mixes composed of asphaltenes-modified binder using the IDEAL-CT test following ASTM D8225-19 [113]. There is very relatively little research specifically examining the combined effect of PET fibres (of varying lengths) and asphaltenes modification on asphalt cracking resistance. As such, this study sought to bridge this gap in the existing literature by providing valuable insights into an area that remains relatively unexplored.

4.3 Objectives

The main objective of this study was to investigate how modifying asphalt binder with asphaltenes, incorporating PET fibre in the asphalt mix, and varying the fibre lengths would affect the cracking performance of HPAC. To achieve this, the cracking behaviour of HPAC was evaluated using the IDEAL-CT at two test temperatures (25 °C and 37 °C). Test specimens were prepared using an unmodified asphalt binder and modified asphalt binders with three different PET fibre lengths (6-mm, 12-mm, and 18-mm) in order to assess the impact of different fibre lengths on the cracking performance.

4.4 Methodology

Dynamic Shear Rheometer (DSR) and Bending Beam Rheometer (BBR) binder tests were carried out to determine the PG of both the base binder and the asphaltenes-modified binder. The IDEAL-CT test was carried out using a Universal Testing Machine (UTM), with the purpose of this test being to obtain cracking parameters such as cracking tolerance index (CT_{Index}), failure energy (FE), pre-crack FE, post-crack FE, and indirect tensile strength (ITS). These parameters were analyzed in order to determine the impact of fibre addition on the asphalt mixes. Figure 4-1 shows the methodology flowchart underlying this research.
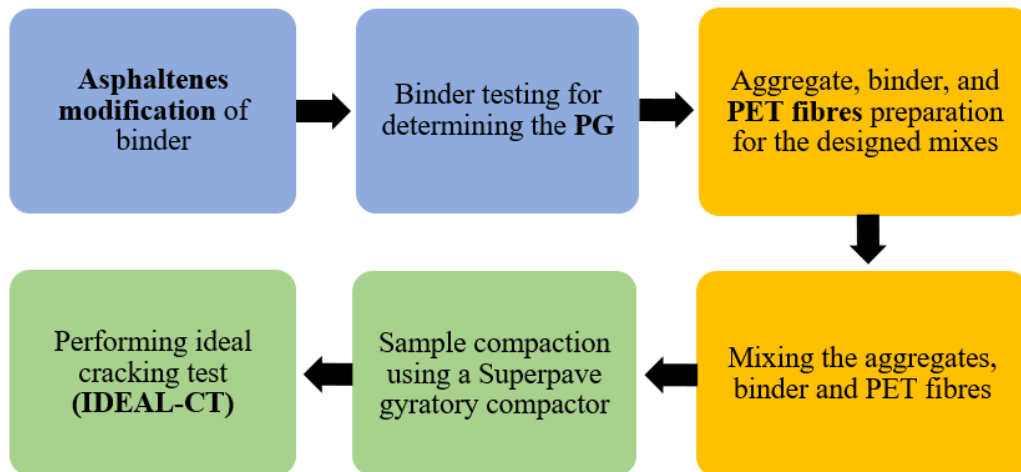
Figure 4-1. Methodology flowchart

4.5 Experimental Procedure

4.5.1 Materials

4.5.1.1 Aggregate Properties

Some of the properties of the aggregate used in this study needed to be determined as a preliminary step. The properties are specific gravity of coarse and fine aggregates, water absorption and Los Angeles (LA) abrasion. Based on the results, the aggregate requirements for HPAC preparation are met according to the results provided in Table 4-1.

68

Table 4-1. Aggregate properties

Specific Gravity				
	Aggregate Portion (%)	Bulk Specific Gravity	Bulk Specific Gravity (SSD*)	Apparent Specific Gravity
Coarse aggregate (≥ 4.75 mm)	39.7	2.618	2.652	2.666
Fine aggregate (< 4.75 mm)	60.3	2.502	2.600	2.617
Water Absorption				
	Water Absorption (%)		Criterion [91]	
Coarse aggregate (≥ 4.75 mm)	0.3		≤1.0	
Fine aggregate (< 4.75 mm)	0.4		≤1.5	
Los Angeles (LA) abrasion				
	Value Obtained (%)		Standard Range (%) [165]	
Coarse aggregate (≥ 9.5 mm)	23		10 - 45	

*SSD is Saturated Surface Dry.

4.5.1.2 Asphaltenes as Binder Additive

The most important component in the elastic behaviour of the asphalt binder is asphaltenes [16].

Asphaltenes, a waste by-product of oil refining with insignificant applications in the oil industry,

have various rich sources including crude oil, asphaltite, oilsands, tar sand, and bituminous coal

[166]. Most asphaltenes is extracted from the source using solvent extraction or solvent

deasphalting [57]. The asphaltenes used in this study were derived from Alberta oil-sand bitumen

as a by-product of the solvent deasphalting process. The material was obtained in solid form

(Figure 4-2(a)), then ground and sieved using a No. 100 sieve with a mesh size of 150 µm to turn

it into powder form (Figure 4-2(b)). The SARA components of asphaltenes, it should be noted, are

as follows: saturates make up 6.85%, aromatics account for 9.68%, resins represent 3.84%, while

the majority is made up of asphaltenes at 79.62%. In our study the asphalt binder was modified by

adding asphaltenes at a concentration of 12% (by weight of binder) and mixing it using a high

shear mixer with a speed of 2,000 rpm for 60 min at a temperature of 140 °C (Figure 4-2(c)).

Figure 4-2. Asphaltenes (a) Solid form, (b) Powder form, (c) Binder modification using a high shear mixer

4.5.1.3 Polyethylene Terephthalate (PET) Fibres

The PET fibres used in this research were generated from municipal solid waste. PET fibres of this

origin offer durability, strength, low gas permeability, as well as thermal and chemical stability

[167]. The physical and mechanical properties of the PET fibres are presented in Table 4-2.

Table 4-2. Properties of PET fibres

Property	Value
Length (mm)	6, 12, and 18
Diameter (μm)	20
Density (g/cm³)	1.41
Tensile strength (MPa)	≥ 500
Melting point (°C)	≥ 256

The PET fibres of varying lengths (6 mm, 12 mm, and 18 mm) are displayed in Figure 4-3.

Figure 4-3. Polyethylene Terephthalate (PET) fibres in different lengths (from left to right: 6-mm, 12-mm, and 18-mm)

4.5.2 Mix Design

4.5.2.1 Aggregate Gradation

To establish the most suitable mixture design approach, an extensive review of established standards and literature from various countries, including Australia, France, South Africa, and the United Kingdom, was conducted [5], [91]–[93]. Based on these sources, a final gradation envelope was selected. The selected gradation envelope was compliant with European specifications and drew inspiration from the French envelopes, maximum density curves, and relevant literature. It featured a nominal maximum aggregate size (NMAS) of 19 mm. Figure 4-4 provides a visual representation of the selected gradation, alongside the French envelopes and maximum density curves. As illustrated in the figure, this gradation falls within the boundaries defined by the French envelopes [93].
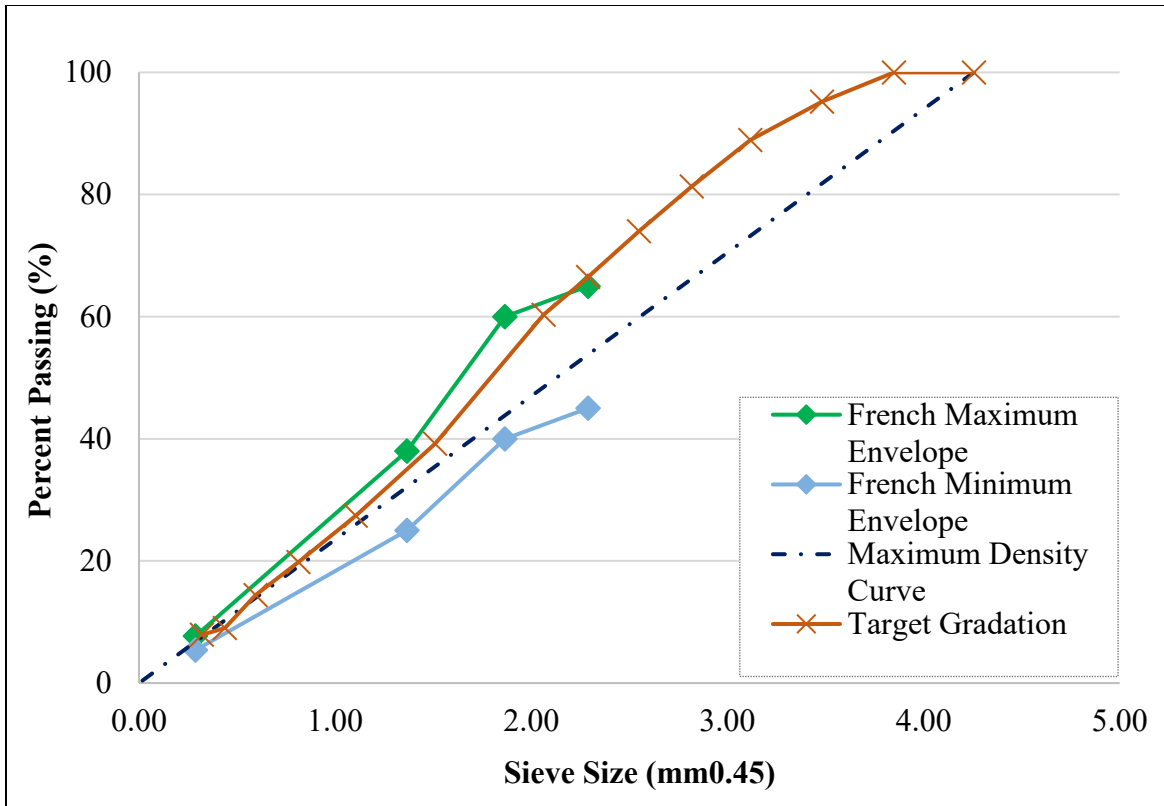
Figure 4-4. Selected aggregate grain size distribution

4.5.2.2 Binder Content

The binder used in this study was a crude oil binder with a PG of 70-22. The binder content for the

HPAC was calculated following the method developed by Denneman et al. in 2011 [91]. In their

method, the richness modulus (K) (a measure of the thickness of the binder film surrounding the

aggregate) and the aggregate type and gradation are used to calculate the binder content for the

mixture design. The optimum binder content was calculated to be 5.6% by the weight of the total

mixture, as per Equation 4-1.

$$TL_{est} = K\alpha\sqrt[5]{\Sigma} \qquad\qquad (4\text{-}1)$$

where,

TL_{est} = percent binder by mass of mixture,

K = richness factor,

α = correction coefficient for relative density of aggregates, and

Σ = specific surface area of aggregates.

4.5.2.3 PET Fibre Content

The dosage in which the PET fibres are added to asphalt mixtures is an important consideration. Increasing the fibre content enhances the effectiveness of the fibres in improving the properties of the mix up to a certain threshold. However, surpassing this threshold with excessive fibre content can compromise workability and lead to an uneven distribution within the mixture [168]. As such, the optimum content of 0.15% (by the weight of total mixture) PET fibres was determined following a novel framework (developed at the University of Alberta) based on practical considerations in road construction and laboratory performance tests that reflect field functionality [85]. Several criteria, such as compactibility, dynamic modulus, as well as ITS and fracture energy, are analyzed in this framework.

4.5.2.4 Asphalt Mixture Preparation

The mixing and compaction temperature ranges for unmodified (PG 70-22) and asphaltenes-modified (PG 70-22 + 12% Asph) binders were determined based on the viscosity results over a wide range of temperatures, as shown in Figure 4-5. The mixing temperature range for unmodified binder was 152 °C to 158 °C, while the range increased to 167 °C to 173 °C for asphaltenes-modified binder. The selected mixing temperatures for the mixes were 158 °C for unmodified binder and 173 °C for the asphaltenes-modified binder. A laboratory bucket mixer was used to mix the aggregates, binder, and fibres. The asphalt mixture was then divided into flat aluminum trays. The trays with the mixture, in turn, were conditioned in an oven for 4 h at 135 °C as per AASHTO R30 [169]. Suitable compaction temperature ranges for unmodified and asphaltenes-modified binders are 141 °C to 145 °C and 154 °C to 160 °C, respectively. For our study, the chosen

compaction temperatures for the mixes with unmodified and asphaltenes-modified binders were 145 °C and 160 °C, respectively. The choice of higher temperatures within the acceptable ranges of mixing and compaction temperatures was made to ensure the workability, quality, and consistency of the asphalt mixes.
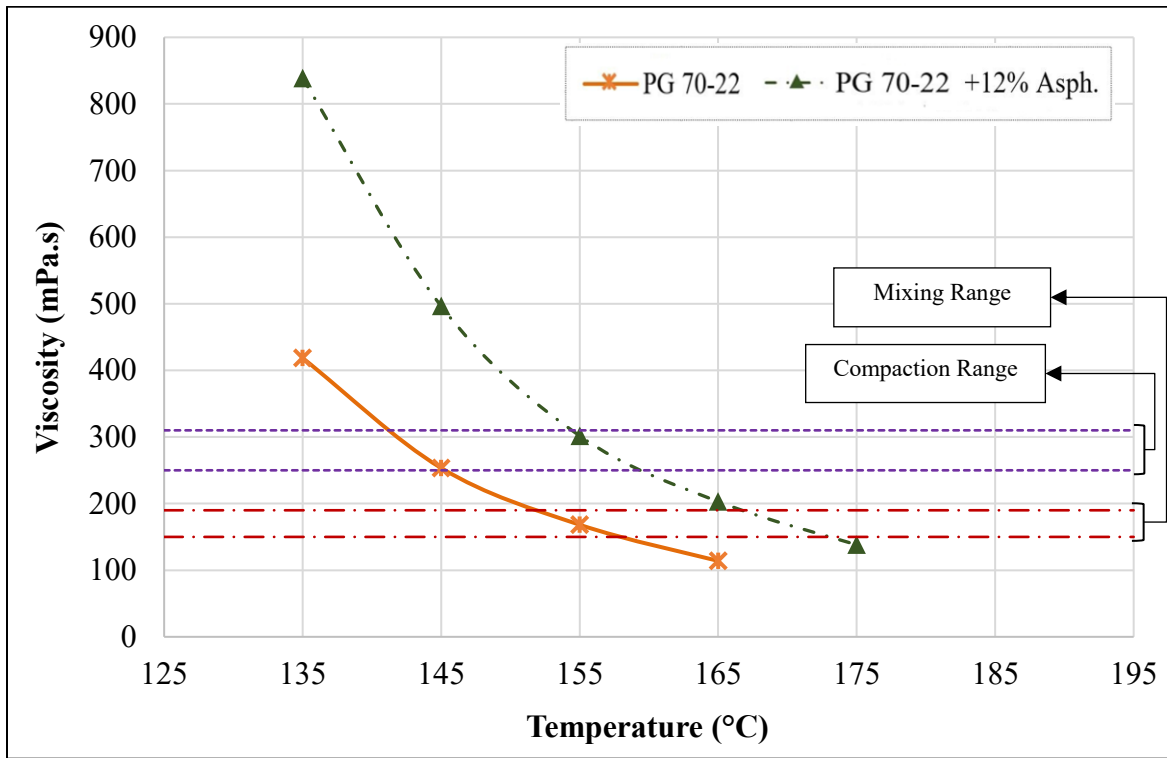
Figure 4-5. Viscosity of asphalt binders versus temperature

A Superpave gyratory compactor was used to compact the control (with no fibre), and PET fabricated mixes with three different fibre lengths (6 mm, 12 mm, and 18 mm). Control Unmodified (CU) samples were prepared with unmodified asphalt binder without the addition of PET fibres, while Control Asphaltenes-Modified (CM) samples were prepared with asphaltenes-modified binder with no PET fibres added in the mix. Asphaltenes-modified binder was used for all the specimens prepared with PET fibres.

The volumetric properties used for the mixes (Table 4-3) were adopted from a recent study on high modulus asphalt concrete [90].

Table 4-3. Volumetric properties of High-performance Asphalt Concrete (HPAC) mixes with nominal maximum aggregate size of 19 mm [90]

Property	Value
Design air voids (%)	1.5 ± 0.5
Voids in the Mineral Aggregate (VMA) (%)	15
Voids Filled with Asphalt (VFA) (%)	90
Effective binder content by volume (%)	13.5 ± 0.5

4.5.3 Aging Process

A Rolling Thin Film Oven (RTFO) was used for the laboratory simulation of the short-term aging of asphalt that typically occurs during production and compaction of HMA mixtures, the simulation having been conducted in accordance with the AASHTO T240-17 standard [38]. In this process, RTFO glass containers were filled with asphalt binder samples of approximately 35 ± 0.5 g. The RTFO glass containers with asphalt binder samples were then placed into the RTFO carriage inside the oven. Each container was placed in such a way that the top opening of the glass containers was directly facing a jet of air supply inside the oven. The oven was then closed, and the temperature was kept at 163 °C, with the carriage set at a rotating speed of 15 rpm throughout the 85-min aging process.

A sample from the RTFO-aged residue was used to simulate long-term aging of asphalt, using a Pressure-Aging Vessel (PAV) for the assessment of the intermediate- and low-temperature performance grade of the asphalt binder in accordance with AASHTO R28-16 [39]. Approximately 50 g of the RTFO-aged residue was used to fill in each of the PAV pans, which were then placed in a PAV sample rack. The samples were then subjected to 2.1 MPa of pressure and a constant temperature of 100 °C for a duration of 20 h. Finally, the residue in each pan was scraped into a

single container and placed inside a vacuum oven at 170 °C for 30 min for the removal of excess gas from the sample.

4.5.4 Dynamic Shear Rheometer (DSR) Test

An Anton Paar SmartPave 102 DSR was used to obtain data on the intermediate- and high-temperature rheological properties of the asphalt binder. DSR is capable of determining rheological characteristics of asphalt binder under sinusoidal loading. One of two setups, depending on the test temperature—either a parallel plate and 8-mm spindle with 2-mm gap or a 25-mm spindle with 1-mm gap—was used for the rheological evaluation, as per the Superpave binder specifications in AASHTO T315-16 [41]. The PG of the asphalt binder was calculated using the main rheological viscoelastic properties, expressed in terms of complex shear modulus (G^*) and phase angle (δ).

4.5.5 Bending Beam Rheometer (BBR) Test

A Cannon BBR was used to determine the cracking resistance of the asphalt binder at low temperatures following AASHTO T313-16 [43]. In this method, two replicate asphalt binder samples with dimensions of $125 \times 6.35 \times 12.7$ mm were prepared from PAV-aged samples of each binder type, where the parameters, creep stiffness (S), and creep rate (m-value) were used to determine the asphalt's low-temperature PG. The low-temperature PG, it should be noted in this regard, is the temperature at which the creep stiffness (S) is 300 MPa and the m-value is 0.30 at 60 s of loading.

4.5.6 Indirect Tensile Cracking Test (IDEAL-CT)

The IDEAL-CT test is simple (without any cutting, gluing, drilling, or notching of test specimens), practical (minimal training is required for regular operation), and efficient (usually completed within minutes). Moreover, this test has a much lower coefficient of variation compared to traditional repeated load cracking tests [112]. In our study, the IDEAL-CT test is carried out as per

ASTM D8225-19 [113], where the width of the loading strips was 19.05 ± 0.3 mm. Three specimens with a diameter of 150 ± 2 mm and thickness of 62 ± 1 mm were prepared at 1.5 ± 0.5% air void content. According to ASTM D8225-19, the typical target intermediate test temperature is 25 °C, and the preconditioning of the test specimen is done in an environmental chamber for 2 h ± 10 min. Other target intermediate test temperatures can be calculated as per Equation 4-2 [113]:

$$PG\ IT = \frac{PG\ HT + PG\ LT}{2} + 4 \tag{4-2}$$

where:

> $PG\ IT$ = intermediate-performance grade temperature (°C),
>
> $PG\ HT$ = climatic high-performance grade temperature (°C), and
>
> $PG\ LT$ = climatic low-performance grade temperature (°C).

In our study, the selected test temperatures were the typical intermediate test temperature of 25 °C as well as 37 °C (based on the PG of the binder as determined in accordance with Equation 4-2). Given that the test temperature can have a significant impact on the performance of asphalt mixes, these two different test temperatures were employed.

The specimen was centered in the fixture, and it was observed that the specimen maintained uniform contact on the support. A constant compressive load with a rate of 50 ± 2 mm/min was applied during the test. The respective test temperatures of 25 °C and 37 °C were maintained as the load and displacement were measured, and the test was stopped when the load dropped below 100 N. The time, load, and Load-Line Displacement (LLD) data were collected at a minimum rate of 40 sampling data points per second for a smooth load-LLD curve. The IDEAL-CT test setup is shown in Figure 4-6.

Figure 4-6. IDEAL-CT test setup

FE was calculated using the area under the load-displacement graph following Equation 4-3, while

Equation 4-4 was used to determine the CT_{Index} [113].

$$G_f = \frac{W_f}{D \times t} \times 10^6 \qquad (4\text{-}3)$$

where:

    G_f = FE (J/m^2),

    W_f = work of failure (J), which is simply the area under the load-displacement curve,

    D = specimen diameter (mm), and

    t = specimen thickness (mm).

$$CT_{Index} = \frac{t}{62} \times \frac{l_{75}}{D} \times \frac{G_f}{|m_{75}|} \times 10^6 \qquad (4\text{-}4)$$

where:

    CT_{Index} = cracking tolerance index,

$|m_{75}|$ = absolute value of the post-peak slope m75 (N/m),

l_{75} = displacement at 75% the peak load after the peak (mm), and

$\frac{t}{62}$ = unitless correction factor for specimen thickness.

The ITS was calculated using Equation 4-5, in accordance with ASTM D6931-17 [115].

$$ITS = \frac{2000.P}{\pi.t.D}$$
(4-5)

where:

ITS = indirect tensile strength (kPa), and

P = maximum load (N).

4.6 Results and Discussion

4.6.1 Performance Grading (PG) Results

Table 4-4 displays the continuous high and low PG temperatures of both unmodified and asphaltenes-modified binders. As can be seen, the standard performance grading of asphaltenes-modified binder was found to be 82-16, meaning that the rate of increase in high-temperature performance grading was much greater than the rate of decrease in the low-temperature performance grading. To clarify, the high-temperature PG increased from 70 to 82, while the low temperature increased from −22 °C to −16 °C following modification with asphaltenes.

Table 4-4. Performance Grading (PG) results of asphalt binders before and after modification

Asphalt Binder Type	Continuous High Grade (°C)	Continuous Intermediate Grade (°C)	Continuous Low Grade (°C)	Standard High Grade (°C)	Standard Low Grade (°C)	True Grade (°C)	Standard Grade (°C)
Unmodified binder	70.2	20.2	−25.9	70	−22	70.2−25.9	70−22
Binder + 12% Asphaltenes	82.9	29.0	−21.8	82	−16	82.9−21.8	82−16

4.6.2 IDEAL-CT Test Results

The IDEAL-CT test is used to determine the crack indices of asphalt mixes, thereby aiding in the identification of the mix design with the highest crack-resistance. In our research, the IDEAL-CT test was conducted in order to assess the cracking behaviour of asphalt mixtures at temperatures of 25 and 37 °C (the latter having been selected based upon the performance grading of the asphalt binder, as noted above). During a close inspection of the cracked samples prepared with PET fibres, a noteworthy phenomenon was observed. Fine, thread-like fibrils were found bonding to the mastic and aggregates, as depicted in Figure 4-7. This observation may have implications for the crack resistance of the asphalt mixtures.
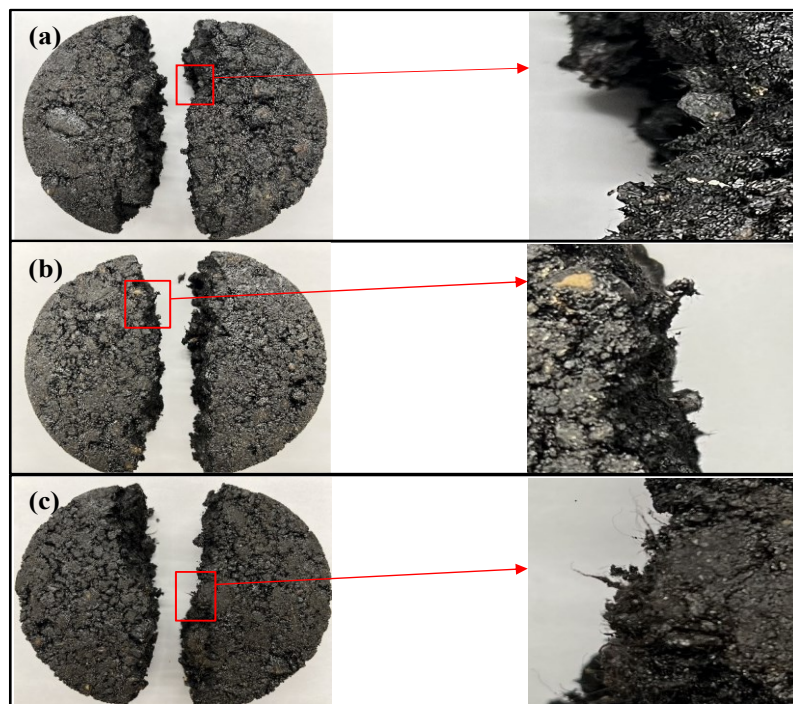
Figure 4-7. Close-up view showing fibrils bonding in the Polyethylene Terephthalate (PET) fabricated mixes (a) 0.15% 6-mm PET, (b) 0.15% 12-mm PET, (c) 0.15% 18-mm PET

The load-displacement graphs shown in Figure 4-8(a) reveal some interesting findings. First, the failure load for the control unmodified samples at 25 °C was found to be 11.6 kN, i.e., significantly lower than those of both the control asphaltenes-modified sample (22.3 kN) and the fibre-

reinforced samples (23 kN, 22.9 kN, and 22.5 kN for 6-mm, 12-mm, and 18-mm samples, respectively); however, it is worth noting that the crack propagation was slower in the post-crack stage for the control unmodified samples, as evidenced by the lower slope of the post-crack curve (slope value of 2,192 kN/m). In contrast, the slope values of the post-crack curves for the control asphaltenes-modified sample and the samples with 6-mm, 12-mm, and 18-mm PET fibres were 6,127 kN/m, 6,149 kN/m, 6,068 kN/m, and 6,161 kN/m, respectively.

The failure loads decreased significantly when the asphaltenes-modified specimens were tested at the higher temperature of 37 °C, as shown in Figure 4-8(b), with respective failure loads of 10.7 kN, 12 kN, 11.9 kN, and 11 kN observed for the control asphaltenes-modified sample and the 6-mm, 12-mm, and 18-mm PET fabricated samples. Nevertheless, it is important to highlight that the rate of crack propagation decreased during the post-crack phase for all of the asphaltenes-modified test specimens tested at 37 °C. The lowest slope value observed (1,979 kN/m) was that of the sample with 12-mm PET fibres. The other slope values were 2,761 kN/m for the control asphaltenes-modified sample, 2,374 kN/m for the sample with 6-mm PET fibres, and 2,163 kN/m for the sample with 18-mm PET fibres.
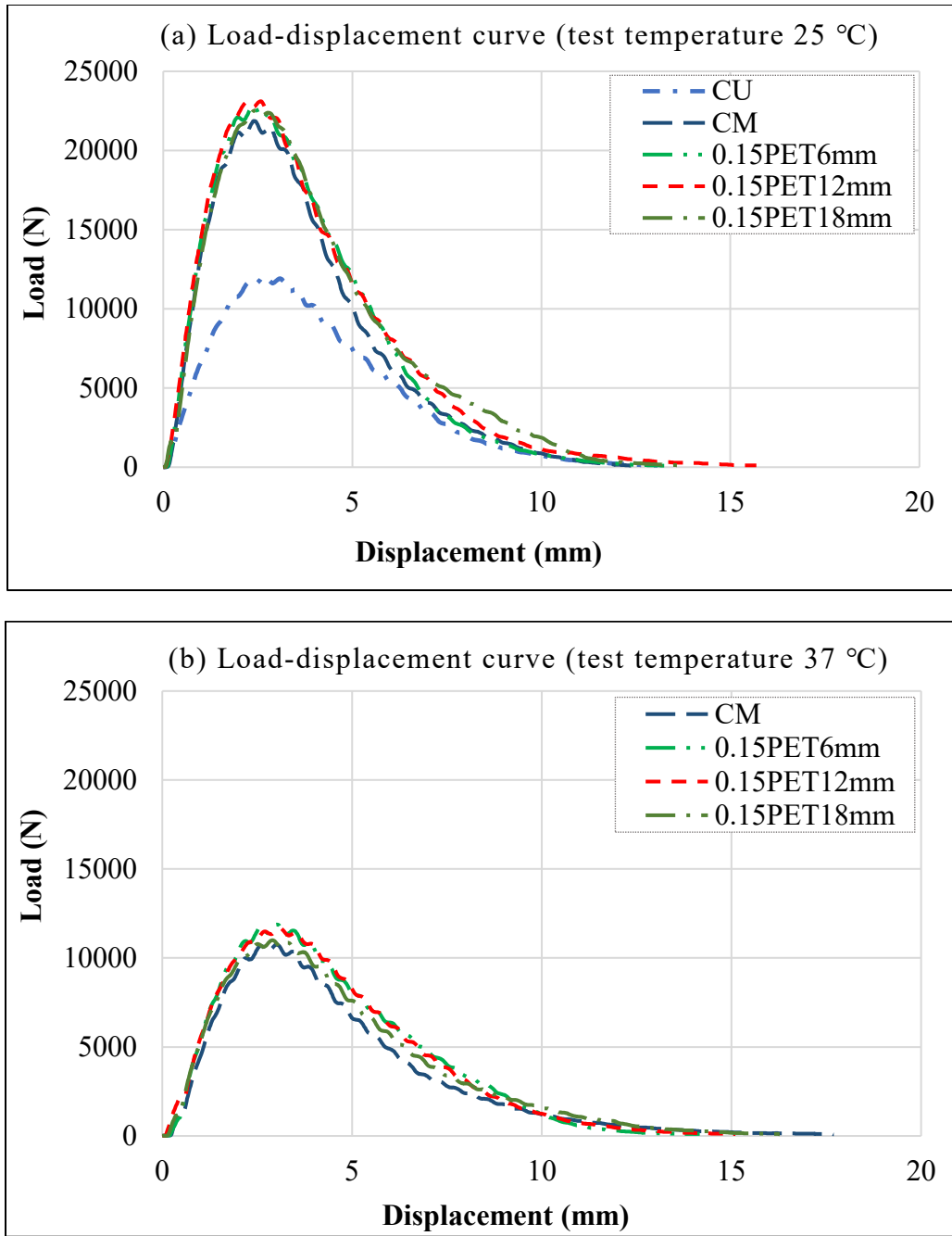
Figure 4-8. Load-displacement graphs (a) 25 °C, (b) 37 °C

From Figure 4-9, it can be seen that all the asphaltenes-modified specimens had significantly higher ITS values when tested at 25 °C test temperature compared to when tested at 37 °C, and the comparison with the control unmodified sample is not reasonable. These elevated ITS values could also be a reason why the impact of the addition of fibres was not apparent at 25 °C. The ITS values

at 37 °C were reduced by half compared to the results obtained at 25 °C. Marín-Uribe and Restrepo-Tamayo have observed in this regard that the tensile strength drops rapidly as the test temperature rises in asphalt mixtures, this being primarily due to the decrease in the viscosity and cohesion of the asphalt binder [170]. However, our results at the higher temperature, in contrast to the results obtained at 25 °C, were comparable to those of the control unmodified samples. The ITS value for the control unmodified sample was 791 kPa, while, when the asphaltenes-modified specimens were tested at 37 °C, the ITS values were found to be 729 kPa for the control asphaltenes-modified sample, 818 kPa for the sample with 6-mm PET fibres, 814 kPa for the sample with 12-mm PET fibres, and 753 kPa for the sample with 18-mm PET fibres.
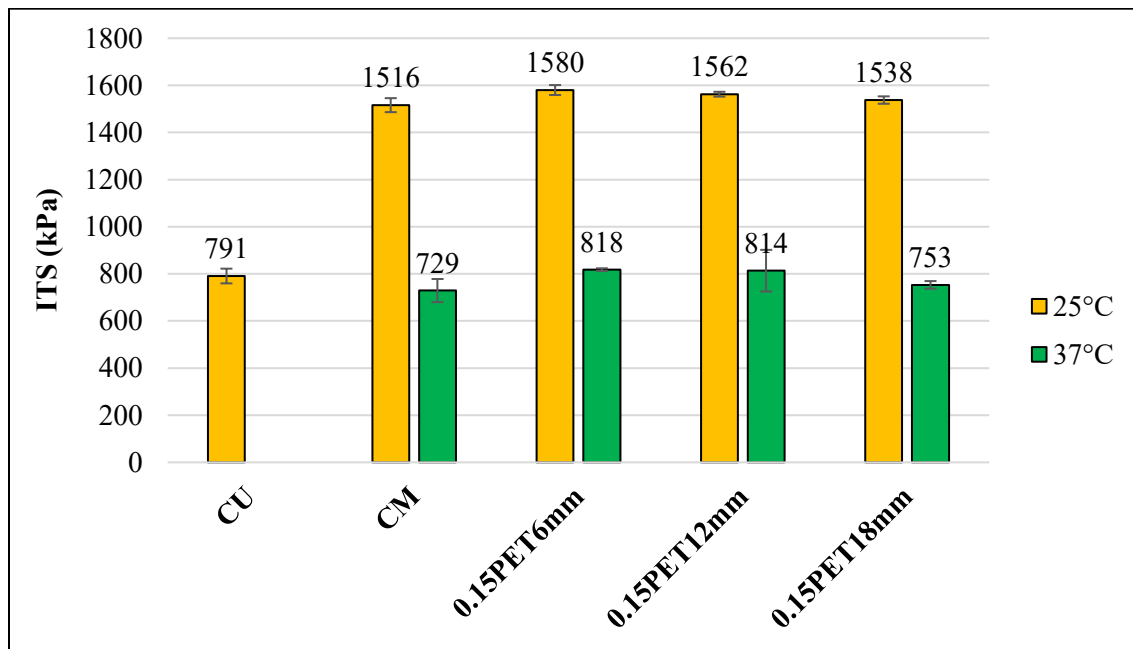

Figure 4-9. Comparison of indirect tensile strength values at 25 °C and 37 °C

The total FE comprises two components: pre-crack FE, which reflects cracking resistance, and post-crack FE, representing energy dissipation and crack propagation assessment in the mixture [171]. Figure 4-10(a) illustrates that, at a test temperature of 25 °C, the 6-mm PET samples showed the highest pre-crack FE result, with an 8.9% rise relative to the control asphaltenes-modified

samples, while the greatest increase in post-crack FE was 14.8%, this being for the samples with 18-mm PET fibres (Figure 4-10(b)). However, both the pre-crack and post-crack FE values saw a significant drop when the asphaltenes-modified specimens were tested at 37 °C. Nevertheless, an overall trend of increasing FE was observed with the addition of PET fibres in the mixes. The highest pre-crack FE (2,277 J/m^2), representing a 23% increase compared to the control asphaltenes-modified samples, was observed in the 12-mm PET samples. The post-crack FE, meanwhile, climbed to 4,864 J/m^2 for the 18-mm PET samples, this being the highest value among all the specimens at 37 °C, although the 12-mm PET samples were not far behind with a post-crack FE of 4,728 J/m^2.
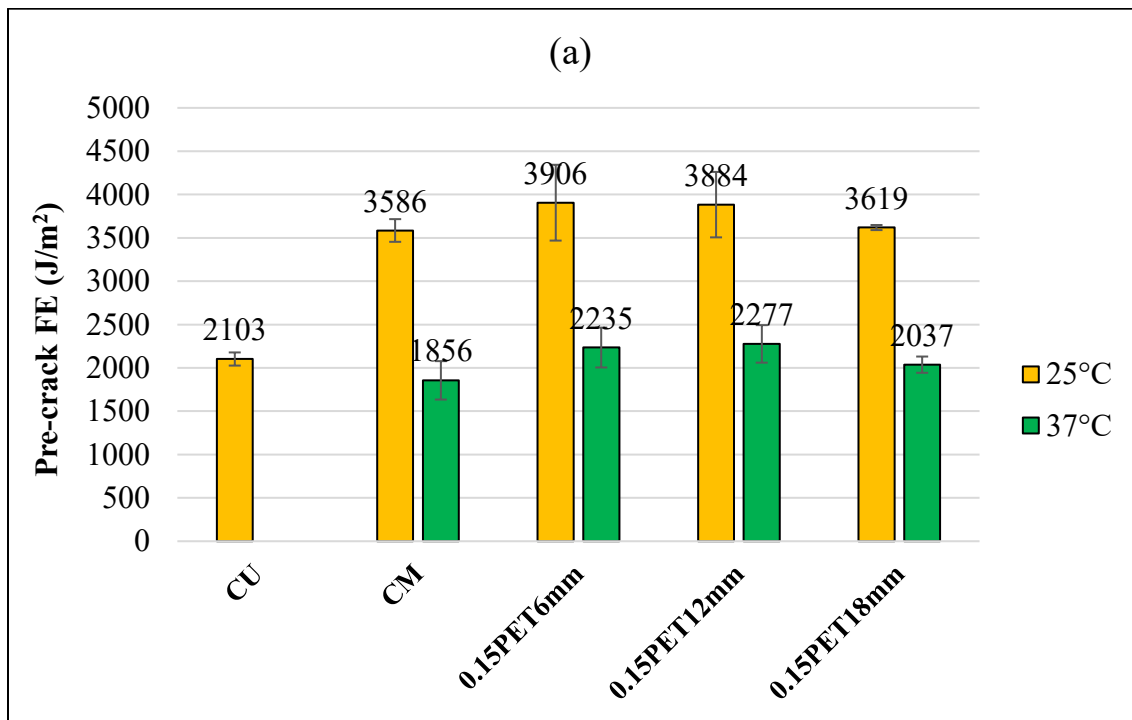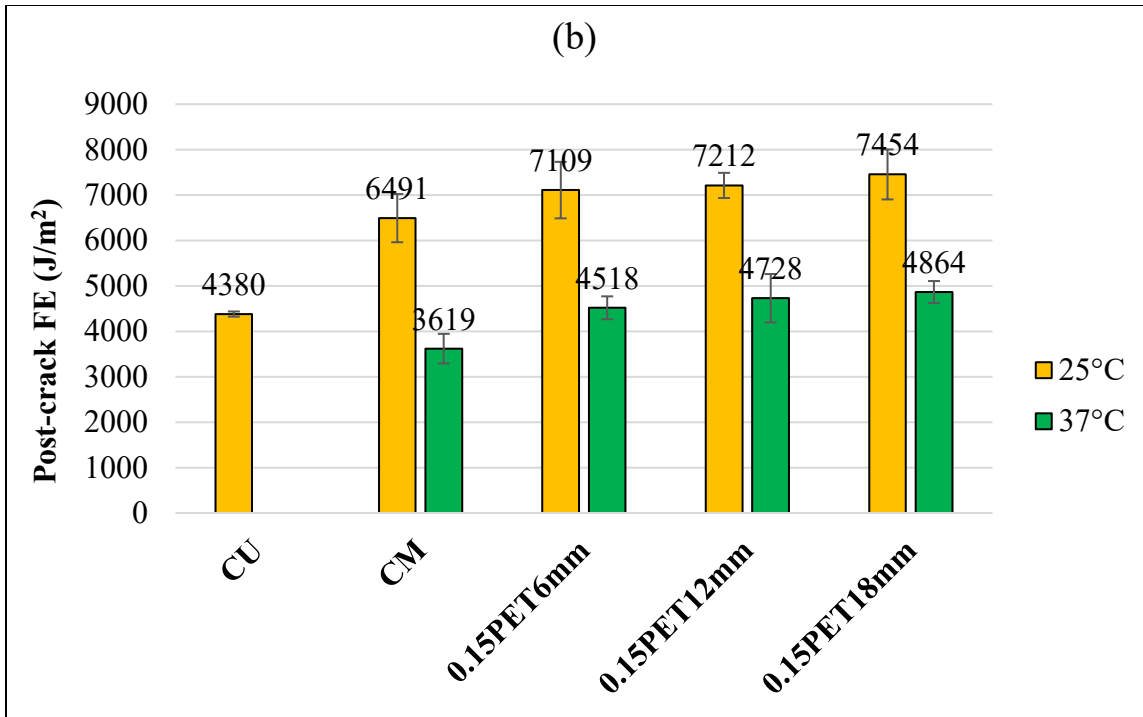
Figure 4-10. Comparison of (a) Pre-crack FE, (b) Post-crack FE results at 25 °C and 37 °C

The total FE is a critical parameter for assessing the potential for cracking in an asphalt mix. As can be seen from Figure 4-11, at the intermediate test temperature of 25 °C, the total FE was 6,482 J/m^2 for the control unmodified sample, this being significantly lower than those of all the asphaltenes-modified samples tested at the same temperature. The samples with 6-mm PET saw a jump of 9.3% in total FE when compared with the control asphaltenes-modified samples. The greatest increase (around 10%) was observed in the case of the samples with 12-mm PET fibres, while the samples with 18-mm PET fibres also saw a sharp increase. At 37 °C, the 12-mm PET samples had a total FE of 7,005 J/m^2 with a considerable increase, relative to the control asphaltenes-modified samples, of 28%. As can be seen, the FE results obtained for the asphaltenes-modified samples at the test temperature of 37 °C are comparable to those of the control unmodified samples.
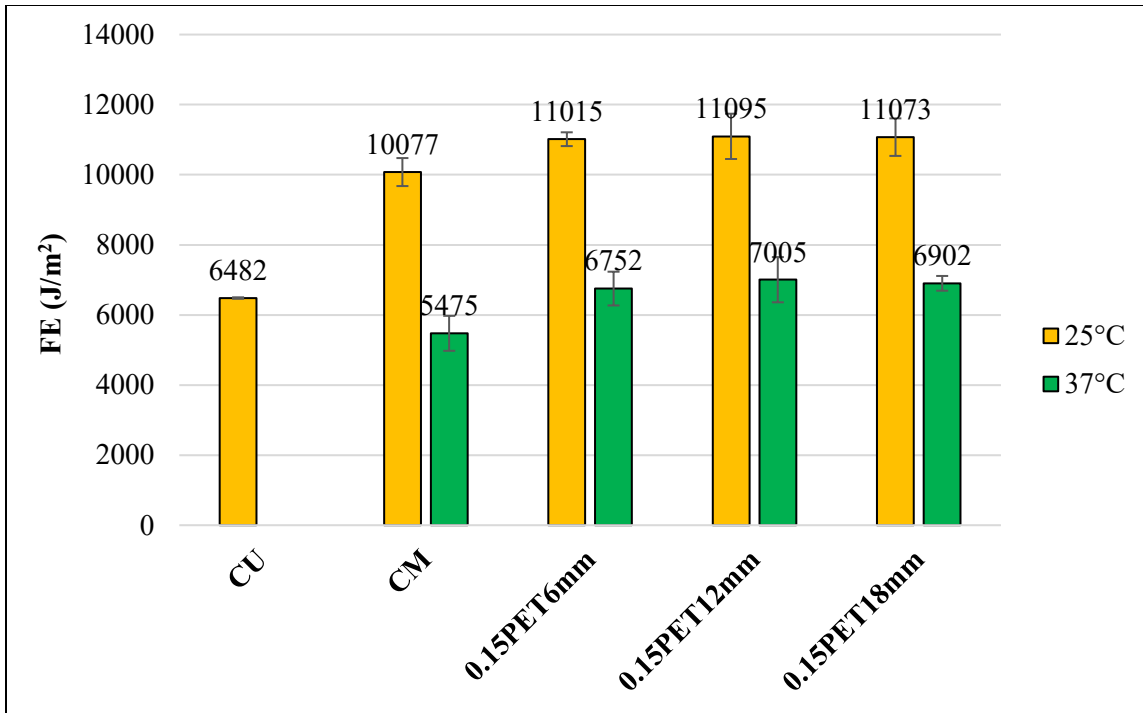
Figure 4-11. Comparison of FE results at 25 °C and 37 °C

Figure 4-12 provides a comparison of cracking tolerance (CT) index values from which it is apparent that, at 25 °C, the CT_{Index} value was highest (i.e., 91) for the control unmodified samples, while it decreased to 42 for the control samples with asphaltenes modification. Interestingly, there was not a significant change in CT_{Index} for the samples containing PET fibres. When the specimens were tested at 37 °C, on the other hand, the CT_{Index} values increased significantly for all the asphaltenes-modified samples, and the impact of the addition of PET fibres was more evident. The highest CT_{Index} value, 105, was observed in the case of the sample with 12-mm PET fibres, which saw an increase of 72% compared to the control asphaltenes-modified samples. The CT_{Index} value of the 18-mm PET samples was 99—slightly lower than that of the 12-mm PET samples. It can thus be concluded that a test temperature of 37 °C is more suitable for determining the CT_{Index} of asphaltenes-modified samples.
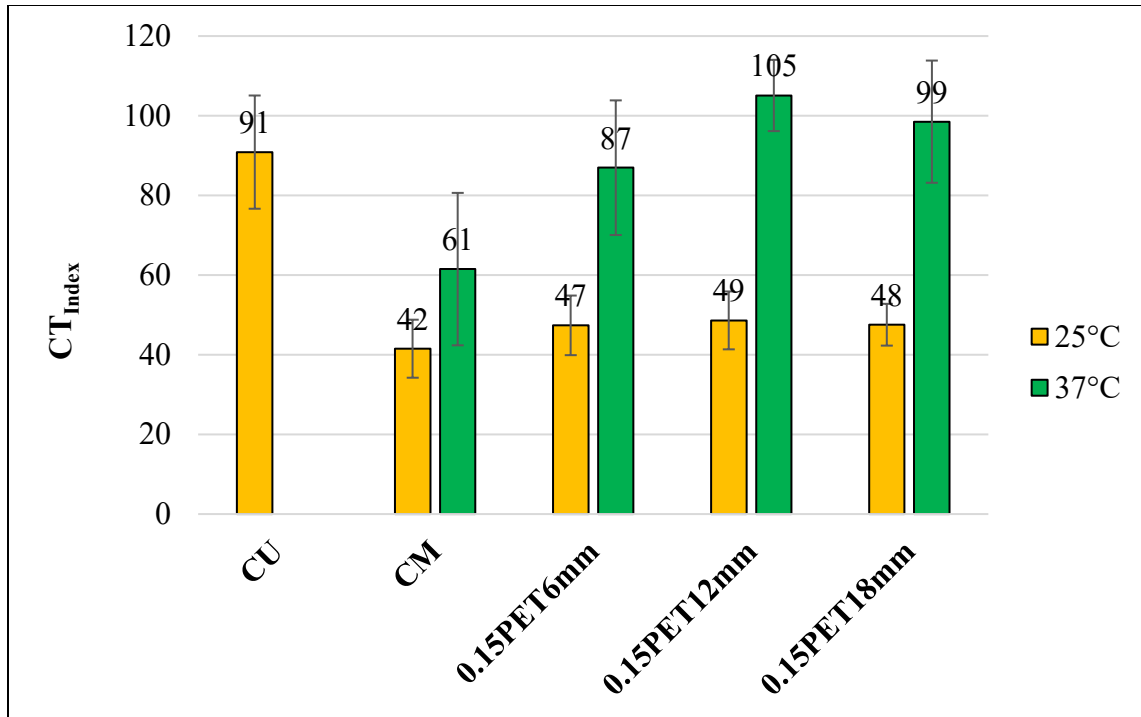
Figure 4-12. Comparison of CT_{Index} values at 25 °C and 37 °C

An Analysis of Variance (ANOVA) on various parameters, including the CT_{Index}, FE, and ITS values, and for both the Control Asphaltenes-Modified (CM) and PET fabricated specimens, was conducted. A significance level (α) of 0.05 was used to assess the statistical significance of the differences observed. In ANOVA, it should be noted, the variability within groups to the variability between groups is compared and the F-values are calculated. In our analysis, the F-critical values obtained for mix type and fibre length were 9.277 and 19, respectively. For temperature the value was 10.128.

Table 4-5. ANOVA results

Index	Mix type		Fibre length		Temperature	
	P-value	F-value[a]	P-value	F-value[b]	P-value	F-value[c]
CT_{Index}	0.307	1.890	0.394	1.537	0.015	25.546
FE	0.010	28.693	0.209	3.777	0.000	1447.727
ITS	0.027	14.572	0.099	9.149	0.000	6714.461

[a] F-crit (mix type) = 9.277, [b] F-crit (fibre length) = 19, [c] F-crit (temperature) = 10.128.

The results presented in Table 4-5 reveal that, with a few exceptions, such as the CT_{Index} for different mix types, the calculated F-values consistently exceeded the corresponding F-critical values. This finding implies that both the type of mix and the temperature have a statistically significant impact on the CT_{Index}, FE, and ITS values. However, the impact of fibre lengths on the resulting parameters was seen to be insignificant with F-values being consistently lower than the respective F-critical values. Additionally, the influence of temperature is more significant compared to the influence of mix type, as the F-critical values are nearly the same for both factors, while the F-values for temperature are notably higher than those for mix type. Moreover, the differences observed in these parameters are unlikely to have occurred randomly. Instead, they can be attributed to the specific mix type or temperature conditions, highlighting the importance of these factors in influencing the outcomes of the analysis.

4.7 Conclusion

In this study, a neat asphalt binder was modified with asphaltenes, a waste material generated as a result of processing of Alberta oil sands. Both the unmodified and asphaltenes-modified binders were tested for performance grading analysis, and were used to prepare HPAC mixes with different lengths of PET fibres. A cracking performance test (IDEAL-CT) was performed to evaluate the cracking properties of asphalt mixes reinforced with PET fibres (of three lengths—6-mm, 12-mm, and 18-mm) and a comparison with the control samples was carried out. The specimens were tested at two test temperatures—25 °C, which is the standard intermediate test temperature, and 37 °C, which was selected based on the PG of the asphaltenes-modified binder. In light of the test results obtained, the following conclusions can be drawn:

- The true performance grading of the neat binder changed from PG 70.2-25.9 to 82.9-21.8 as a result of asphaltenes modification, indicating ideal rheological characteristics at high-performance temperatures.

- In terms of the IDEAL-CT test results obtained at 25 °C test temperature, the ITS values for the asphaltenes-modified samples were significantly higher than those for the control unmodified samples. These higher ITS values overshadow the potential crack resistance improvement brought about by the addition of the fibres. As such, the evaluation of the impact of PET fibres was inconclusive at this test temperature.

- When the test temperature was raised to 37 °C, the ITS values decreased considerably. This reduction in ITS values made it more reasonable to compare results between the control unmodified and asphaltenes-modified samples. Additionally, the impact of adding PET fibres of varying lengths became more apparent at this elevated temperature. The reduction in ITS values can be attributed to the decrease in the viscosity and cohesion of the asphaltenes-modified binder used in the mixes at the higher temperature of 37 °C. As such, for the IDEAL-CT test, it is recommended to determine the test temperature according to the performance grading of the binder in order to obtain more reliable results.

- At a test temperature of 37 °C, the addition of PET fibres resulted in considerable improvements for several different parameters, particularly when using a fibre length of 12 mm. The 12-mm PET samples exhibited the highest CT_{Index} (105), the highest pre-crack FE (23% increase), a 31% increase in post-crack FE, and the highest FE of 7,005 J/m^2 compared to the control asphaltenes-modified samples. It can thus be concluded that the samples with 12-mm PET fibres performed the best among the test specimens considered in this study. This may be

attributable to the effective dispersion and comparably less clustering and "balling" in the mixes containing a dosage of 0.15% of 12-mm PET fibres.

- The ANOVA results suggest that both mix type and temperature had a statistically significant impact on the results obtained in this study. However, the impact of different fibre lengths was found to be insignificant.

In future studies, additional performance tests, such as IDT creep and compliance at lower temperatures, as well as the Hamburg Wheel-Tracking test, could be conducted. These tests would provide a more comprehensive understanding of how the inclusion of PET fibres in the asphalt mixture influences its behaviour and performance at both low and high temperatures.

Chapter 5. Summary and Conclusions

5.1 Summary

Asphalt pavement distresses have been a cause for concern for a long time since they have a significant impact on the performance and overall lifespan of a pavement. The asphalt binder and mix properties play a vital role in determining the pavement's effectiveness over time. Employing waste materials, such as asphaltenes and PET fibres, in the development of HPAC emerges as a sustainable strategy to enhance pavement performance. In the initial phase of this study, an assessment was conducted to investigate the impact of asphaltenes modification on the rheological and aging properties of asphalt binders, utilizing two distinct binders, denoted as A and B. Results from the MSCR and FS tests revealed a notable enhancement in elasticity, rutting resistance, and resistance to short-term aging following the introduction of asphaltenes.

In the second stage of this research, asphaltenes-modified binders were used to develop HPAC mixtures, incorporating varying lengths of PET fibres. The cracking behavior of these asphalt mixes, reinforced with PET fibres measuring 6-, 12-, and 18-mm, was evaluated using the IDEAL-CT test, and comparisons were drawn against control samples. Testing was conducted at two temperatures: 37 °C, aligned with the PG of the asphaltenes-modified binder, and 25 °C, which is the typical intermediate test temperature. The test findings showed that the asphalt mixtures fabricated with PET had better resilience to cracking.

The results from all the testing programs are summarized in Table 5-1.

Table 5-1. Summary of all the test results

Test program	Result parameter	Control values	Other values
Multiple stress creep recovery (MSCR)	Average non-recoverable creep compliance, J_{nr}	100%	• -88% for modified binder A at 3.2 kPa • -84% for modified binder B at 3.2 kPa
	Stress sensitivity index, $J_{nr\,diff}$	100%	• -21% for modified binder A • -11.5% for modified binder B
	Modified stress sensitivity index, $J_{nr\,slope}$	100%	• -90.6% for modified binder A • -85% for modified binder B
	Average percent recovery, R	100%	• 437% for modified binder A at 0.1 kPa • 385% for modified binder B at 0.1 kPa
Frequency sweep (FS)	Complex shear modulus, G^*	100%	• 546% for modified binder A at 1 rad/s • 497% for modified binder B at 1 rad/s
	Phase angle, δ	100%	• -16.5% for modified binder A at 1 rad/s • -15% for modified binder B at 1 rad/s
	Rutting parameter, $G^*/\sin[\delta]$	100%	• 604% for modified binder A at 1 rad/s • 542% for modified binder B at 1 rad/s
	Complex shear modulus aging index, CAI	100%	• -19.7% for modified binder A at 1 rad/s • -21% for modified binder B at 1 rad/s
	Phase angle aging index, PAI	100%	• 0.22% for modified binder A at 100 rad/s • 1.8% for modified binder B at 100 rad/s
Ideal cracking test (IDEAL-CT)	Indirect tensile strength, ITS	100%	• 11.7% for 12-mm PET fabricated asphalt mix at 37 °C
	Failure energy, FE	100%	• 28% for 12-mm PET fabricated asphalt mix at 37 °C
	Cracking tolerance index, CT_{Index}	100%	• 72% for 12-mm PET fabricated asphalt mix at 37 °C

5.2 Conclusions

The main conclusions obtained from this study are summarized below:

- Incorporation of 12% asphaltenes concentration helped to achieve the required high PG of 82 °C for HMAC. The lower temperature performance of the asphalt binders was not compromised, and the results of CI suggested a well-maintained asphalt binder stability at this concentration of asphaltenes.

- The incorporation of asphaltenes into the binders led to a noteworthy reduction in average non-recoverable creep compliance (J_{nr}) results, indicating improved elasticity and enhanced resistance to rutting. Particularly, the lowest J_{nr} value, measuring 0.29 kPa^{-1}, was observed in binder A modified with asphaltenes under a maximum stress level of 3.2 kPa. These modified binders met the requirements for 'E' grade, indicating their ability to withstand the demands of extremely heavy traffic and high-stress conditions.

- All asphalt binders met stress sensitivity criteria, with $J_{nr\ diff}$ values falling below 75%. Noteworthy is the significant decrease in $J_{nr\ slope}$ values—90.6% for binder A and 85% for binder B—underscoring a diminished sensitivity to stress in the modified binders, post asphaltenes introduction.

- The G* master curves pointed to a significant rise in stiffness for binders with asphaltenes modification, particularly after RTFO aging, enhancing their ability to resist rutting. Lower δ values, on the other hand, indicated increased elasticity and reduced viscosity in asphaltenes-modified binders. Additionally, Rutting parameter (G*/sin[δ]) values saw a considerable increase, especially in RTFO-aged asphaltenes-modified binders, emphasizing their superior resistance to deformation. Moreover, CAI results indicated enhanced aging resistance due to asphaltenes

inclusion, credited to their intricate molecular structure and antioxidant qualities. However, the differences between the PAI values were insignificant, as verified by the statistical analysis.

- At 25 °C, asphalt mixes with asphaltenes-modified binder exhibited considerably higher ITS values compared to mixes with unmodified binder, overshadowing the potential enhancement in crack resistance attributed to PET fibres addition. Conversely, at 37 °C, ITS values declined, facilitating a more reasonable comparison. The influence of PET fibres, particularly of different lengths, became noticeable at this temperature due to decreased viscosity and cohesion in the asphaltenes-modified binder. To ensure more reliable results in IDEAL-CT testing, it is recommended to select the test temperature based on the PG of the asphalt binder.

- The incorporation of 12-mm PET fibres yielded considerable improvements across various parameters, displaying superior performance in terms of CT_{Index} (105), pre-crack FE (23% rise), post-crack FE (31% increase), and total FE (7,005 J/m^2) when compared with control asphaltenes-modified mixes, at 37 °C test temperature. The favorable outcome could be attributed to the efficient dispersion and minimal clustering observed in the 0.15% dosage of 12-mm PET fibres. Additionally, ANOVA underscored the significant impact of both mix type and temperature on the obtained results.

Future performance tests, such as Hamburg Wheel-Tracking (HWT), and IDT creep and compliance tests at lower temperatures, can be carried out to better understand the rutting performance of asphalt mixes containing asphaltenes-modified binder and the combined impact of asphaltenes and PET fibres on the asphalt mixtures in cold climatic conditions.

References

[1] L.A.P. Callomamani, N. Bala, and L. Hashemian, "Comparative analysis of the impact of synthetic fibers on cracking resistance of asphalt mixes," International Journal of Pavement Research and Technology, vol. 16, no. 4, pp. 992–1008, 2023.

[2] B.N. Mills, S.L. Tighe, J. Andrey, J.T. Smith, and K. Huen, "Climate change implications for flexible pavement design and performance in southern Canada," Journal of Transportation Engineering, vol. 135, no. 10, pp. 773–782, 2009.

[3] M.V. Mohod and K.N. Kadam, "A comparative study on rigid and flexible pavement: A review," IOSR Journal of Mechanical and Civil Engineering (IOSR-JMCE), vol. 13, no. 3, pp. 84–88, 2016.

[4] C. Si, X. Zhou, Z. You, Y. He, E. Chen, and R. Zhang, "Micro-mechanical analysis of high modulus asphalt concrete pavement," Construction and Building Materials, vol. 220, pp. 128–141, 2019.

[5] P.J. Sanders and M.E. Nunn, "The application of Enrobe a Module Eleve in flexible pavements," Transport Research Laboratory Crowthorne, UK, 2005.

[6] M. Shimazaki, M. Konno, M. Takahashi, and A. Kasahara, "Development of high-performance asphalt for prevention of reflective cracking," in First International Conference on Pavement Preservation California Department of Transportation Federal Highway Administration Foundation for Pavement Preservation, 2010.

[7] V. Haritonovs, J. Tihonovs, and J. Smirnovs, "High modulus asphalt concrete with dolomite aggregates," in IOP Conference Series: Materials Science and Engineering, IOP Publishing, p. 12084, 2015.

[8] T.B. Moghaddam and H. Baaj, "The use of compressible packing model and modified asphalt binders in high-modulus asphalt mix design," Road Materials and Pavement Design, vol. 21, no. 4, pp. 1061–1077, 2020.

[9] F. Olard and D. Perraton, "On the optimization of the aggregate packing characteristics for the design of high-performance asphalt concretes," Road Materials and Pavement Design, vol. 11, no. sup1, pp. 145–169, 2010.

[10] H. Fazaeli, Y. Samin, A. Pirnoun, and A.S. Dabiri, "Laboratory and field evaluation of the warm fiber reinforced high-performance asphalt mixtures (case study Karaj–Chaloos Road)," Construction and Building Materials, vol. 122, pp. 273–283, 2016.

[11] L.J. Ma, J.Y. Zhang, and Z. Li, "The road-test of high-performance asphalt mixture with Superpave," Applied Mechanics and Materials, vol. 361, pp. 1576–1579, 2013.

[12] R.N. Hunter, A. Self, J. Read, and E. Hobson, "The shell bitumen handbook," vol. 514. Ice Publishing London, UK, 2015.

[13]   U. Isacsson and H. Zeng, "Relationships between bitumen chemistry and low temperature behaviour of asphalt," Construction and Building Materials, vol. 11, no. 2, pp. 83–91, 1997.

[14]   A. Behnood and M.M. Gharehveran, "Morphology, rheology, and physical properties of polymer-modified asphalt binders," European Polymer Journal, vol. 112, pp. 766–791, 2019.

[15]   S.H. Firoozifar, S. Foroutan, and S. Foroutan, "The effect of asphaltene on thermal properties of bitumen," Chemical Engineering Research and Design, vol. 89, no. 10, pp. 2044–2048, 2011.

[16]   Y. Xu, E. Zhang, and L. Shan, "Effect of SARA on rheological properties of asphalt binders," Journal of Materials in Civil Engineering, vol. 31, no. 6, p. 4019086, 2019.

[17]   H.K. Webb, J. Arnott, R.J. Crawford, and E.P. Ivanova, "Plastic degradation and its environmental implications with special reference to poly (ethylene terephthalate)," Polymers (Basel), vol. 5, no. 1, pp. 1–18, 2012.

[18]   F. Awaja and D. Pavel, "Recycling of PET," European Polymer Journal, vol. 41, no. 7, pp. 1453–1477, 2005.

[19]   T.B. Moghaddam, M. Soltani, and M.R. Karim, "Evaluation of permanent deformation characteristics of unmodified and Polyethylene Terephthalate modified asphalt mixtures using dynamic creep test," Materials & Design, vol. 53, pp. 317–324, 2014.

[20]   N. Usman, M. Masirin, K.A. Ahmad, and A.A. Wurochekke, "Reinforcement of asphalt concrete mixture using recycle polyethylene terephthalate fibre," Indian Journal of Science and Technology, vol. 9, no. 46, p. 107143, 2016.

[21]   N. Usman and M.I.M. Masirin, "Performance of asphalt concrete with plastic fibres," in Use of recycled plastics in eco-efficient concrete, Elsevier, pp. 427–440, 2019.

[22]   Y. Huang, R.N. Bird, and O. Heidrich, "A review of the use of recycled solid waste materials in asphalt pavements," Resources, Conservation and Recycling, vol. 52, no. 1, pp. 58–73, 2007.

[23]   T.V. Mathew and K.V.K. Rao, "Capacity and Level of service," Introduction to Transportation Engineering, NPTEL, 2007.

[24]   J.G. Speight, "Asphalt materials science and technology," Butterworth-Heinemann is, 2016.

[25]   P.K. Gautam, P. Kalla, A.S. Jethoo, R. Agrawal, and H. Singh, "Sustainable use of waste in flexible pavement: A review," Construction and Building Materials, vol. 180, pp. 239–253, 2018.

[26]   M. Sarireh, "Flexible pavement distress evaluation and analysis," International Journal of Advanced Research in Engineering, vol. 2, no. 4, pp. 1–7, 2016.

[27] J.S. Miller and W.Y. Bellinger, "Distress identification manual for the long-term pavement performance program," United States. Federal Highway Administration. Office of Infrastructure, 2003.

[28] The Constructor, "Types of Failures in Flexible Pavements and their Repair Techniques," [Online]. Available: https://theconstructor.org/transportation/types-failures-in-flexible-pavements-repair/16124/.

[29] S.W. Haider and K. Chatti, "Effect of design and site factors on fatigue cracking of new flexible pavements in the LTPP SPS-1 experiment," International Journal of Pavement Engineering, vol. 10, no. 2, pp. 133–147, 2009.

[30] C.L. Monismith, "Analytically based asphalt pavement design and rehabilitation: Theory to practice," 1962-1992, no. 1354. 1992.

[31] M.N. Nagabhushana, D. Tiwari, and P.K. Jain, "Rutting in flexible pavement: an approach of evaluation with accelerated pavement testing facility," Procedia-Social and Behavioral Sciences, vol. 104, pp. 149–157, 2013.

[32] N.K. Tamrakar, "Overview on causes of flexible pavement distresses," Bull. Nepal Geol. Soc, vol. 36, pp. 245–250, 2019.

[33] J.G. Speight, "Introduction to enhanced recovery methods for heavy oil and tar sands," Gulf Professional Publishing, 2016.

[34] F. Povolo and M. Fontelos, "Time-temperature superposition principle and scaling behaviour," Journal of Materials Science, vol. 22, pp. 1530–1534, 1987.

[35] W. Zeiada, H. Liu, H. Ezzat, G.G. Al-Khateeb, B.S. Underwood, A. Shanableh, and M.W. Samarai, "Review of the Superpave performance grading system and recent developments in the performance-based test methods for asphalt binder characterization," Construction and Building Materials, vol. 319, p. 126063, 2022.

[36] A. Abbas, B.C. Choi, E. Masad, and T. Papagiannakis, "The influence of laboratory aging method on the rheological properties of asphalt binders," Journal of Testing and Evaluation, vol. 30, no. 2, pp. 171–176, 2002.

[37] C.H. Domke, M. Liu, R.R. Davison, J.A. Bullin, and C.J. Glover, "Study of strategic highway research program pressure aging vessel procedure using long-term, low-temperature aging experiments and asphalt kinetics," Transportation Research Record, vol. 1586, no. 1, pp. 10–15, 1997.

[38] AASHTO T240-17, "Effect of Heat and Air on a Moving Film of Asphalt Binder (Rolling Thin-Film Oven Test)," American Association of State Highway and Transportation Officials.: AASHTO provisional standards. Washington, D.C., 2017.

[39] AASHTO R28-16, "Accelerated Aging of Asphalt Binder Using a Pressurized Aging Vessel (PAV)," American Association of State Highway and Transportation Officials.: AASHTO provisional standards, Washington, D.C., 2016.

[40]   AASHTO R29-18, "Grading or Verifying the Performance Grade (PG) of an Asphalt Binder," American Association of State Highway and Transportation Officials.: AASHTO provisional standards, Washington, D.C., 2018.

[41]   AASHTO T315-16, "Determining the Rheological Properties of Asphalt Binder Using a Dynamic Shear Rheometer (DSR)," American Association of State Highway and Transportation Officials.: AASHTO provisional standards, Washington, D.C., 2016.

[42]   AASHTO M320-17, "Performance-Graded Asphalt Binder," American Association of State Highway and Transportation Officials.: AASHTO provisional standards, Washington, D.C., 2017.

[43]   AASHTO T313-16, "Determining the Flexural Creep Stiffness of Asphalt Binder Using the Bending Beam Rheometer (BBR)," American Association of State Highway and Transportation Officials.: AASHTO provisional standards, Washington, D.C., 2016.

[44]   S. Fundamentals, "Superpave Fundamentals Reference Manual," Federal Highway Administration-FHWA, National Highway Institute: NHI (National Highway Institute), 2000.

[45]   H.A. Omar, N.I.M. Yusoff, M. Mubaraki, and H. Ceylan, "Effects of moisture damage on asphalt mixtures," Journal of Traffic and Transportation Engineering (English Edition), vol. 7, no. 5, pp. 600–628, 2020.

[46]   H. Luo, X. Huang, T. Rongyan, H. Ding, J. Huang, D. Wang, Y. Liu, and Z. Hong, "Advanced method for measuring asphalt viscosity: Rotational plate viscosity method and its application to asphalt construction temperature prediction," Construction and Building Materials, vol. 301, p. 124129, 2021.

[47]   I.L. Al-Qadi, H. Wang, P. J. Yoo, and S.H. Dessouky, "Dynamic analysis and in situ validation of perpetual pavement response to vehicular loading," Transportation Research Record, vol. 2087, no. 1, pp. 29–39, 2008.

[48]   N.W. McLeod, "Influence of viscosity of asphalt-cements on compaction of paving mixtures in the field and discussion," Highway Research Record, no. 158, 1967.

[49]   N.M. Wasiuddin, R. Saha, W. King Jr, and L. Mohammad, "Effects of temperature and shear rate on viscosity of Sasobit®-modified asphalt binders," International Journal of Pavement Research and Technology, vol. 5, no. 6, p. 369, 2012.

[50]   AASHTO T316-17, "Viscosity Determination of Asphalt Binder Using Rotational Viscometer," American Association of State Highway and Transportation Officials.: AASHTO provisional standards, Washington, D.C., 2017.

[51]   R.C. West, D.E. Watson, P.A. Turner, and J.R. Casola, "Mixing and compaction temperatures of asphalt binders in hot-mix asphalt," no. Project 9-39. 2010.

[52] M. Guo, Y. Tan, L. Wang, and Y. Hou, "Diffusion of asphaltene, resin, aromatic and saturate components of asphalt on mineral aggregates surface: molecular dynamics simulation," Road Materials and Pavement Design, vol. 18, no. sup3, pp. 149–158, 2017.

[53] J. Zhao, X. Huang, and T. Xu, "Combustion mechanism of asphalt binder with TG–MS technique based on components separation," Construction and Building Materials, vol. 80, pp. 125–131, 2015.

[54] L.W. Corbett, "Composition of asphalt based on generic fractionation, using solvent deasphaltening, elution-adsorption chromatography, and densimetric characterization," Analytical Chemistry, vol. 41, no. 4, pp. 576–579, 1969.

[55] J.M. Dealy, "Rheological properties of oil sand bitumens," The Canadian Journal of Chemical Engineering, vol. 57, no. 6, pp. 677–683, 1979.

[56] P. Zuo, S. Qu, and W. Shen, "Asphaltenes: Separations, structural analysis and applications," Journal of Energy Chemistry, vol. 34, pp. 186–207, 2019.

[57] B. Hofko, L. Eberhardsteiner, J. Füssl, H. Grothe, F. Handle, M. Hospodka, D. Grossegger, S.N. Nahar, A.J.M. Schmets, and A. Scarpas, "Impact of maltene and asphaltene fraction on mechanical behavior and microstructure of bitumen," Materials and Structures, vol. 49, pp. 829–841, 2016.

[58] ASTM D6560-17, "Standard Test Method for Determination of Asphaltenes (Heptane Insolubles) in Crude Petroleum and Petroleum Products," ASTM International, West Conshohocken, PA, 2017.

[59] C. Yang, J. Xie, S. Wu, S. Amirkhanian, X. Zhou, Q. Ye, D. Yang, and R. Hu, "Investigation of physicochemical and rheological properties of SARA components separated from bitumen," Construction and Building Materials, vol. 235, p. 117437, 2020.

[60] M.M. Ramirez-Corredores, "The science and technology of unconventional oils: finding refining opportunities," Academic press, 2017.

[61] ASTM D2007-19, "Standard test method for characteristic groups in rubber extender and processing oils and other petroleum–derived oils by the clay–gel absorption chromatographic method," ASTM International, West Conshohocken, PA, 2019.

[62] H. Shi, T. Xu, P. Zhou, and R. Jiang, "Combustion properties of saturates, aromatics, resins, and asphaltenes in asphalt binder," Construction and Building Materials, vol. 136, pp. 515–523, 2017.

[63] J. Wang, T. Wang, X. Hou, and F. Xiao, "Modelling of rheological and chemical properties of asphalt binder considering SARA fraction," Fuel, vol. 238, pp. 320–330, 2019.

[64] M.N. Siddiqui and M.F. Ali, "Investigation of chemical transformations by NMR and GPC during the laboratory aging of Arabian asphalt," Fuel, vol. 78, no. 12, pp. 1407–1416, 1999.

[65] D. Lesueur, "The colloidal structure of bitumen: Consequences on the rheology and on the mechanisms of bitumen modification," Advances in Colloid and Interface Science, vol. 145, no. 1–2, pp. 42–82, 2009.

[66] H. Li, J. Zhang, Q. Xu, C. Hou, Y. Sun, Y. Zhuang, S. Han, and C.H. Wu, "Influence of asphaltene on wax deposition: Deposition inhibition and sloughing," Fuel, vol. 266, p. 117047, 2020.

[67] S. Alimohammadi, S. Zendehboudi, and L. James, "A comprehensive review of asphaltene deposition in petroleum reservoirs: Theory, challenges, and tips," Fuel, vol. 252, pp. 753–791, 2019.

[68] M.E. Moir, "Asphaltenes, what art thou? Asphaltenes and the Boduszynski Continuum," in The Boduszynski Continuum: Contributions to the Understanding of the Molecular Composition of Petroleum, ACS Publications, pp. 3–24, 2018.

[69] J. Ancheyta, G. Centeno, F. Trejo, G. Marroquin, J.A. García, E. Tenorio, and A. Torres, "Extraction and characterization of asphaltenes from different crude oils and solvents," Energy & Fuels, vol. 16, no. 5, pp. 1121–1127, 2002.

[70] V. Calemma, R. Rausa, P. D'Anton, and L. Montanari, "Characterization of asphaltenes molecular structure," Energy & Fuels, vol. 12, no. 2, pp. 422–428, 1998.

[71] A. Demirbas, "Deposition and flocculation of asphaltenes from crude oils," Petroleum Science and Technology, vol. 34, no. 1, pp. 6–11, 2016.

[72] J.G. Speight, "Petroleum Asphaltenes-Part 1: Asphaltenes, resins and the structure of petroleum," Oil & Gas Science and Technology, vol. 59, no. 5, pp. 467–477, 2004.

[73] L. Eberhardsteiner, J. Füssl, B. Hofko, F. Handle, M. Hospodka, R. Blab, and H. Grothe, "Influence of asphaltene content on mechanical bitumen behavior: experimental investigation and micromechanical modeling," Materials and Structures, vol. 48, pp. 3099–3112, 2015.

[74] C. Varanda, I. Portugal, J. Ribeiro, A. Silva, and C.M. Silva, "Influence of polyphosphoric acid on the consistency and composition of formulated bitumen: standard characterization and NMR insights," Journal of analytical methods in chemistry, vol. 2016, 2016.

[75] S. Sultana, and A. Bhasin, "Effect of chemical composition on rheology and mechanical properties of asphalt binder," Construction and Building Materials, vol. 72, pp. 293–300, 2014.

[76] M. da C. C. Lucena, S. de A. Soares, and J.B. Soares, "Characterization and thermal behavior of polymer-modified asphalt," Materials Research, vol. 7, pp. 529–534, 2004.

[77] A. Ghasemirad, N. Bala, and L. Hashemian, "High-temperature performance evaluation of asphaltenes-modified asphalt binders," Molecules, vol. 25, no. 15, p. 3326, 2020.

[78] S. Mangiafico, H. Di Benedetto, C. Sauzéat, F. Olard, S. Pouget, and L. Planque, "Effect of colloidal structure of bituminous binder blends on linear viscoelastic behaviour of mixtures containing Reclaimed Asphalt Pavement," Materials & Design, vol. 111, pp. 126–139, 2016.

[79] N.A.A. Mazalan, M.K.I.M. Satar, A. Mohamed, and M.N.M. Warid, "Rheological properties of asphaltene-modified asphalt binder and mastic," Physics and Chemistry of the Earth, Parts A/B/C, vol. 131, p. 103422, 2023.

[80] S. Fakirov, "Fundamentals of polymer science for engineers," John Wiley & Sons, 2017.

[81] C. Bach, X. Dauchy, M.C. Chagnon, and S. Etienne, "Chemical compounds and toxicological assessments of drinking water stored in polyethylene terephthalate (PET) bottles: a source of controversy reviewed," Water Research, vol. 46, no. 3, pp. 571–583, 2012.

[82] K. Simon, and M. Milad, "Recycling Plastic Bottle into Synthetic Fiber," IUBAT - International University of Business Agriculture and Technology, Dhaka, 2019.

[83] M.E. Sánchez, A. Morán, A. Escapa, L.F. Calvo, and O. Martínez, "Simultaneous thermogravimetric and mass spectrometric analysis of the pyrolysis of municipal solid wastes and polyethylene terephthalate," Journal of Thermal Analysis and Calorimetry, vol. 90, pp. 209–215, 2007.

[84] J. Ma, and S.A.M. Hesp, "Effect of recycled polyethylene terephthalate (PET) fiber on the fracture resistance of asphalt mixtures," Construction and Building Materials, vol. 342, p. 127944, 2022.

[85] M. Saleh, N. Ahmed, T.B. Moghaddam, and L. Hashemian, "A novel framework for determining optimum fibre content in high-performance asphalt concrete mixes for low temperature applications.," in Transportation Association of Canada 2023 Conference and Exhibition-Lessons in Leadership, 2023.

[86] E. Ahmadinia, M. Zargar, M.R. Karim, M. Abdelaziz, and E. Ahmadinia, "Performance evaluation of utilization of waste Polyethylene Terephthalate (PET) in stone mastic asphalt," Construction and Building Materials, vol. 36, pp. 984–989, 2012.

[87] Z. Dehghan and A. Modarres, "Evaluating the fatigue properties of hot mix asphalt reinforced by recycled PET fibers using 4-point bending test," Construction and Building Materials, vol. 139, pp. 384–393, 2017.

[88] R. Izaks, L. Gebauere, R. Sparans, R. Kornisovs, and V. Haritonovs, "Use of Recycled Asphalt and Waste Materials in Production of High-Performance Asphalt Mixtures," The Baltic Journal of Road and Bridge Engineering, vol. 17, no. 4, pp. 120–145, 2022.

[89] H.M.R.D. da Silva, A.V. Machado, J. Oliveira, and L.M.B. Costa, "Waste polymers recycling in high performance asphalt mixtures," 2011.

[90] F. Leiva-Villacorta, A. Taylor, and R. Willis, "High-modulus asphalt concrete (HMAC) mixtures for use as base course," National Center for Asphalt Technology Report, pp. 4–17, 2017.

[91] E. Denneman, M. Nkgapele, J. Anochie-Boateng, and J.W. Maina, "Transfer of high modulus asphalt mix technology to South Africa," in Proceedings of the 10th conference on asphalt pavements for Southern Africa, Champagne Sports Resort. Google Scholar, 2011.

[92] L. Petho and E. Denneman, "Implementing EME2, the French high modulus asphalt in Australia," in 6th Eurasphalt & Eurobitume Congress, 2016.

[93] J.L. Delorme, C. De la Roche, and L. Wendling, "LPC bituminous mixtures design guide," Laboratoire Central des Ponts et Chaussées, 2007.

[94] A. Ghassemirad, N. Bala, L. Hashemian, and A. Bayat, "Application of asphaltenes in high modulus asphalt concrete," Construction and Building Materials, vol. 290, p. 123200, 2021.

[95] L. Wang, H. Meng, Q. Wang, Z. Liu, and S. Xue, "Application Research of High Modulus Asphalt Mixture Using Hard Grade Binder," J DEStech Transactions on Engineering Technology Research, 2016.

[96] H. Liu, W. Zeiada, G.G. Al-Khateeb, A. Shanableh, and M. Samarai, "Use of the multiple stress creep recovery (MSCR) test to characterize the rutting potential of asphalt binders: A literature review," Construction and Building Materials, vol. 269, p. 121320, 2021.

[97] H. Liu, W. Zeiada, G.G. Al-Khateeb, H. Ezzet, A. Shanableh, and M. Samarai, "Analysis of MSCR test results for asphalt binders with improved accuracy," Materials and Structures, vol. 54, pp. 1–14, 2021.

[98] J. Zhang, L.F. Walubita, A.N.M. Faruk, P. Karki, and G.S. Simate, "Use of the MSCR test to characterize the asphalt binder properties relative to HMA rutting performance–A laboratory study," Construction and Building Materials, vol. 94, pp. 218–227, 2015.

[99] AASHTO T350–19, "Standard method of test for multiple stress creep recovery (MSCR) test of asphalt binder using a dynamic shear rheometer (DSR)," American Association of State Highway and Transportation Officials.: AASHTO provisional standards, Washington, D.C., 2019.

[100] J. De Visscher, A. Paez-Dueñas, P. Cabanillas, V. Carrera, R. Cerny, G. Durand, T. Hagner, and I. Lancaster, "European round robin tests for the multiple stress creep recovery test and contribution to the development of the European standard test method," in 6th Eurobitumen and Euraspahlt Congress, Prague, Czech Republic, 2016.

[101] H. Liu, W. Zeiada, G.G. Al-Khateeb, A. Shanableh, and M. Samarai, "Characterization of the shear-thinning behavior of asphalt binders with consideration of yield stress," Materials and Structures, vol. 53, pp. 1–13, 2020.

[102] F.S. Bhat and M.S. Mir, "Rheological investigation of asphalt binder modified with nanosilica," International Journal of Pavement Research and Technology, vol. 14, pp. 276–287, 2021.

[103] S.M. Asgharzadeh, N. Tabatabaee, K. Naderi, and M.N. Partl, "Evaluation of rheological master curve models for bituminous binders," Materials and Structures, vol. 48, pp. 393–406, 2015.

[104] G.D. Airey, "Rheological characteristics of polymer modified and aged bitumens." University of Nottingham, Nottingham, 1997.

[105] M. Elkashef, J. Podolsky, R.C. Williams, and E. Cochran, "Preliminary examination of soybean oil derived material as a potential rejuvenator through Superpave criteria and asphalt bitumen rheology," Construction and Building Materials, vol. 149, pp. 826–836, 2017.

[106] G. Cerni, F. Cardone, and S. Colagrande, "Low-temperature tensile behaviour of asphalt binders: Application of loading time–temperature–conditioning time superposition principle," Construction and Building Materials, vol. 25, no. 4, pp. 2133–2145, 2011.

[107] A.M. Rodríguez-Alloza, J. Gallego, and F. Giuliani, "Complex shear modulus and phase angle of crumb rubber modified binders containing organic warm mix asphalt additives," Materials and Structures, vol. 50, pp. 1–9, 2017.

[108] H. Zhang, Z. Chen, G. Xu, and C. Shi, "Evaluation of aging behaviors of asphalt binders through different rheological indices," Fuel, vol. 221, pp. 78–88, 2018.

[109] C. Zhu, H. Zhang, G. Xu, and C. Shi, "Aging rheological characteristics of SBR modified asphalt with multi-dimensional nanomaterials," Construction and Building Materials, vol. 151, pp. 388–393, 2017.

[110] Q. Li, H. Zhang, C. Shi, and Z. Chen, "A novel warm-mix additive for SBR modified asphalt binder: Effects of Sasobit/epoxidized soybean oil compound on binder rheological and long-term aging performance," Journal of Cleaner Production, vol. 326, p. 129405, 2021.

[111] H. Chen, Y. Zhang, and H.U. Bahia, "The role of binders in mixture cracking resistance measured by ideal-CT test," International Journal of Fatigue, vol. 142, p. 105947, 2021.

[112] F. Zhou, "Development of an IDEAL cracking test for asphalt mix design, quality control and quality assurance," NCHRP-IDEA Program Project Final Report, no. 195, 2019.

[113] ASTM D8225-19, "Standard Test Method for Determination of Cracking Tolerance Index of Asphalt Mixture Using the Indirect Tensile Cracking Test at Intermediate Temperature," ASTM International, West Conshohocken, PA, 2019.

[114] P.S. Chowdhury, S.L.A. Noojilla, and M.A. Reddy, "Evaluation of fatigue characteristics of asphalt mixtures using Cracking Tolerance index (CTIndex)," Construction and Building Materials, vol. 342, p. 128030, 2022.

[115] ASTM D6931-17, "Standard Test Method for Indirect Tensile (IDT) Strength of Asphalt Mixtures," ASTM International, West Conshohocken, PA, 2017.

[116] R.B. Ahmed and K. Hossain, "Waste cooking oil as an asphalt rejuvenator: A state-of-the-art review," Construction and Building Materials, vol. 230, p. 116985, 2020.

[117] Y. Du, J. Chen, Z. Han, and W. Liu, "A review on solutions for improving rutting resistance of asphalt pavement and test methods," Construction and Building Materials, vol. 168, pp. 893–905, 2018.

[118] Y. Bi, S. Wu, J. Pei, Y. Wen, and R. Li, "Correlation analysis between aging behavior and rheological indices of asphalt binder," Construction and Building Materials, vol. 264, p. 120176, 2020.

[119] F.S. Almadwi and G.J. Assaf, "Effects of asphalt binders on pavement mixtures using an optimal balance of desert sand," Construction and Building Materials, vol. 220, pp. 415–425, 2019.

[120] V. Radhakrishnan, M.R. Sri, and K.S. Reddy, "Evaluation of asphalt binder rutting parameters," Construction and Building Materials, vol. 173, pp. 298–307, 2018.

[121] T. Xu and X. Huang, "Investigation into causes of in-place rutting in asphalt pavement," Construction and Building Materials, vol. 28, no. 1, pp. 525–530, 2012.

[122] F.L. Roberts, P.S. Kandhal, E.R. Brown, D.Y. Lee, and T.W. Kennedy, "Hot mix asphalt materials, mixture design and construction," The National Academies of Sciences, Engineering, and Medicine, Washington, D.C., 1996.

[123] M.O. Hamzah, S.R. Omranian, and B. Golchin, "A Review on the Effects of Aging on Properties of Asphalt Binders and Mixtures," Caspian Journal of Applied Sciences Research, vol. 4, no. 6, 2015.

[124] T. Yi-qiu, Z. Lei, G. Wei-qiang, and G. Meng, "Investigation of the effects of wax additive on the properties of asphalt binder," Construction and Building Materials, vol. 36, pp. 578–584, 2012.

[125] S. Rahmad, N.I.M. Yusoff, S.M. Fadzil, K.H. Badri, A.K. Arshad, I. Widyatmoko, and S.A.P. Rosyidi, "The effects of polymer modified asphalt binder incorporating with chemical warm mix additive towards water quality degradation," Journal of Cleaner Production, vol. 279, p. 123698, 2021.

[126] L. Monteiro, T.B. Moghaddam, M. Shafiee, and L. Hashemian, "Investigating the Addition of Organomontmorillonite Nanoclay and Its Effects on the Performance of Asphalt Binder," Journal of Materials in Civil Engineering, vol. 35, no. 8, p. 4023267, 2023.

[127] M.R.M. Hasan, B. Colbert, Z. You, A. Jamshidi, P.A. Heiden, and M.O. Hamzah, "A simple treatment of electronic-waste plastics to produce asphalt binder additives with improved properties," Construction and Building Materials, vol. 110, pp. 79–88, 2016.

[128] M. Mazumder, H. Kim, and S.J. Lee, "Performance properties of polymer modified asphalt binders containing wax additives," International Journal of Pavement Research and Technology, vol. 9, no. 2, pp. 128–139, 2016.

[129] J. Choudhary, B. Kumar, and A. Gupta, "Utilization of solid waste materials as alternative fillers in asphalt mixes: A review," Construction and Building Materials, vol. 234, p. 117271, 2020.

[130] D. Wang, A. Baliello, L. Poulikakos, K. Vasconcelos, M.R. Kakar, G. Giancontieri, E. Pasquini, L. Porot, M. Tušar, C. Riccardi, and M. Pasetto, "Rheological properties of asphalt binder modified with waste polyethylene: An interlaboratory research from the RILEM TC WMR," Resources, Conservation and Recycling, vol. 186, p. 106564, 2022.

[131] A. Meisen, "Bitumen Beyond Combustion (BBC) Project Phase 1 Report. BBC Project - Phase 1 Report 0416x.docx: Prepared for Alberta Innovates," Alberta, Canada, 2017.

[132] T. Ling, Y. Lu, Z. Zhang, C. Li, and M. Oeser, "Value-added application of waste rubber and waste plastic in asphalt binder as a multifunctional additive," Materials, vol. 12, no. 8, p. 1280, 2019.

[133] C. Hu, W. Lin, M. Partl, D. Wang, H. Yu, and Z. Zhang, "Waste packaging tape as a novel bitumen modifier for hot-mix asphalt," Construction and Building Materials, vol. 193, pp. 23–31, 2018.

[134] L. Feng, J. Liu, and L. Hu, "Rheological behavior of asphalt binder and performances of asphalt mixtures modified by waste soybean oil and lignin," Construction and Building Materials, vol. 362, p. 129735, 2023.

[135] S. Dreessen, J.P. Planche, and V. Gardel, "A new performance related test method for rutting prediction: MSCRT," Advanced Testing and Characterization of Bituminous Materials, vol. 1, pp. 971–980, 2009.

[136] N. Saboo, and P. Kumar, "Analysis of different test methods for quantifying rutting susceptibility of asphalt binders," Journal of Materials in Civil Engineering, vol. 28, no. 7, p. 4016024, 2016.

[137] J. Stempihar, A. Gundla, and B.S. Underwood, "Interpreting stress sensitivity in the multiple stress creep and recovery test," Journal of Materials in Civil Engineering, vol. 30, no. 2, p. 4017283, 2018.

[138] A.K. Apeagyei, "Laboratory evaluation of antioxidants for asphalt binders," Construction and Building Materials, vol. 25, no. 1, pp. 47–53, 2011.

[139] J.A. D'Angelo, "The relationship of the MSCR test to rutting," Road Materials and Pavement Design, vol. 10, no. sup1, pp. 61–80, 2009.

[140] T.L.J. Wasage, J. Stastna, and L. Zanzotto, "Rheological analysis of multi-stress creep recovery (MSCR) test," International Journal of Pavement Engineering, vol. 12, no. 6, pp. 561–568, 2011.

[141] AASHTO M332-20, "Standard Specification for Performance-Graded Asphalt Binder Using Multiple Stress Creep Recovery (MSCR) Test," American Association of State Highway and Transportation Officials.: AASHTO provisional standards, 2020.

[142] R. Chang, A. Sha, P. Zhao, S. Huang, and C. Qi, "Evaluation of susceptibility of asphalt binders to rutting through MSCR test," Advances in Materials Science and Engineering, vol. 2021, pp. 1–10, 2021.

[143] O.V. Laukkanen, H. Soenen, T. Pellinen, S. Heyrman, and G. Lemoine, "Creep-recovery behavior of bituminous binders and its relation to asphalt mixture rutting," Materials and Structures, vol. 48, pp. 4039–4053, 2015.

[144] H. Zhang, Z. Chen, L. Li, and C. Zhu, "Evaluation of aging behaviors of asphalt with different thermochromic powders," Construction and Building Materials, vol. 155, pp. 1198–1205, 2017.

[145] K. Kołodziej, L. Bichajło, and T. Siwowski, "Effects of aging on the physical and rheological properties of trinidad lake asphalt modified bitumen," Materials, vol. 14, no. 10, p. 2532, 2021.

[146] P. Yee, B. Aida, S.A.M. Hesp, P. Marks, and K.K. Tam, "Analysis of premature low-temperature cracking in three Ontario, Canada, pavements," Transportation Research Record, vol. 1962, no. 1, pp. 44–51, 2006.

[147] T.M.A. Al-Ani, "Modification of asphalt mixture performance by rubber-silicone additive," Anbar Journal of Engineering Sciences, vol. 71, 2009.

[148] E. Masad, K.L. Roja, A. Rehman, and A. Abdala, "A review of asphalt modification using plastics: a focus on polyethylene," Texas A&M University: Qatar, Doha, 2020.

[149] R.S. McDaniel, "Fiber additives in asphalt mixtures," no. Project 20-05 (Topic 45-15), 2015.

[150] C.J. Slebi-Acevedo, P. Lastra-González, P. Pascual-Muñoz, and D. Castro-Fresno, "Mechanical performance of fibers in hot mix asphalt: A review," Construction and Building Materials, vol. 200, pp. 756–769, 2019.

[151] F. Morea, and R. Zerbino, "Improvement of asphalt mixture performance with glass macro-fibers," Construction and Building Materials, vol. 164, pp. 113–120, 2018.

[152] A. Muftah, A. Bahadori, F. Bayomy, and E. Kassem, "Fiber-reinforced hot-mix asphalt: Idaho case study," Transportation Research Record, vol. 2633, no. 1, pp. 98–107, 2017.

[153] P. Jaskuła, M. Stienss, and C. Szydłowski, "Effect of polymer fibres reinforcement on selected properties of asphalt mixtures," Procedia Engineering, vol. 172, pp. 441–448, 2017.

[154] S. Badeli, A. Carter, G. Doré, and S. Saliani, "Evaluation of the durability and the performance of an asphalt mix involving Aramid Pulp Fiber (APF): Complex modulus

before and after freeze-thaw cycles, fatigue, and TSRST tests," Construction and Building Materials, vol. 174, pp. 60–71, 2018.

[155] S.M. Abtahi, M. Sheikhzadeh, and S.M. Hejazi, "Fiber-reinforced asphalt-concrete–a review," Construction and Building Materials, vol. 24, no. 6, pp. 871–877, 2010.

[156] M. Amuchi, S.M. Abtahi, B. Koosha, S.M. Hejazi, and H. Sheikhzeinoddin, "Reinforcement of steel-slag asphalt concrete using polypropylene fibers," Journal of Industrial Textiles, vol. 44, no. 4, pp. 526–541, 2015.

[157] A.F. Ahmad, A.R. Razali, and I.S.M. Razelan, "Utilization of polyethylene terephthalate (PET) in asphalt pavement: A review," in IOP Conference Series: Materials Science and Engineering, IOP Publishing, p. 12004, 2017.

[158] A. Usman, M.H. Sutanto, M. Napiah, S.E. Zoorob, S. Abdulrahman, and S.M. Saeed, "Irradiated polyethylene terephthalate fiber and binder contents optimization for fiber-reinforced asphalt mix using response surface methodology," Ain Shams Engineering Journal, vol. 12, no. 1, pp. 271–282, 2021.

[159] T.B. Moghaddam, M.R. Karim, and T. Syammaun, "Dynamic properties of stone mastic asphalt mixtures containing waste plastic bottles," Construction and Building Materials, vol. 34, pp. 236–242, 2012.

[160] N. Jegatheesan, T.M. Rengarasu, and W. Bandara, "Effect of polyethylene terephthalate (PET) fibres as binder additive in hot mix asphalt concrete," Annual Sessions of IESL, pp. 175–182, 2018.

[161] V. Haritonovs, M. Zaumanis, J. Tihonovs, and J. Smirnovs, "Development of high-performance asphalt concrete using low quality aggregates," Civil Engineering'13, vol. 100, p. 197, 2013.

[162] H. Ziari, M.R.M. Aliha, A. Moniri, and Y. Saghafi, "Crack resistance of hot mix asphalt containing different percentages of reclaimed asphalt pavement and glass fiber," Construction and Building Materials, vol. 230, p. 117015, 2020.

[163] L.A.P. Callomamani, N. Bala, and L. Hashemian, "Comparative analysis of the impact of synthetic fibers on cracking resistance of asphalt mixes," International Journal of Pavement Research and Technology, pp. 1–17, 2022.

[164] T. Johnson, N. Bala, A. Bayat, and L. Hashemian, "Laboratory evaluation of cracking resistance for asphalt mixtures modified with nanoclay and nanocellulose," Canadian Journal of Civil Engineering, vol. 48, no. 12, pp. 1674–1682, 2021.

[165] ASTM C131, "Resistance to degradation of small-size coarse aggregate by abrasion and impact in the Los Angeles Machine," ASTM Designation, Philadelphia, 2014.

[166] A. Demirbaş, "Asphaltene yields from five types of fuels via different methods," Energy Conversion and Management, vol. 43, no. 8, pp. 1091–1097, 2002.

[167] F. Awaja, and D. Pavel, "Recycling of PET," European Polymer Journal, vol. 41, no. 7, pp. 1453–1477, 2005.

[168] H. Noorvand, M. Mamlouk, and K. Kaloush, "Evaluation of optimum fiber length in fiber-reinforced asphalt concrete," Journal of Materials in Civil Engineering, vol. 34, no. 3, p. 4021494, 2022.

[169] AASHTO R30, "Standard Practice for Laboratory Conditioning of Asphalt Mixtures," American Association of State Highway and Transportation Officials.: AASHTO provisional standards, 2022.

[170] C.R. Marín-Uribe, and L.M. Restrepo-Tamayo, "Experimental study of the tensile strength of hot asphalt mixtures measured with indirect tensile and semi-circular bending tests," Construction and Building Materials, vol. 339, p. 127651, 2022.

[171] K.L. Vasconcelos, L.B. Bernucci, and J.M. Chaves, "Effect of temperature on the indirect tensile strength test of asphalt mixtures," in 5th Eurasphalt & Eurobitume congress, p. 9, 2012.